

AD-A196 014

DTIC ELECT COPY

2

"Simulation of a Two Link Robot Manipulator with Elastic Members"

ILT John C. Hinds
HQDA, MILPERCEN (DAPC-OPA-E)
200 Stovall Street
Alexandria, VA 22332

Final report completed and approved 6 May 1988

DTIC
ELECTE
MAY 31 1988
S D
CAD

Approved for public release; distribution is unlimited.

A thesis submitted to The University of Pennsylvania
in partial fulfillment of the requirements for the degree of
Master of Science in Mechanical Engineering.

88 5 01 089

REPORT DOCUMENTATION PAGE

Form Approved
OMB No 0704-0188
Exp Date Jun 30, 1986

1a. REPORT SECURITY CLASSIFICATION		1b. RESTRICTIVE MARKINGS	
2a. SECURITY CLASSIFICATION AUTHORITY		3. DISTRIBUTION / AVAILABILITY OF REPORT	
2b. DECLASSIFICATION / DOWNGRADING SCHEDULE			
4. PERFORMING ORGANIZATION REPORT NUMBER(S) "Simulation of a Two Link Robot Manipulator with Elastic Members"		5. MONITORING ORGANIZATION REPORT NUMBER(S) Final report and thesis approved 6 May88	
6a. NAME OF PERFORMING ORGANIZATION	6b. OFFICE SYMBOL (if applicable)	7a. NAME OF MONITORING ORGANIZATION US Army Student Detachment w/dty station @ The University of Pennsylvania	
6c. ADDRESS (City, State, and ZIP Code)		7b. ADDRESS (City, State, and ZIP Code) Dept. of Mechanical Engineering, 11A Towne Bldg., 220 S. 33rd Street Philadelphia, PA 19104-6315	
8a. NAME OF FUNDING / SPONSORING ORGANIZATION	8b. OFFICE SYMBOL (if applicable)	9. PROCUREMENT INSTRUMENT IDENTIFICATION NUMBER Student, HQDA, MILPERCEN (DAPC-OPA-E) 200 Stovall St., Alexandria, VA 22332	
8c. ADDRESS (City, State, and ZIP Code)		10. SOURCE OF FUNDING NUMBERS	
		PROGRAM ELEMENT NO.	PROJECT NO.
		TASK NO.	WORK UNIT ACCESSION NO.
11. TITLE (Include Security Classification) HQDA, MILPERCEN, ATTN: DAPC-OPA-E 200 Stovall Street, Alexandria VA 22332			
12. PERSONAL AUTHOR(S) 6 May 1988			
13a. TYPE OF REPORT Thesis	13b. TIME COVERED FROM 1SEP 88 TO 6MAY88	14. DATE OF REPCRT (Year, Month, Day)	15. PAGE COUNT 117
16. SUPPLEMENTARY NOTATION Approved for public release; distribution unlimited.			
17. COSATI CODES		18. SUBJECT TERMS (Continue on reverse if necessary and identify by block number)	
FIELD	GROUP	SUB-GROUP	
19. ABSTRACT (Continue on reverse if necessary and identify by block number)			
<p>The elastic behavior of the components of a robot manipulator will tend to induce both static and dynamic errors between desired and actual trajectories and end-effector positions. Currently, most researchers consider joint compliance - as opposed to link displacements - to be the dominant source of these errors. This conclusion is based on the the fact that when compared to the yielding typically seen in gears, motor shafts, bearings, etc., the links appear almost perfectly rigid. However, current efforts to lighten robot manipulators and increase their operating speeds also tends to increase the significance of link elasticity. This study considers the dynamic effects of elastic link displacements in a two-link robot manipulator as simulated by a hierarchy of models. Model TTFEL allows both manipulator links to bend in a single plane and to twist. Therefore, the effects of bending-torsion vibrations in each link may be observed when the manipulator attempts motion with an inertially asymmetric payload grasped in its end-effector. This elasto-dynamic behavior is simulated, and results indicate a definite disturbance of the joint angle trajectories. The use of structural damping to eliminate these high frequency vibrations and increase the manipulator's accuracy is evaluated.</p>			
20. DISTRIBUTION / AVAILABILITY OF ABSTRACT <input checked="" type="checkbox"/> UNCLASSIFIED/UNLIMITED <input type="checkbox"/> SAME AS RPT. <input type="checkbox"/> DTIC USERS		21. ABSTRACT SECURITY CLASSIFICATION	
22a. NAME OF RESPONSIBLE INDIVIDUAL		22b. TELEPHONE (Include Area Code)	22c. OFFICE SYMBOL

Block 18 cont'd. : All pertinent symbols identified within.

UNIVERSITY OF PENNSYLVANIA
SCHOOL OF ENGINEERING AND APPLIED SCIENCE

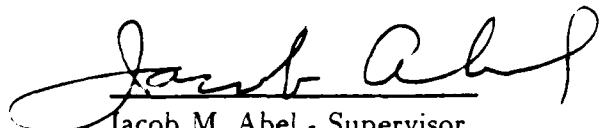
**SIMULATION OF A TWO LINK
ROBOT MANIPULATOR WITH
ELASTIC MEMBERS**

John C. Hinds

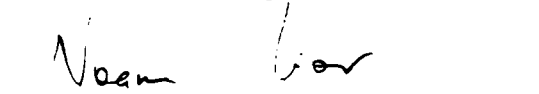
Philadelphia, Pennsylvania

May 1988

A thesis presented to the Faculty of Engineering and Applied Science of the University of Pennsylvania in partial fulfillment of the requirements for the degree of Master of Science in Engineering for graduate work in Mechanical Engineering and Applied Mechanics.



Jacob M. Abel - Supervisor



Noam Lior - Graduate Group Chairman

Abstract

The elastic behavior of the components of a robot manipulator will tend to induce (both static and dynamic errors between desired and actual trajectories and end-effector positions. Currently, most researchers consider joint compliance - as opposed to link displacements - to be the dominant source of these errors. This conclusion is based on the the fact that when compared to the yielding typically seen in gears, motor shafts, bearings, etc., the links appear almost perfectly rigid. However, current efforts to lighten robot manipulators (and increase their operating speeds also tends to increase the significance of link elasticity. This study considers the dynamic effects of elastic link displacements in a two-link robot manipulator) as simulated by a hierarchy of models. In all, five separate system models are developed. The last model, TTFEL, allows *both* manipulator links to bend in a single plane and to twist. Therefore, the effects of bending-torsion vibrations in each link may be observed when the manipulator attempts motion with an inertially asymmetric payload grasped in its end-effector. This elasto-dynamic behavior is simulated, and results indicate a definite disturbance of the joint angle trajectories. The use of structural damping to eliminate these high frequency vibrations and increase the manipulator's accuracy is evaluated. (118)

I would like to express my deep appreciation to Dr. Jacob M. Abel for his continuing technical advice, guidance, patience and inspiration. Special thanks also go to my friends Pramath Raj Sinha and Stephen Klemick for their suggestions, assistance and constructive criticism.

Finally, I would like to thank my mother and father, for without their constant support and encouragement this work would not have been possible.

Financial support for this research has been provided by the Department of the Army's Technological Enrichment Program.

Table of Contents

Nomenclature	1
Introduction	3
Development of System Models	9
Control	41
Numerical Simulation	45
Results and Discussion	47
Summary and Conclusions	56
Figures	60
Appendix A	95
Appendix B	99
Bibliography	115

Nomenclature

N	gear ratio
T_1	motor torque applied to first joint
T_2	motor torque applied to second joint
l_1	length of link one
l_2	length of link two
g	acceleration due to gravity
ρ	material density
I	link cross sectional moment of inertia
K_p	forward path gain
K_T	torque sensitivity
R	D.C. motor resistance
J_m	motor armature inertia
J_L	load inertia at motor shaft
J_T	total inertia at motor shaft
K_b	motor back e.m.f. constant
K_v	motor voltage sensitivity
T_{grav}	gravity torque
$\theta_d(t)$	desired joint angle
$\theta_m(t)$	actual motor angle
$\theta_L(t)$	actual link angle
$\theta_1(t)$	first link joint angle
$\theta_2(t)$	second link joint angle
$\Lambda(t)$	generalized time coordinate, first link torsion
$\alpha(t)$	generalized time coordinate, second link torsion
$q(t)$	generalized time coordinate, first link flexure
$b(t)$	generalized time coordinate, second link flexure
$\Gamma(y_1)$	mode shape, first link torsion
$\lambda(y_2)$	mode shape, second link torsion
$\psi(y_1)$	mode shape, first link flexure

$\epsilon(y_2)$	mode shape, second link flexure
\vec{e}	vector in end-effector coord. frame to eccentric payload
e	scalar distance to payload from origin of end-effector c. frame
GJ	torsional rigidity
EI	flexural rigidity
M_{pL}	payload mass
m_1	mass of link one
m_2	mass of link two
$\eta_1(y_1, t)$	first link torsional displacement
$\eta_2(y_2, t)$	second link torsional displacement
$w_1(y_1, t)$	first link flexural displacement
$w_2(y_2, t)$	second link flexural displacement
ζ_1	small angle due to first link flexural displacement
ζ_2	small angle due to second link flexural displacement
β	$(\theta_1 + \theta_2 + \zeta_1) \dots$ unless stated otherwise
A_1	cross sectional area of link one
A_2	cross sectional area of link two
I_{x_3}	moment of inertia of payload about axis x_3
I_{y_3}	moment of inertia of payload about axis y_3

Chapter 1

Introduction

When robot manipulators were first introduced into the automated manufacturing industry, they were usually tasked with only the simplest repetitive jobs. Today, however, they are finding their way into many different technical industries with various scientific as well as industrial applications. Many of these jobs place great expectations and demands upon the manipulators - often calling for high levels of accuracy, reliability, speed, strength, and efficiency. Considering all of these requirements, and then designing a suitably swift-moving, mechanically smooth, efficient, and powerful manipulator with high end-effector accuracy is no easy task to say the least. One is often forced into a compromise since improvement of one characteristic often dictates a reduction in performance in another. Consider, as a case in point, the demand for greater manipulator strength. This problem has been typically dealt

with through the application of more and stronger load bearing materials and more powerful joint motors [3]. However, this solution tends to increase the armweight to payload weight ratio drastically e.g. the Cincinatti Milicron robot for which payload capacity is only 10% of the system's weight. The increased weight in turn creates the need for higher joint torques, higher feedback gains, and causes greater overall power consumption. Efficiency, speed of response, and smooth operation will obviously also deteriorate.

However, another option does exist. Specifically, it is possible to meet these demands with lighter, more efficient, and *knowingly* flexible robots. It is true that manipulator performance and accuracy would be severely threatened by the inevitable *structural deformations and vibrations* that result when such a machine is expected to operate at higher speeds and/or handle substantial payloads. Yet, indications do exist that the need to be able to control this type of device is significant. For example, future applications of robotics to space exploration - some of which has already been seen with the use of the "arm" on the space shuttle - suggest the need to be able to effectively control lighter, more slender robot arms where link flexibility poses a serious challenge to accurate arm trajectories and end-effector positioning. Even at this moment, the desire for very light weight high-speed robots has been expressed through various DOD contracts. For example, the Army is currently funding research to develop reliable high speed manipulators for use in vehicle refueling operations, and explosive ordnance handling [9]. Low weight is of prime concern for ease of mobility, while long link lengths are needed for reach and powerful motor torques are

needed for potentially heavy payloads (0 – 1500lbs.). The need for light weight, high speed of operation, strength and accuracy coupled with the flexible displacements and vibrations that would be expected obviously pose the need for a mechanism with a kinematic/dynamic design that considers this and a control policy that compensates for the elastic phenomena.

These considerations motivate investigations aimed at developing a greater understanding of the dynamic behavior of flexible robotic systems. With this knowledge it may be possible to develop manipulator control schemes in order to minimize the effects of link flexibility on the desired dynamic response and accuracy of the robot.

To date, a considerable amount of research concerning the effects of elasticity in robot manipulators has been performed. Understandably, a good deal of time has been spent analyzing the effects of joint compliance because in many of the robots in use today, the links themselves are short and heavy enough to justify the assumption of rigidity. In these cases, the compliance observed is attributed to the elasticity found in the gears, belts, tendons, bearings, and hydraulic lines. This problem has been thoroughly investigated by Spong [12].

In the consideration of link deflections, considerable research producing dynamic models and suggestions for control strategies has also been published. Gebler considers a two joint, two link manipulator with link flexibility in a single plane coupled with joint compliance[7]. He proposes a feed-forward control strategy to correct the

link's trajectory. A similar analysis is performed by Tang and Wang [17], however they also allow for out-of-plane bending and torsional link displacements. Their result is an algorithm which predicts the actual position and orientation of the end-effector of a two link robot. However, the manipulator considered has only one moveable joint angle and carries no payload. Naganathan and Soni [14] also consider lateral deflection in two planes plus torsional displacements in a two link manipulator, but instead resort to a finite element model to determine the nonlinear effects of link flexibility. Nicosia and Tomei [15], who use the Lagrangian approach to obtain a dynamic model of a single and a double link planar manipulator, also employ the symbolic algebraic manipulation language MACSYMA to assist their efforts. Their study is limited to a consideration of in-plane link distortion only. Dubowsky and Sunada [5] provide a powerful finite element routine which considers the effects of distributed mass and flexibility and produces a model of the dynamic behaviour of manipulators composed of arbitrarily shaped links. Rakhsha and Goldenberg [16] use the Newton-Euler approach to develop a dynamic model of a single link robot with a payload. Lateral bending motion is considered, and the natural frequencies and mode shapes describing the vibratory behavior are found using a constrained mode approach [18]. Moreover, the flexibility influence is modeled as a disturbance torque affecting the rigid body motion. This paper serves as a good foundation for more comprehensive efforts. Several other works have also been completed, however the first to consider and analyze the limitations of a rigid-link assumption in the dynamic analysis of manipulators was Book. For example, in 1975 he, along with Whitney and Maizzo-Neto [3], published a paper describing a model of a two link, two joint

flexible manipulator. Lateral in-plane link flexibility was allowed in each link, and various control schemes were compared and contrasted. Specifically, individual joint control (IJC) was compared and contrasted with the feedback of flexible coefficients (FFC). Since then, Book has made various other contributions including models and suggested control methods [2].

In light of these efforts, the purpose of this research was to generate explicit closed-form models capable of simulating the motion of an arbitrary two-link revolute jointed manipulator wherein single-plane and torsional link flexure may occur while the arm is tasked to move various payloads. Dynamic behavior is also considered when the payload is grasped at a point removed from its mass center - hence making it inertially asymmetric. Following the analysis performed by Book in '86 [2], first the complete kinetic and potential energy expressions for each system are found. The vibratory displacements are represented through the method of assumed modes [13], and each complete system Lagrangian is then used to derive the set of governing equations of motion for each model which consists of a set of second order nonlinear differential equations. The dynamic behavior of the systems is simulated on a VAX 8560 digital computer wherein a straightforward IJC control policy is applied. The effectiveness of this control method is observed and compared with the same policy's strong effectiveness on a rigid two-link manipulator with a payload. Deviations in the joint angle trajectories and the end-effector position accuracy are examined and again the flexible-link robot performance is compared to that of the rigid link manipulator. Furthermore, the effects of increasing payload inertia are considered along

with possible compensation techniques.

Chapter 2

Development of System Models

In this study, five separate system models have been developed. Each model simulates the three dimensional motion of an upright serial two-link manipulator carrying a payload fixed at its end-effector (see fig.2). Gravitational effects are included, and each model introduces various elastic degrees of freedom. Furthermore, the links are assumed to behave as continuous slender beams modeled by the Bernoulli - Euler beam equations [13], and power is delivered to the system by standard servomotors.

The first model, RR (fig. 2), simulates the performance of a two-link robot manipulator wherein the links are assumed to be absolutely rigid. This model serves to provide a base of reference for "ideal" system behavior.

In the second model, TT (fig. 3), each link is permitted to vibrate in torsion about an axis passing longitudinally through the center of each link's cross section. The payload is gripped firmly at the end-effector, and the system motion is then analyzed following an initial twist to the end of the second link. The third model, TTEL (fig. 4), extends this problem by allowing the payload to be gripped eccentrically - i.e. not at its center of gravity. No initial torsional excitation is given in this case because even rigid body movement will excite second link, and then first link vibration.

Second link in-plane flexural vibration is then added to the problem defined by model TTEL, thus raising the number of degrees of freedom in the fourth model, TTFEL (fig. 5), to five. Here, the payload may be gripped at or off its center of gravity - which will tend to excite second link bending torsion-vibration. Finally, the fifth model, TFTFEL (fig. 6), permits each link to vibrate both torsionally and laterally thus raising the number of degrees of freedom in the system to six. In this case, the payload may also be held at any point.

Each of these system models yields a governing set of coupled second order non-linear differential equations of motion. The first step in deriving these equations is the development of a proper kinematic representation for each system. Specifically, robot arm kinematics is concerned with analytically describing the manipulator's and end-effector's spatial orientation, which entails mathematically illustrating the relationships between the joint variables and the operating space. This is actually a forward kinematics problem which results in a mathematical description of the robot's

position and orientation based upon a prior knowledge of the link parameters and the joint angle trajectories as a function of time. It should be mentioned that the Denavit Hartenberg formulation is very useful in forward kinematics for it conveniently represents the spatial relationships between the coordinate frames of the adjacent links forming the manipulator in a compact 4×4 homogeneous transformation matrix [6]. Thus the forward kinematics problem is reduced to the problem of obtaining the appropriate 4×4 homogeneous matrix which will yield the overall relationship between the end-effector and the stationary base or "inertial" reference frame. In this study, 3×3 rotation matrices and accompanying relative position vectors between the origins of the joint coordinate frames is used in lieu of the Denavit Hartenberg technique.

Once the kinematics have been formulated, the derivation of the equations of motion may begin. Note that the development of a proper control scheme is facilitated by reference to the closed form governing equations, and the resulting dynamic behavior of the manipulator is therefore a direct function of the efficiency and accuracy of them. There are a variety of methods available to develop them, however the two conventional approaches are the Newton - Euler (NE) formulation and the Lagrange - Euler (LE) formulation which rely on the principles of Newtonian and Lagrangian mechanics, respectively. These two methods are favored in fundamental studies and analysis because of their systematic methods and reliability.

The NE approach, which was developed in order to reduce the computational

burden of numerically solving these equations, involves relatively complex vector manipulations and appears to be quite uninviting. Yet once properly applied, it allows for a fast computational algorithm in which the time needed for calculations is linearly proportional to the number of joints of the robot arm and is independent of its configuration [6]. Thus, this method allows for the real-time control of the manipulator.

The LE method, on the other hand, provides a clearer and more appealing systematic method to obtain the manipulator's governing equations of motion. Based on Lagrangian dynamics, it relieves one of the burden of expressing and evaluating complex vector relationships, and requires simply the determination of the mechanism's proper kinetic and potential energy expressions. The resulting equations, as stated earlier, are nonlinear and include coupling forces between the joints - such as Coriolis and centrifugal forces - and gravitational effects. One also notices that the LE formulation clearly expresses these terms as an explicit function of the manipulator's physical characteristics such as link lengths and masses, material stiffness, and payload mass. As such, the LE approach yields the explicit closed - form state equations necessary for a dynamic analysis and control scheme design [6]. Through the use of conventional and compact transformation matrix relationships (such as the Denavit Hartenberg formulation previously mentioned) this method also lends itself to a smooth transition from analytic model to coded algorithm needed for computer simulation of the robot's movement.

Of the methods described, the LE approach generates equations which are the

most difficult to integrate numerically. Thus, this method really does not lend itself to use in the real - time control of a robot manipulator, for which most people rely on more efficient NE and d'Alembert techniques. (Variations of the basic LE method are available, however, such as the recursive Lagrangian formulation suggested by Hollerbach in 1980 [10] which alters a manipulator's standard LE equations, permitting their application to real - time control schemes.) However, since the purpose of this study has been to obtain insight to the elasto - dynamic behavior of these systems from computer simulations of their motion, the LE method was considered to be quite adequate. Furthermore, its systematic application allows for a simplified treatment of the great complexities normally introduced by the material flexibility. Also, the closed - form equations produced are then easily translateable into FORTRAN codes.

2.1 Model RR

We define the system Lagrangian, L , to be the difference between the kinetic energy T and the potential energy V of the system. ie.

$$L = T - V$$

Here T and V are themselves functions of variables that give the position and orientation of the system in a "base" or inertial frame of reference.

To obtain the kinetic energy of a rigid body in three dimensional motion relative

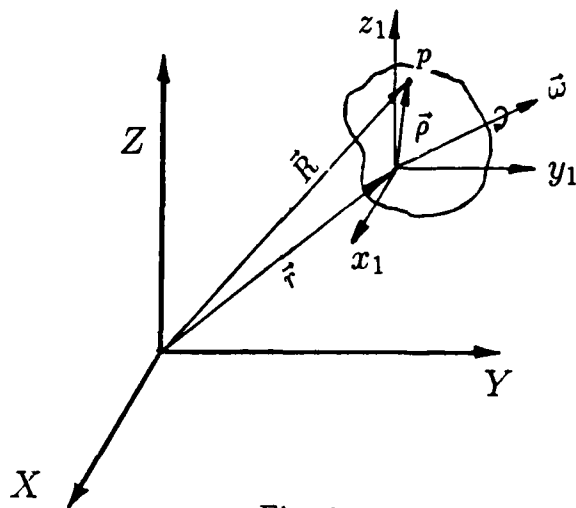


Fig. 1

to an inertial frame of reference XYZ, a moving reference frame or “body frame” $x_1y_1z_1$ is fixed to the body’s mass center G. A vector \vec{r} is defined to extend from the origin of the inertial frame to the origin of the body frame. Another vector $\vec{\rho}$ is defined to extend from the origin of the body frame to a generic point p in the body. (See fig. 1).

Then, with the vector

$$\vec{R} = \vec{r} + \vec{\rho}$$

the velocity of the point in the body is then expressed as

$$\vec{V} = \dot{\vec{r}} + \vec{\omega} \times \vec{\rho}$$

... where $\vec{\omega}$ is the angular velocity of the body at the instant considered.

The total kinetic energy expression becomes

$$T = \frac{1}{2} \int \vec{V} \cdot \vec{V} dm$$

Applying this method to the rigid link revolute-joint serial link manipulator of Model RR, "body frames" of reference are first placed at the revolute joints as shown in fig. 2.

The vectors depicted in fig. 1 are defined below:

\vec{r}_{p1} = from origin of first link coordinate frame to a generic point in link 1

\vec{r}_{e1} = from origin of first link coordinate frame to end of link 1

\vec{r}_{p2} = from origin of second link coordinate frame to a generic point in link2

\vec{r}_{pL} = from the origin of the inertial frame to the end of link2

Therefore,

$$\vec{V}_{p1}^o = \vec{\omega}_{link1} \times \vec{r}_{p1}^o$$

$$\vec{r}_{p2}^o = \vec{r}_{e1}^o + \vec{r}_{p2}^o$$

and so

$$\vec{V}_{p2}^o = \vec{\omega}_{link1} \times \vec{r}_{e1}^o + \vec{\omega}_{link2} \times \vec{r}_{p2}^o$$

$$\vec{r}_{pL} = \vec{r}_{e1} + \vec{r}_{e2}$$

$$\vec{V}_{PL}^o = \vec{\omega}_{link1} \times \vec{r}_{e1}^o + \vec{\omega}_{link2} \times \vec{r}_{e2}^o$$

assuming rigid links. (Note that the superscript "o" indicates with respect to the inertial frame of reference.)

At this point, further computations can be greatly simplified and the non-rigid body terms which will appear later due to link flexibility can be accounted for far

more easily if rotation matrix relationships are employed instead of the above vector expressions. As the name implies, a rotation matrix gives the “rotated” orientation of one link’s coordinate frame with respect to another’s. For example, R_1^0 expresses the rotated orientation of the first link’s coordinate frame with respect to the inertial frame of reference. It should be mentioned that the standard 3×3 rotation matrix does not express the translated position of the coordinate frame origin as do the standard 4×4 homogenous transformation matrices usually employed in robotics studies. Instead, this displacement is represented throughout this analysis by a separate relative position vector.

Thus, the following rotation matrices are defined:

$$R_1^0 = \begin{bmatrix} 1 & 0 & 0 \\ 0 & C\theta_1 & -S\theta_1 \\ 0 & S\theta_1 & C\theta_1 \end{bmatrix}$$

where $C\theta_1$ and $S\theta_1$ are the cosine and sine of the first and second joint angles, respectively.

$$R_2^1 = \begin{bmatrix} 1 & 0 & 0 \\ 0 & C\theta_2 & -S\theta_2 \\ 0 & S\theta_2 & C\theta_2 \end{bmatrix}$$

Therefore, in this case,

$$\vec{r}_{p1}^0 = R_1^0 \vec{r}_{p1}^1$$

$$\vec{v}_{p1}^0 = \dot{R}_1^0 \vec{r}_{p1}^1$$

$$\vec{v}_{p1}^{\circ} = \dot{\theta}_1 \begin{bmatrix} 0 & 0 & 0 \\ 0 & -S\theta_1 & -C\theta_1 \\ 0 & C\theta_1 & -S\theta_1 \end{bmatrix} \begin{bmatrix} 0 \\ y_1 \\ 0 \end{bmatrix} = \begin{bmatrix} 0 \\ -y_1 \dot{\theta}_1 S\theta_1 \\ y_1 \dot{\theta}_1 C\theta_1 \end{bmatrix}$$

$$\vec{r}_{p2}^{\circ} = R_1^0 \vec{r}_{e1}^{\circ} + R_1^0 R_2^1 \vec{r}_{p2}^{\circ} = R_1^0 \vec{r}_{e1}^{\circ} + R_2^0 \vec{r}_{p2}^{\circ}$$

$$\vec{v}_{p2}^{\circ} = \dot{R}_1^0 \vec{r}_{e1}^{\circ} + \dot{R}_2^0 \vec{r}_{p2}^{\circ}$$

$$\vec{v}_{p2}^{\circ} = \begin{bmatrix} 0 \\ -\dot{\theta}_1 l_1 S\theta_1 - (\dot{\theta}_1 + \dot{\theta}_2) y_2 S(\theta_1 + \theta_2) \\ l_1 \dot{\theta}_1 + (\dot{\theta}_1 + \dot{\theta}_2) y_2 C(\theta_1 + \theta_2) \end{bmatrix}$$

$$\vec{r}_{pL} = R_1^0 \vec{r}_{e1} + R_2^0 \vec{r}_{e2}$$

$$\vec{v}_{pL} = \dot{R}_1^0 \vec{r}_{e1} + \dot{R}_2^0 \vec{r}_{e2}$$

$$\vec{v}_{pL}^{\circ} = \begin{bmatrix} 0 \\ -l_1 \dot{\theta}_1 S\theta_1 - l_2 (\dot{\theta}_1 + \dot{\theta}_2) S(\theta_1 + \theta_2) \\ l_1 \dot{\theta}_1 C\theta_1 + l_2 (\dot{\theta}_1 + \dot{\theta}_2) C(\theta_1 + \theta_2) \end{bmatrix}$$

At this point, the kinetic energy expressions may now be defined as follows:

$$T_{link1} = \frac{1}{2} \int_0^{l_1} A_1(y_1) \rho(y_1) \vec{v}_{p1}^{\circ} \bullet \vec{v}_{p1}^{\circ} dy_1$$

Assuming the links to be uniform, this becomes

$$T_{link1} = \frac{1}{2} \rho A_1 \int_0^{l_1} \vec{v}_{p1}^\circ \bullet \vec{v}_{p1}^\circ dy_1 = \frac{1}{6} \dot{\theta}_1^2 m_1 l_1^2$$

Also,

$$T_{link2} = \frac{1}{2} \rho A_1 \int_0^{l_2} \vec{v}_{p2}^\circ \bullet \vec{v}_{p2}^\circ dy_2 = \frac{1}{2} m_2 \left[(\dot{\theta}_1 l_1)^2 + l_2^2 (\dot{\theta}_1 + \dot{\theta}_2)^2 / 3 + \dot{\theta}_1 l_1 l_2 C \theta_2 (\dot{\theta}_1 + \dot{\theta}_2) \right]$$

$$T_{payload} = \frac{1}{2} M_{pL} \vec{v}_{pL}^\circ \bullet \vec{v}_{pL}^\circ = \frac{1}{2} M_{pL} \left[(\dot{\theta}_1 l_1)^2 + l_2^2 (\dot{\theta}_1 + \dot{\theta}_2)^2 + 2 \dot{\theta}_1 l_1 l_2 C \theta_2 (\dot{\theta}_1 + \dot{\theta}_2) \right]$$

In this first model, where each link is assumed to be rigid, the only potential energy that needs to be accounted for is that due to gravity. The rotation matrix relationships just established allow this to be conveniently expressed as

$$V_{link1} = \int g \vec{r}_{p1}^\circ dm_1$$

$$V_{link2} = \int g \vec{r}_{p2}^\circ dm_2$$

$$V_{payload} = M_{pL} g \vec{r}_{pL}^\circ$$

Finally, the system Lagrangian can be defined as follows

$$L = T_{link1} + T_{link2} + T_{payload} - V_{link1} - V_{link2} - V_{payload}$$

and from this the manipulator's governing differential equations of motion can be derived in terms of the system's generalized coordinates $\theta_1(t)$ and $\theta_2(t)$.

$$d/dt \left\{ \partial L / \partial \dot{\theta}_1 \right\} - \partial L / \partial \theta_1 = T_1$$

$$d/dt \{ \partial L / \partial \dot{\theta}_2 \} - \partial L / \partial \theta_2 = T_2$$

Omitting all of the computational steps, the resulting equations of motion for the rigid two link manipulator (Model RR) are then obtained through the application of these expressions. Refer to Appendix B for the equations in their complete form.

2.2 Model TT and Model TTEL

The principles used to derive the equations of motion for the previous case are also applied in the derivation of models TT and TTEL. However, the torsional displacements which are now permitted to occur in each link and the consequences of this motion have to be accounted for in the system's kinematic representation and in the kinetic and potential energy expressions forming the system's Lagrangian. This has been accomplished through the use of the method of assumed modes [13] and "special" rotation matrices containing the flexibility variables.

Specifically, the torsional displacement in links one and two have been identified as $\eta_1(y_1, t)$ and $\eta_2(y_2, t)$, respectively.

The method of assumed modes is applied to express each of these displacements as a summation of the products of a generalized time coordinate and an associated

mode shape. In other words, let

$$\eta_1(y_1, t) = \sum_{i=1}^{\infty} \Lambda_i(t) \Gamma_i(y_1)$$

$$\eta_2(y_2, t) = \sum_{i=1}^{\infty} \alpha_i(t) \lambda_i(y_2)$$

where $\Gamma_i(y_1)$ and $\lambda_i(y_2)$ each represent the first mode shape of a cantilever shaft and payload in torsional vibration for $i=1$, second mode for $i=2$, and so on. The fundamental mode shape is

$$\Gamma_1(y) = \lambda_1(y) = A_1 \sin(\beta y)$$

where $\beta^2 = \omega^2 I/GJ$ [18]. Note that Appendix A focuses on the difficulties introduced here by the time varying inertial load present at the end of the first link due to the movement of the second link.

In an analysis completed by Book [3], a two mode shape approximation was used to represent flexural link displacements for the reason that the amplitudes of the higher mode shapes were assumed to be small. In this study, all flexural displacements have been represented with a single mode approximation. ie.

$$\eta_1(y_1, t) = \sum_{i=1}^{\infty} \Lambda_i(t) \Gamma_i(y_1) \approx \Lambda_1(t) \Gamma_1(y_1)$$

$$\eta_2(y_2, t) = \sum_{i=1}^{\infty} \alpha_i(t) \lambda_i(y_2) \approx \alpha_1(t) \lambda_1(y_2)$$

Furthermore, to maintain kinematic accuracy, it was also decided to employ a rotation matrix to account for the re-orientation of the second link's coordinate frame due to the twisting of the first link.

Specifically, fig. 3 illustrates how the second link coordinate frame experiences an additional small rotation about axis y_1 . Hence, the matrix R_2^0 used in the development of the system Lagrangian, which was previously defined as

$$R_2^0 = R_1^0 R_2^1$$

where

$$R_1^0 = ROT(x_1, \theta_1) \quad R_2^1 = ROT(x_2, \theta_2)$$

has been re-defined as

$$R_2^0 = R_1^0 R' R_2^1$$

where the matrix R' represents the rotation of the $x_2 y_2 z_2$ frame about axis y_1 through small angle $\eta_1(l_1, t)$. In other words $R' = ROT(y_1, \eta_1(l_1, t))$

$$R' = \begin{bmatrix} C(\eta_1(l_1, t)) & 0 & S(\eta_1(l_1, t)) \\ 0 & 1 & 0 \\ -S(\eta_1(l_1, t)) & 0 & C(\eta_1(l_1, t)) \end{bmatrix}$$

Therefore, the complete expression for R_2^0 becomes

$$R_2^0 = \begin{bmatrix} C\eta_1 & S\eta_1 S\theta_2 & S\eta_1 C\theta_2 \\ S\theta_1 S\eta_1 & C\theta_1 C\theta_2 - S\theta_1 C\eta_1 S\theta_2 & -C\theta_1 S\theta_2 - S\theta_1 C\eta_1 C\theta_2 \\ -C\theta_1 S\eta_1 & S\theta_1 C\theta_2 + C\theta_1 C\eta_1 S\theta_2 & C\theta_1 C\eta_1 C\theta_2 - S\theta_1 S\theta_2 \end{bmatrix}$$

note $\eta_1 \equiv \eta_1(l_1, t)$.

A similar matrix representation is also required to properly develop the kinetic energy expressions for the case when the payload is grasped eccentrically. This situation has been represented in model TTEL by placing a point mass at a distance from the end of link two, thus simulating an eccentric grasp (see fig.4).

Therefore, the required rotation matrix $R'' \equiv ROT(y_2, \eta_2(l_2, t))$ can be defined as follows:

$$R'' = \begin{bmatrix} C(\eta_2(l_2, t)) & 0 & S(\eta_2(l_2, t)) \\ 0 & 1 & 0 \\ -S(\eta_2(l_2, t)) & 0 & C(\eta_2(l_2, t)) \end{bmatrix}$$

R'' permits the calculation of the rotation matrix R_3^0 that defines the re-orientation of the end-effector coordinate frame $x_3y_3z_3$ relative to the inertial frame of reference XYZ due to the motion of each joint angle and the torsional displacements in each link.

$$R_3^0 = R_1^0 R' R_2^1 R''$$

$$R_3^0 = \begin{bmatrix} 1 - \eta_1 \eta_2 C \theta_2 & \eta_1 S \theta_2 & \eta_2 + \eta_1 \eta_2 C \theta_2 \\ S \theta_1 \eta_1 + \eta_2 S(\theta_1 + \theta_2) & C(\theta_1 + \theta_2) & \eta_1 \eta_2 S \theta_1 - S(\theta_1 + \theta_2) \\ -C \theta_1 \eta_1 - \eta_2 C(\theta_1 + \theta_2) & S(\theta_1 + \theta_2) & -\eta_1 \eta_2 C \theta_1 + C(\theta_1 + \theta_2) \end{bmatrix}$$

where $\eta_1 \equiv \eta_1(l_1, t)$ and $\eta_2 \equiv \eta_2(l_2, t)$.

At this point, the development of the kinetic energy due to each link's motion may begin. As shown earlier, a vector \vec{r}_{p1} is defined to extend from the origin of the first

link's coordinate frame to an arbitrary point in the first link. Relating this vector to the inertial frame through R_1^0 yields

$$\begin{aligned}\vec{r}_{p1}^\circ &= R_1^0 \vec{r}_{p1} \\ \vec{v}_{p1}^\circ &= \dot{R}_1^0 \vec{r}_{p1} = \begin{bmatrix} 0 \\ -y_1 \dot{\theta}_1 S\theta_1 \\ y_1 \dot{\theta}_1 C\theta_1 \end{bmatrix}\end{aligned}$$

Similarly, the angular velocity $\dot{\eta}_1(y_1, t)$ due to link one's torsional vibration is related to the inertial frame through R_1^0

$$\dot{\eta}_1^\circ(y_1, t) = R_1^0 \dot{\eta}_1 = \begin{bmatrix} 1 & 0 & 0 \\ 0 & C\theta_1 & -S\theta_1 \\ 0 & S\theta_1 & C\theta_1 \end{bmatrix} \begin{bmatrix} 0 \\ \dot{\eta}_1(y_1, t) \\ 0 \end{bmatrix}$$

$$\ddot{\eta}_1^\circ(y_1, t) = \begin{bmatrix} 0 \\ C\theta_1 \dot{\eta}_1(y_1, t) \\ S\theta_1 \dot{\eta}_1(y_1, t) \end{bmatrix}$$

Thus,

$$\begin{aligned}T_{link1} &= \frac{1}{2} \int_0^{l_1} \rho(y_1) A(y_1) (\vec{v}_{p1}^\circ \cdot \vec{v}_{p1}^\circ) dy_1 + \frac{1}{2} \int_0^{l_1} I(y_1) (\dot{\eta}_1^\circ(y_1, t) \cdot \dot{\eta}_1^\circ(y_1, t)) dy_1 \\ T_{link1} &= \frac{1}{2} A_1 \rho \dot{\theta}_1^2 \int_0^{l_1} y_1^2 dy_1 + \frac{1}{2} I \dot{\Lambda}^2 \int_0^{l_1} \Gamma_1^2(y_1) dy_1\end{aligned}$$

assuming a one mode approximation.

The expression for the kinetic energy of the second link also follows the example set by the earlier derivation.

$$\vec{r}_{p2}^{\circ} = R_1^0 \vec{r}_{e1} + R_2^0 \vec{r}_{p2}$$

$$\vec{v}_{p2}^{\circ} = \dot{R}_1^0 \vec{r}_{e1} + \dot{R}_2^0 \vec{r}_{p2}$$

$$\vec{v}_{p2}^{\circ} = \left\{ \begin{array}{l} y_2 (\eta_1 \dot{\theta}_2 C \theta_2 + \dot{\eta} S \theta_2) \\ -\dot{\theta}_1 l_1 S \theta_1 - y_2 (\dot{\theta}_1 S(\theta_1 + \theta_2) + \dot{\theta}_2 S(\theta_1 + \theta_2) - S \theta_1 \dot{\eta}_1 S \theta_2 \eta_1) \\ \dot{\theta}_1 l_1 C \theta_1 + y_2 (\dot{\theta}_1 C(\theta_1 + \theta_2) + \dot{\theta}_2 C(\theta_1 + \theta_2) - \dot{\eta}_1 C \theta_1 S \theta_2 \eta_1) \end{array} \right\}$$

... again where $\eta_1 = \eta_1(l_1, t)$ and $\dot{\eta}_1 = \dot{\eta}_1(l_1, t)$.

Furthermore, the angular velocity due to the torsional vibration of link two can also be related to the inertial frame of reference as follows

$$\dot{\vec{\eta}}_2^{\circ}(y_2, t) = R_1^0 \dot{\vec{\eta}}_1 + R_2^0 \dot{\vec{\eta}}_2$$

$$= \left[\begin{array}{l} \eta_1(l_1, t) \dot{\eta}_2(y_2, t) S \theta_2 \\ C(\theta_1 + \theta_2) \dot{\eta}_2(y_2, t) + C \theta_1 \dot{\eta}_1(l_1, t) \\ S(\theta_1 + \theta_2) \dot{\eta}_2(y_2, t) + S \theta_1 \dot{\eta}_1(l_1, t) \end{array} \right]$$

And so,

$$T_{link2} = \frac{1}{2} \int_0^{l_2} \rho(y_2) A_2(y_2) (\vec{v}_{p2}^{\circ} \bullet \vec{v}_{p2}^{\circ}) dy_2 + \frac{1}{2} \int_0^{l_2} I(y_2) (\dot{\vec{\eta}}_2^{\circ}(y_2, t) \bullet \dot{\vec{\eta}}_2^{\circ}(y_2, t)) dy_2$$

In model TT, the payload is grasped at its center of gravity and is therefore represented as a rigid body mounted at the end of link two. Hence, the kinetic energy

due to the motion of the payload must account for the movement of its center of gravity (developed in Model RR) and the body's rotation about the center of gravity due to the twist at the end of link two.

$$T_{payload\ rotation} = \frac{1}{2} I_{pL} \dot{\eta}_2^{\circ}(l_2, t) \bullet \dot{\eta}_2^{\circ}(l_2, t)$$

However, if the payload is not grasped exactly at its center of gravity, as shown in fig. 4, then the kinetic energy due to the motion of the payload is found as follows

$$\vec{r}_{pL}^{\circ} = R_1^0 \vec{r}_{e1} + R_2^0 \vec{r}_{e2} + R_3^0 \vec{e}$$

where

$$\vec{e} = \begin{bmatrix} e \\ 0 \\ e \end{bmatrix}$$

$$\vec{v}_{pL}^{\circ} = \dot{R}_1^0 \vec{r}_{e1} + \dot{R}_2^0 \vec{r}_{e2} + \dot{R}_3^0 \vec{e}$$

$$T_{payload} = \frac{1}{2} M_{pL} \vec{v}_{pL}^{\circ} \bullet \vec{v}_{pL}^{\circ}$$

The gravitational energy expressions previously obtained in model RR also apply to these two models, however the elastic potential energy levels due to link torsion must now be included as well.

$$V_{link1,elas.} = \frac{1}{2} \int_0^{l_1} GJ(y_1) (\partial \eta_1(y_1, t) / \partial y_1)^2 dy_1$$

$$= \frac{1}{2} GJ \Lambda^2(t) \int_0^{l_1} (\Gamma_1'(y_1))^2 dy_1$$

$$V_{link2,elas.} = \frac{1}{2} \int_0^{l_2} GJ(y_2) (\partial \eta_2(y_2, t) / \partial y_2)^2 dy_2$$

$$= \frac{1}{2} GJ \alpha^2(t) \int_0^{l_2} (\lambda'_1(y_2))^2 dy_2$$

assuming uniform links.

Finally, the additional gravitational potential energy due to an eccentrically grasped payload is easily included as

$$V_{pL\ grav.} = M_{pL} g [l_1 S \theta_1 + l_2 S(\theta_1 + \theta_2) + e(C(\theta_1 + \theta_2) - \eta_2 \eta_1 C \theta_1 - C \theta_1 \eta_1 - \eta_2 C(\theta_1 + \theta_2))]$$

... where $\eta_1 = \eta_1(l_1, t)$ and $\eta_2 = \eta_2(l_2, t)$

The Lagrangian for models TT and TTEL is then formed as the difference between the sum of the kinetic and the sum of the potential energy expressions pertaining to each. Unlike the previous derivation of model RR, the current two models incorporate four degrees of freedom each. Therefore, models TT and TTEL are both governed by a set of four coupled, second order, nonlinear differential equations of motion - which are derived as follows :

$$d/dt \{ \partial L / \partial \dot{\theta}_1 \} - \partial L / \partial \theta_1 = T_1$$

$$d/dt \{ \partial L / \partial \dot{\theta}_2 \} - \partial L / \partial \theta_2 = T_2$$

$$d/dt \{ \partial L / \partial \dot{\Lambda}_1 \} - \partial L / \partial \Lambda_1 = 0$$

$$d/dt \{ \partial L / \partial \dot{\alpha}_1 \} - \partial L / \partial \alpha_1 = 0$$

The resulting equations of motion are listed below in an abbreviated format. The equations can be obtained in explicit form by referring to the discussion in Appendix

B.

$$\begin{bmatrix} I'_{11} & I'_{12} & I'_{13} & I'_{14} \\ I'_{21} & I'_{22} & I'_{23} & I'_{24} \\ I'_{31} & I'_{32} & I'_{33} & I'_{34} \\ I'_{41} & I'_{42} & I'_{43} & I'_{44} \end{bmatrix} \begin{bmatrix} \ddot{\theta}_1 \\ \ddot{\theta}_2 \\ \ddot{\Lambda} \\ \ddot{\alpha} \end{bmatrix} + \begin{bmatrix} \dot{\theta}_1 B'_{11} \\ \dot{\theta}_2 B'_{21} \\ \dot{\Lambda} B'_{31} \\ \dot{\alpha} B'_{41} \end{bmatrix} + \begin{bmatrix} C'_{11} \\ C'_{21} \\ C'_{31} \\ C'_{41} \end{bmatrix} = \begin{bmatrix} T_1 \\ T_2 \\ 0 \\ 0 \end{bmatrix}$$

The form in which these equations appear will also be used in the following cases.

Note that the first coefficient matrix on the far left is equivalent to the system's inertia matrix. The second matrix contains the second derivatives of the system's generalized time coordinates. The third matrix from the left contains the system's complex damping terms, its Coriolis and centripetal terms, and various velocity cross-product coupling terms. The fourth matrix contains the system's stiffness terms, and its gravitational terms. Finally, the far right-hand matrix contains the system forcing functions, which in all cases are the motor torques applied at the first and second revolute joints.

2.3 Models TTFEL and TTFTEL

The problem defined by model TTEL is extended in model TTFEL by permitting lateral second link flexure to occur, and model TTFTEL takes this one step further by allowing lateral flexibility in both of the manipulator's links. As was done earlier to define torsional link vibrations, these lateral flexural displacements are represented through the method of assumed modes in a one mode approximation. Moreover, the

effect that the added degrees of freedom have upon the orientation of link coordinate frames is expressed through additional - and more complex - “special” rotation matrices. (See fig.5 and fig.6).

Specifically, the lateral single-plane bending of link one is designated in model TTFEL as $w_1(y_1, t)$. The same motion of the second link is designated as $w_2(y_2, t)$ in both models TTFEL and TTFEL. Also, the single mode approximation of these displacements is

$$w_1(y_1, t) = \sum_{i=1}^{\infty} q_i(t) \psi_i(y_1) \approx q_1(t) \psi_1(y_1)$$

$$w_2(y_2, t) = \sum_{i=1}^{\infty} b_i(t) \epsilon_i(y_2) \approx b_1(t) \epsilon_1(y_2)$$

where $\psi_1(y_1)$ and $\epsilon_1(y_2)$ each represent the fundamental mode shape of a cantilever beam with payload in lateral vibration [13]. ie.

$$\psi_1(y) \equiv \epsilon_1(y) \equiv A \left\{ (\sinh \beta y - \sin \beta y) - \left[\frac{(\sin \beta l + \sinh \beta l)}{(\cos \beta l + \cosh \beta l)} \right] (\cosh \beta y - \cos \beta y) \right\}$$

where $\beta^4 = \rho A_1 \omega^2 / EI$ and A is an arbitrary constant.

Just as rotation matrices were employed in the kinematic description of models TT and TTEL to account for coordinate frame rotations as a result of torsional link flexure, “special” rotation matrices are also employed in both of these models to describe the coordinate frame re-orientations due to the lateral flexure at the link ends.

Specifically, due to the additional lateral flexure at the very end of link two, the end-effector coordinate frame $x_3 y_3 z_3$ rotates through a small angle ζ_2 about axis x_2 .

This rotation is *in addition* to the rotation through small angle $\eta_2(l_2, t)$ about axis y_2 that the end-effector's coordinate frame already experiences due to the link's torsional vibration (see figs. 7 and 7.1).

This small angle ζ_2 is defined as follows

$$\zeta_2 \approx \left[\frac{\partial w_2(y_2, t)}{\partial y_2} \right]_{y=l_2}$$

which in a single-mode approximation becomes

$$\zeta_2 = \sum_{i=1}^{\infty} b_i(t) \epsilon'_i(l_2) \approx b_1(t) \epsilon'_1(l_2)$$

Thus, the matrix R_3^0 used to determine the payload kinetic energy for the case described by model TTFEL becomes

$$R_3^0 = R_1^0 R' R_2^1 R'' R'''$$

where

$$R_1^0 \equiv ROT(x_1, \theta_1)$$

$$R' \equiv ROT(y_1, \eta_1(l_1, t))$$

$$R_2^1 \equiv ROT(x_2, \theta_2)$$

$$R'' \equiv ROT(x_2, \zeta_2)$$

$$R''' \equiv ROT(y_2, \eta_2(l_2, t))$$

and where

$$R'' = \begin{bmatrix} 1 & 0 & 0 \\ 0 & C\zeta_2 & -S\zeta_2 \\ 0 & S\zeta_2 & C\zeta_2 \end{bmatrix}$$

ie. $R'' \equiv ROT(x_2, \zeta_2)$.

Employing small angle approximations, R_3^0 becomes

$$R_3^0 \approx \begin{bmatrix} 1 - \eta_2\eta_1C(\theta_1 + \theta_2 + \zeta_2) & \eta_1S(\theta_2 + \zeta_2) & S\eta_2 + C\eta_2\eta_1C(\theta_1 + \theta_2 + \zeta_2) \\ \eta_1S\theta_1 + \eta_2S(\theta_1 + \theta_2 + \zeta_2) & C(\zeta_2 + \theta_1 + \theta_2) & \eta_1S\theta_1S\eta_2 - C\eta_2S(\theta_1 + \theta_2 + \zeta_2) \\ -\eta_1C\theta_1 - \eta_2C(\theta_1 + \theta_2 + \zeta_2) & S(\zeta_2 + \theta_1 + \theta_2) & C\eta_2C(\theta_1 + \theta_2 + \zeta_2) - \eta_1C\theta_1S\eta_2 \end{bmatrix}$$

It is also noted that the lateral flexibility of link two dictates no change in the matrix R_2^0 as it is defined in model TTEL. On the contrary, the matrix R_2^0 used in the kinematic description of model TTFEL differs for the fact that the effects of first link lateral flexure must now be included in it in order to express the re-orientation of the second link coordinate frame. In other words, the second link coordinate frame not only rotates through small angle $\eta_1(l_1, t)$ about axis y_1 , but it also rotates through small angle ζ_1 about axis x_1 due to the flexure $w_1(l_1, t)$ at the end of link one (see figs. 8 and 8.1).

This small angle is defined as

$$\zeta_1 \approx \left[\frac{\partial w_1(y_1, t)}{\partial y_1} \right]_{y_1=l_1}$$

$$\zeta_1 = \sum_{j=1}^{\infty} q_j(t) \psi'_j(l_1) \approx q_1(t) \psi'_1(l_1)$$

As a result, R_2^0 for model TTFEL becomes

$$R_2^0 = R_1^0 R' R'' R_2^1$$

where

$$R_1^0 \equiv ROT(x_1, \theta_1)$$

$$R' \equiv ROT(x_1, \zeta_1)$$

$$R'' \equiv ROT(y_1, \eta_1(l_1, t))$$

$$R_2^1 \equiv ROT(x_2, \theta_2)$$

and

$$R' = \begin{bmatrix} 1 & 0 & 0 \\ 0 & C\zeta_1 & -S\zeta_1 \\ 0 & S\zeta_1 & C\zeta_1 \end{bmatrix}$$

Therefore,

$$R_2^0 = \begin{bmatrix} 1 & \eta_1 S \theta_2 & \eta_1 C \theta_2 \\ S(\theta_1 + \zeta_1) \eta_1 & C\beta & -S\beta \\ -C(\theta_1 + \zeta_1) \eta_1 & S\beta & C\beta \end{bmatrix}$$

where $\beta = (\theta_1 + \theta_2 + \zeta_1)$ and $\eta_1 = \eta_1(l_1, t)$.

Moreover, an additional consequence of the lateral flexibility of the first link is that the rotation matrix R_3^0 used in model TTFEL becomes even more complex :

$$R_3^0 = R_1^0 R' R'' R_2^1 R''' R''''$$

where

$$R_1^0 \equiv ROT(x_1, \theta_1)$$

$$R' \equiv ROT(x_1, \zeta_1)$$

$$R'' \equiv ROT(y_1, \eta_1(l_1, t))$$

$$R_2^1 \equiv ROT(x_2, \theta_2)$$

$$R''' \equiv ROT(x_2, \zeta_2)$$

$$R'''' \equiv ROT(y_2, \eta_2(l_1, t))$$

Therefore,

$$R_3^0 \approx \begin{bmatrix} C\eta_2 - S\eta_2\eta_1C(\theta_2 + \zeta_2) & \eta_1S(\theta_2 + \zeta_2) & S\eta_2 + C\eta_2\eta_1C(\theta_2 + \zeta_2) \\ C\eta_2\eta_1S(\theta_1 + \zeta_1) + S\eta_2S(\beta + \zeta_2) & C(\beta + \zeta_2) & S\eta_2\eta_1S(\theta_1 + \zeta_1) - C\eta_2S(\beta + \zeta_2) \\ -C\eta_2\eta_1C(\theta_1 + \zeta_1) - S\eta_2C(\beta + \zeta_2) & S(\beta + \zeta_2) & -S\eta_2\eta_1C(\theta_1 + \zeta_1) + C\eta_2C(\beta + \zeta_2) \end{bmatrix}$$

... assuming small angle approximations.

At this point, the kinematic descriptions for both models TTFEL and TTFEL is complete, and it is now possible to develop the proper kinetic energy expressions needed for the Lagrangian of each. Specifically, for model TTFEL

$$\tilde{r}_{p1}^\circ = R_1^0 \tilde{r}_{p1}$$

$$\tilde{v}_{p1}^\circ = \dot{R}_1^0 \tilde{r}_{p1}$$

$$T_{link1} = \frac{1}{2} \int_0^{l_1} \rho(y_1) A(y_1) (\tilde{v}_{p1}^\circ \bullet \tilde{v}_{p1}^\circ) dy_1 + \frac{1}{2} \int_0^{l_1} I(y_1) (\dot{\tilde{\eta}}_1^\circ(y_1, t) \bullet \dot{\tilde{\eta}}_1^\circ(y_1, t)) dy_1$$

and

$$T_{link1} = \frac{1}{2} A_1 \rho \dot{\theta}_1^2 \int_0^{l_1} y_1^2 dy_1 + \frac{1}{2} I \dot{\Lambda}^2 \int_0^{l_1} \Gamma_1^2(y_1) dy_1$$

assuming a one mode approximation.

Moreover, the kinetic energy for the second link becomes

$$\begin{aligned}\vec{r}_{p2}^{\circ} &= R_1^0 \vec{r}_{e1} + R_2^0 \vec{r}_{p2} \\ \vec{v}_{p2}^{\circ} &= \dot{R}_1^0 \vec{r}_{e1} + \dot{R}_2^0 \vec{r}_{p2} + R_1^0 \dot{\vec{r}}_{p2}\end{aligned}$$

where

$$\vec{r}_{p2} = \begin{Bmatrix} 0 \\ y_2 \\ w_2(y_2, t) \end{Bmatrix} \quad \dot{\vec{r}}_{p2} = \begin{Bmatrix} 0 \\ 0 \\ \dot{w}_2(y_2, t) \end{Bmatrix}$$

$$\vec{v}_{p2}^{\circ} = \begin{Bmatrix} \eta_1 \dot{w}_2(y_2, t) C \theta_2 + y_2 (\eta_1 \dot{\theta}_2 C \theta_2 + \dot{\eta}_1 S \theta_2) + w_2(y_2, t) (\dot{\eta}_1 C \theta_2 - \dot{\theta}_2 S \theta_2 \eta_1) \\ -l_1 \dot{\theta}_1 S \theta_1 - S(\theta_1 + \theta_2) \dot{w}_2(y_2, t) - y_2 (\dot{\theta}_1 + \dot{\theta}_2) S(\theta_1 + \theta_2) - w_2(y_2, t) (\dot{\theta}_1 + \dot{\theta}_2) C(\theta_1 + \theta_2) \\ l_1 \dot{\theta}_1 C \theta_1 + C(\theta_1 + \theta_2) \dot{w}_2(y_2, t) + y_2 (\dot{\theta}_1 + \dot{\theta}_2) C(\theta_1 + \theta_2) - w_2(y_2, t) (\dot{\theta}_1 + \dot{\theta}_2) S(\theta_1 + \theta_2) \end{Bmatrix}$$

(note $\eta_1 = \eta_1(l_1, t)$) and so,

$$T_{link2} = \frac{1}{2} \int_0^{l_2} \rho(y_2) A_2(y_2) (\vec{v}_{p2}^{\circ} \bullet \vec{v}_{p2}^{\circ}) dy_2 + \frac{1}{2} \int_0^{l_2} I(y_2) (\dot{\vec{\eta}}_2^{\circ}(y_2, t) \bullet \dot{\vec{\eta}}_2^{\circ}(y_2, t)) dy_2$$

The total kinetic energy produced by the motion of a *properly* grasped payload includes the energy associated with the motion of the load's center of gravity, and the energy of the two rigid body rotations the load experiences due to the lateral and torsional vibrations at the end of link two (see fig. 9). In other words,

$$\vec{r}_{pL}^{\circ} = R_1^0 \vec{r}_{e1} + R_2^0 \vec{r}_{e2}$$

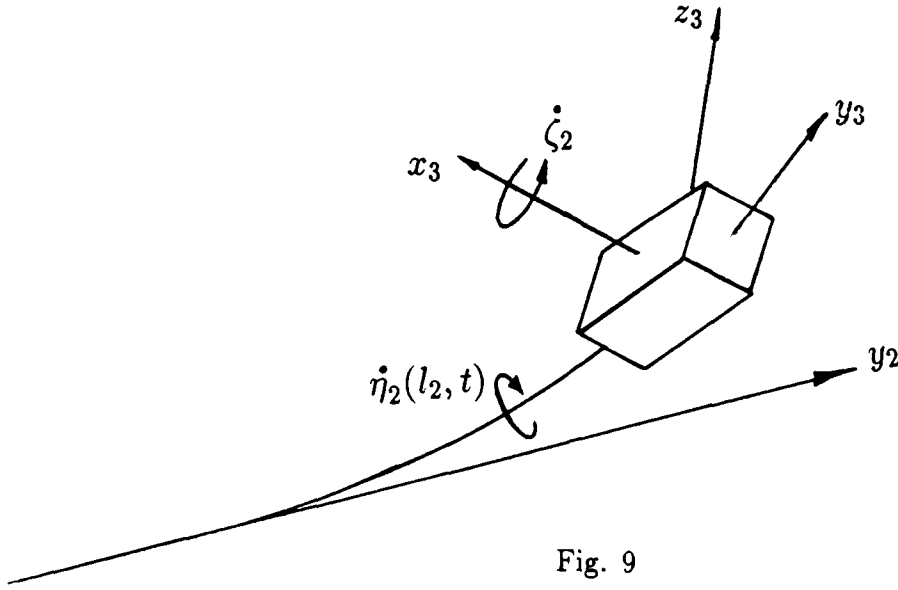


Fig. 9

$$\vec{v}_{pL}^{\circ} = \dot{R}_1^0 \vec{r}_{e1} + \dot{R}_2^0 \vec{r}_{e2} + R_2^0 \dot{\vec{r}}_{e2}$$

and therefore the total kinetic energy associated with the motion of the payload becomes

$$T_{payload} = \frac{1}{2} M_{pL} \vec{v}_{pL}^{\circ} \cdot \vec{v}_{pL}^{\circ} + \frac{1}{2} I_{y_3} \dot{\eta}_2^{\circ}(l_2, t) \cdot \dot{\eta}_2^{\circ}(l_2, t) + \frac{1}{2} I_{x_3} \left(\partial^2 \zeta_2(l_2, t) / \partial y_2 \partial t \right)^2$$

$$T_{payload} = \frac{1}{2} M_{pL} \vec{v}_{pL}^{\circ} \cdot \vec{v}_{pL}^{\circ} + \frac{1}{2} I_{y_3} \dot{\alpha}^2(t) \lambda^2(l_2) + \frac{1}{2} I_{x_3} \dot{b}^2(t) \epsilon' \epsilon'$$

where I_{y_3} and I_{x_3} are equivalent to the moments of inertia of the payload about axis y_3 and x_3 , respectively (see fig.9).

On the other hand, when the payload is grasped eccentrically, the complete kinetic energy expression is conveniently found through the use of rotation matrix R_3^0 (recall that an eccentric load has been modeled as a point mass displaced a distance \vec{e} from the origin of the end-effector coordinate frame).

$$\vec{r}_{pL}^{\circ} = R_1^0 \vec{r}_{e1} + R_2^0 \vec{r}_{e2} + R_3^0 \vec{e}$$

$$\vec{v}_{pL}^{\circ} = \dot{R}_1^0 \vec{r}_{e1} + \dot{R}_2^0 \vec{r}_{e2} + R_2^0 \dot{\vec{r}}_{e2} + \dot{R}_3^0 \vec{e}$$

$$T_{payload} = \frac{1}{2} M_{pL} \vec{v}_{pL}^{\circ} \bullet \vec{v}_{pL}^{\circ}$$

This step completes the kinetic energy formulation for model TTFEL. For model TTFEL, the total system kinetic energy expressions are as follows

$$\vec{r}_{p1}^{\circ} = R_1^0 \vec{r}_{p1}$$

$$\vec{v}_{p1}^{\circ} = \dot{R}_1^0 \vec{r}_{p1} + R_1^0 \dot{\vec{r}}_{p1}$$

where

$$\vec{r}_{p1} = \begin{Bmatrix} 0 \\ y_1 \\ w_1(y_1, t) \end{Bmatrix} \quad \dot{\vec{r}}_{p1} = \begin{Bmatrix} 0 \\ 0 \\ \dot{w}_1(y_1, t) \end{Bmatrix}$$

... and

$$\vec{v}_{p1}^{\circ} = \begin{Bmatrix} 0 \\ -\dot{\theta}_1 (y_1 S \theta_1 + w_1(y_1, t) C \theta_1) - \dot{w}_1(y_1, t) S \theta_1 \\ \dot{\theta}_1 (y_1 C \theta_1 - w_1(y_1, t) S \theta_1) + \dot{w}_1(y_1, t) C \theta_1 \end{Bmatrix}$$

$$T_{link1} = \frac{1}{2} \int_0^{l_1} \rho(y_1) A(y_1) (\vec{v}_{p1}^{\circ} \bullet \vec{v}_{p1}^{\circ}) dy_1 + \frac{1}{2} \int_0^{l_1} I(y_1) (\ddot{\eta}_1^{\circ}(y_1, t) \bullet \ddot{\eta}_1^{\circ}(y_1, t)) dy_1$$

Furthermore, for the second link

$$\vec{r}_{p2}^{\circ} = R_1^0 \vec{r}_{e1} + R_2^0 \vec{r}_{p2}$$

$$\vec{v}_{p2}^{\circ} = \dot{R}_1^0 \vec{r}_{e1} + R_1^0 \dot{\vec{r}}_{e1} + \dot{R}_2^0 \vec{r}_{p2} + R_2^0 \dot{\vec{r}}_{p2}$$

$$\vec{v}_{p2}^{\circ} = \left\{ \begin{array}{l} \eta_1 C \theta_2 \dot{w}_2(y_2, t) + y_2(\eta_1 \dot{\theta}_2 C \theta_2 + \dot{\eta}_1 S \theta_2) + w_2(y_2, t)(\dot{\eta}_1 C \theta_2 - \dot{\theta}_2 \eta_1 S \theta_2) \\ -y_2 \dot{\beta} S \beta - w_2(y_2, t) \dot{\beta} C \beta - \dot{w}_2(y_2, t) S \beta - \dot{\theta}_1(l_1 S \theta_1 + w_1(l_1, t) C \theta_1) - S \theta_1 \dot{w}_1(l_1, t) \\ y_2 \dot{\beta} C \beta - w_2(y_2, t) \dot{\beta} S \beta + \dot{w}_2(y_2, t) C \beta + \dot{\theta}_1(l_1 C \theta_1 - w_1(l_1, t) S \theta_1) + C \theta_1 \dot{w}_1(l_1, t) \end{array} \right\}$$

where $\eta_1 = \eta_1(l_1, t)$. Thus,

$$T_{link2} = \frac{1}{2} \int_0^{l_2} \rho(y_2) A_2(y_2) (\vec{v}_{p2}^{\circ} \bullet \vec{v}_{p2}^{\circ}) dy_2 + \frac{1}{2} \int_0^{l_2} I(y_2) (\ddot{\eta}_2^{\circ}(y_2, t) \bullet \ddot{\eta}_2^{\circ}(y_2, t)) dy_2$$

Finally, the expression for the kinetic energy due to the motion of the payload follows the example set in the development of model TTFEL, although in the present case it is emphasized that the rotation matrices include the effects of first link lateral flexure.

In other words, for a properly grasped payload

$$\vec{r}_{pL}^{\circ} = R_1^0 \vec{r}_{e1} + R_2^0 \vec{r}_{e2}$$

$$\vec{v}_{pL}^{\circ} = \dot{R}_1^0 \vec{r}_{e1} + R_1^0 \dot{\vec{r}}_{e1} + \dot{R}_2^0 \vec{r}_{e2} + R_2^0 \dot{\vec{r}}_{e2}$$

$$T_{payload} = \frac{1}{2} M_{pL} \vec{v}_{pL}^{\circ} \bullet \vec{v}_{pL}^{\circ} + \frac{1}{2} I_{y_3} \dot{\eta}_2^{\circ}(l_2, t) \bullet \dot{\eta}_2^{\circ}(l_2, t) + \frac{1}{2} I_{x_3} (\partial^2 \zeta_2(l_2, t) / \partial y_2 \partial t)^2$$

$$T_{payload} = \frac{1}{2} M_{pL} \vec{v}_{pL}^{\circ} \bullet \vec{v}_{pL}^{\circ} + \frac{1}{2} I_{y_3} \dot{\alpha}^2(t) \lambda^2(l_2) + \frac{1}{2} I_{x_3} \dot{b}^2(t) \epsilon' \epsilon'$$

And for an eccentrically grasped payload

$$\vec{v}_{pL}^{\circ} = \dot{R}_1^0 \vec{r}_{e1} + R_1^0 \dot{\vec{r}}_{e1} + \dot{R}_2^0 \vec{r}_{e2} + R_2^0 \dot{\vec{r}}_{e2} + \dot{R}_3^0 \vec{e}$$

$$T_{payload} = \frac{1}{2} M_{pL} \vec{v}_{pL}^{\circ} \bullet \vec{v}_{pL}^{\circ}$$

With the kinetic energy expressions determined, the complete potential energy levels must now be evaluated in order to form each system's Lagrangian. The potential energy due to gravity remains virtually unchanged from the expression shown in model TTEL. However, the elastic potential energy due to lateral link flexure must now be accounted for as well as the elastic potential energy due to link torsion in both models TTFEL and TTFTEL.

Specifically, as a result of second link flexure in both models

$$V_{flex.link2} = \frac{1}{2} \int_0^{l_2} EI(y_2) \left(\partial^2 w_2(y_2, t) / \partial y_2^2 \right)^2 dy_2$$

$$V_{flex.link2} = \frac{1}{2} \int_0^{l_1} EI(y_2) \sum_{j=1}^{\infty} b_j(t) \epsilon_j''(y_2) \sum_{k=1}^{\infty} b_k(t) \epsilon_k''(y_2) dy_2$$

$$V_{flex.link2} \approx \frac{1}{2} EI b^2(t) \int_0^{l_2} (\epsilon_1''(y_2))^2 dy_2$$

assuming uniform links. Also, as a result of the lateral first link flexure included in model TTFTEL, the following elastic potential energy expression is obtained

$$V_{flex.link1} \approx \frac{1}{2} EI q^2(t) \int_0^{l_1} (\psi_1''(y_1))^2 dy_1$$

also assuming a uniform first link.

Therefore, the total elastic potential energy for model TTFEL is

$$V_{elastic} = \frac{1}{2} EI b^2(t) \int_0^{l_2} (\epsilon_1''(y_2))^2 dy_2$$

$$\begin{aligned}
& + \frac{1}{2} GJ\Lambda^2(t) \int_0^{l_1} (\Gamma'_1(y_1))^2 dy_1 \\
& + \frac{1}{2} GJ\alpha^2(t) \int_0^{l_2} (\lambda'_1(y_1))^2 dy_2
\end{aligned}$$

and the total elastic potential energy for model TTFEL is

$$\begin{aligned}
V_{elastic} &= \frac{1}{2} EIq^2(t) \int_0^{l_1} (\psi''_1(y_1))^2 dy_1 \\
& + \frac{1}{2} EIt^2(t) \int_0^{l_2} (\epsilon''_1(y_2))^2 dy_2 \\
& + \frac{1}{2} GJ\Lambda^2(t) \int_0^{l_1} (\Gamma'_1(y_1))^2 dy_1 \\
& + \frac{1}{2} GJ\alpha^2(t) \int_0^{l_2} (\lambda'_1(y_1))^2 dy_2
\end{aligned}$$

Since the kinetic and potential energy levels have been completely expressed as a function of generalized coordinates with respect to an inertial frame of reference, the complete Lagrangian for each model is

$$L_{TTFEL} = T_{link1} + T_{link2} + T_{payload} - V_{elastic} - V_{gravity}$$

$$L_{TTFEL} = T_{link1} + T_{link2} + T_{payload} - V_{elastic} - V_{gravity}$$

The derivation of the set of governing differential equations of motion for both models is now possible. For model TTFEL, where there are five degrees of freedom, the following expressions are applied to the system Lagrangian L_{TTFEL}

$$d/dt \{ \partial L / \partial \dot{\theta}_1 \} - \partial L / \partial \theta_1 = T_1$$

$$d/dt \{ \partial L / \partial \dot{\theta}_2 \} - \partial L / \partial \theta_2 = T_2$$

$$d/dt \{ \partial L / \partial \dot{\Lambda}_1 \} - \partial L / \partial \Lambda_1 = 0$$

$$d/dt \{ \partial L / \partial \dot{\alpha}_1 \} - \partial L / \partial \alpha_1 = 0$$

$$d/dt \{ \partial L / \partial \dot{b}_1 \} - \partial L / \partial b_1 = 0$$

An abbreviated listing of the five resulting coupled, second order, nonlinear differential equations is shown below. Note that the equations may be obtained in their full form by referring to Appendix B.

$$\begin{bmatrix} I_{11i} & I_{12i} & I_{13i} & I_{14i} & I_{15i} \\ I_{21i} & I_{22i} & I_{23i} & I_{24i} & I_{25i} \\ I_{31i} & I_{32i} & I_{33i} & I_{34i} & I_{35i} \\ I_{41i} & I_{42i} & I_{43i} & I_{44i} & I_{45i} \\ I_{51i} & I_{52i} & I_{53i} & I_{54i} & I_{55i} \end{bmatrix} \begin{bmatrix} \bar{\theta}_1 \\ \bar{\theta}_2 \\ \bar{\Lambda}_1 \\ \bar{\alpha}_1 \\ \bar{b}_1 \end{bmatrix} + \begin{bmatrix} \dot{\theta}_1 B_{11i} \\ \dot{\theta}_2 B_{21i} \\ \dot{\Lambda}_1 B_{31i} \\ \dot{\alpha}_1 B_{41i} \\ \dot{b}_1 B_{51i} \end{bmatrix} + \begin{bmatrix} C_{11i} \\ C_{21i} \\ C_{31i} \\ C_{41i} \\ C_{51i} \end{bmatrix} = \begin{bmatrix} T_1 \\ T_2 \\ 0 \\ 0 \\ 0 \end{bmatrix}$$

For model TTFEL, the application of the following relationships to the total system Lagrangian L_{TTFEL} will yield the complete set of equations of motion governing this six degree of freedom problem.

$$d/dt \{ \partial L / \partial \dot{\theta}_1 \} - \partial L / \partial \theta_1 = T_1$$

$$d/dt \{ \partial L / \partial \dot{\theta}_2 \} - \partial L / \partial \theta_2 = T_2$$

$$d/dt \{ \partial L / \partial \dot{\Lambda}_1 \} - \partial L / \partial \Lambda_1 = 0$$

$$d/dt \{ \partial L / \partial \dot{\alpha}_1 \} - \partial L / \partial \alpha_1 = 0$$

$$d/dt \{ \partial L / \partial \dot{q}_1 \} - \partial L / \partial q_1 = 0$$

$$d/dt \{ \partial L / \partial \dot{b}_1 \} - \partial L / \partial b_1 = 0$$

As before, an abbreviated listing of these equations is shown below, and the full listing may be obtained by referring to Appendix B.

$$\begin{bmatrix} I_{11} & I_{12} & I_{13} & I_{14} & I_{15} & I_{16} \\ I_{21} & I_{22} & I_{23} & I_{24} & I_{25} & I_{26} \\ I_{31} & I_{32} & I_{33} & I_{34} & I_{35} & I_{36} \\ I_{41} & I_{42} & I_{43} & I_{44} & I_{45} & I_{46} \\ I_{51} & I_{52} & I_{53} & I_{54} & I_{55} & I_{56} \\ I_{61} & I_{62} & I_{63} & I_{64} & I_{65} & I_{66} \end{bmatrix} \begin{bmatrix} \ddot{\theta}_1 \\ \ddot{\theta}_2 \\ \ddot{\Lambda}_1 \\ \ddot{\alpha}_1 \\ \ddot{q}_1 \\ \ddot{b}_1 \end{bmatrix} + \begin{bmatrix} \dot{\theta}_1 B_{11} \\ \dot{\theta}_2 B_{21} \\ \dot{\Lambda}_1 B_{31} \\ \dot{\alpha}_1 B_{41} \\ \dot{q}_1 B_{51} \\ \dot{b}_1 B_{61} \end{bmatrix} + \begin{bmatrix} C_{11} \\ C_{21} \\ C_{31} \\ C_{41} \\ C_{51} \\ C_{61} \end{bmatrix} = \begin{bmatrix} T_1 \\ T_2 \\ 0 \\ 0 \\ 0 \\ 0 \end{bmatrix}$$

Chapter 3

Control

The basic objective of a manipulator control scheme is to move the robot arm from an initial position to a desired final position and configuration in an allotted period of time. Once this is achieved, another control scheme is usually utilized to coordinate the movement of the manipulator's end-effector with the environment. In other words, robot arm control as a category includes gross motion control which moves the arm to the vicinity of some desired final position and orientation, and fine motion control which permits the arm to interact dynamically with the object of concern. The focus here is on gross motion control, which can be classified into three groups: joint motion control, resolved motion control (Cartesian space), and adaptive controls [6]. Under the heading of joint motion control fall such techniques as individual joint servomechanism control (IJC), variable structure control, nonlinear feedback,

and feedforward control, among others. Resolved motion control includes position, velocity, and acceleration control methods wherein the desired trajectory of the manipulator is translated from Cartesian world coordinates to joint coordinates through the governing Jacobian matrix. Adaptive control techniques rely on altering feedback signals on the basis of a comparison of the observed performance of the system to the performance of an idealized model.

These three categories include many more control techniques and variations of control schemes than is listed here. Even so, the individual joint control method (IJC) is still commonly applied. In the IJC approach, the motors at each joint are treated as independently functioning servos. Thus, this control method completely ignores the arm's nonlinear dynamics - which include the effects of Coriolis and centripetal forces. Yet, since these effects tend to be primarily velocity dependent, the IJC approach will work fairly well as long as the robot arm is not required to move at high speeds.

In this study, the IJC approach was first applied to the rigid two link model (Model RR) in the form of proportional plus tachometric feedback positional controllers at each joint (see fig. 10).

Note that the desired angular trajectory $\theta_d(t)$ was based upon either a "bang-bang" or a ramped motor acceleration/deceleration profile (see figs. 10.1 & 10.2).

$$\theta_{ramp}(t) = at^3/(3t_f) + \theta(0) \quad 0 \leq t \leq t_f/2$$

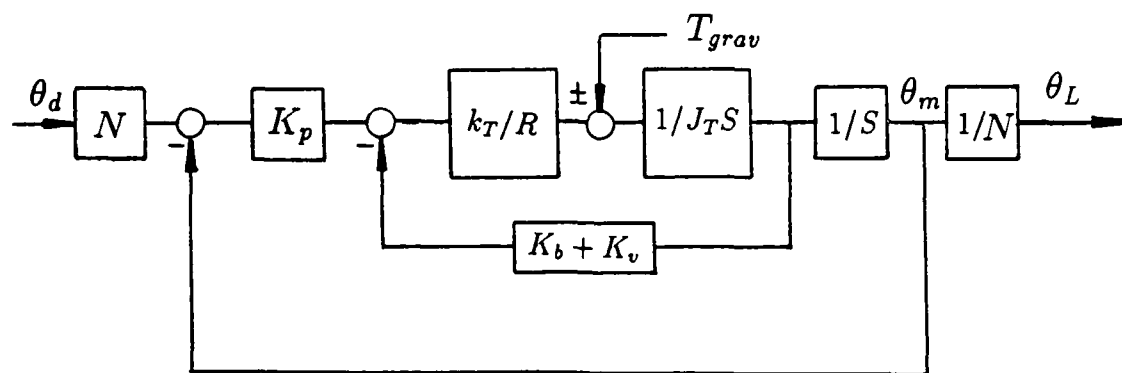


Fig. 10 Joint-Motor Servocontroller

$$\theta_{ramp}(t) = a \left\{ t^2 - t^3/(3t_f) - t t_f/2 + t_f^2/12 \right\} + \theta(0) \quad t_f/2 \leq t \leq t_f$$

$$\theta_{bb} = at^2/2 + \theta(0) \quad 0 \leq t \leq t_f/2$$

$$\theta_{bb} = at_f t - at^2/2 - at_f^2/4 + \theta(0) \quad t_f/2 \leq t \leq t_f$$

... where a is the maximum motor acceleration, t_f represents the target time, and $\theta(0)$ is the initial joint angle measure. Also, first estimates of the gain settings K_p and K_v were evaluated assuming a desired critically damped linear system response (thus placing a double pole at a position of $-P$ on the negative real axis of the system's root locus plot). Better gain estimates were subsequently found through trial and error runs of Model RR (higher gain levels were required for heavier payloads). Also, values of motor resistance, rotor inertia, maximum motor acceleration and torque, etc., were taken from manufacturer's specifications (Kollmorgan Co.).

In an effort to maximize each joint angle's acceleration $\ddot{\theta}_L$ through proper gearing,

gear ratios N were evaluated in the following manner:

$$J_T = J_m + \frac{1}{N^2} J_L$$

$$T_{gen} = (J_m + J_L/N^2)\ddot{\theta}_m$$

... which ignores the adverse effects of friction or the influence of gravity.

$$\ddot{\theta}_m = T_{gen}/J_T$$

$$\ddot{\theta}_L = \ddot{\theta}_m/N$$

$$\ddot{\theta}_L = T_{gen}/(NJ_T) = \frac{T_{gen}}{(NJ_m + J_L/N)}$$

Maximizing $\ddot{\theta}_L$ with respect to N

$$\frac{d\ddot{\theta}_L}{dN} = 0$$

$$\frac{-T_{gen}(J_m - J_L/N)}{(NJ_m + J_L/N)^2} = 0$$

$$N = \sqrt{J_L/J_m}$$

Finally, it was assumed that no lag existed in the feedback loops.

Once it was determined that the IJC control scheme could effectively govern the movement of the rigid two link model, it was applied to each of the flexible-link models in an effort to examine the limitations imposed by the link vibrations.

Chapter 4

Numerical Techniques

The development of the analytic form of each system model was a slow and extremely cumbersome task - given all of the hundreds of terms involved in each of the equations of motion. Hence, the algebraic symbolic manipulation language MACSYMA was employed to some extent to assist in the manipulations of each system's Lagrangian. Thereafter, all models were translated into FORTRAN algorithms and run on a VAX 8650 computer.

The objective of each program was to obtain the simultaneous solutions to each model's set of governing equations of motion. Note that in all cases, the set of differential equations was second order, nonlinear, and fully coupled. Moreover, due to the large disparity between the high natural frequencies of structural link vibrations

and the low frequency of each joint angle trajectory, the family of equations for each flexible-link model was also very "stiff." As a result, the simultaneous numerical integration of these equations proved to be difficult and very time consuming due to the extremely small step sizes required by standard Runge-Kutta techniques. As a matter of fact, the Runge-Kutta method is not well suited for this problem at all. However, modern predictor-corrector techniques which have been specifically designed for stiff systems of equations are available. One such technique, which was developed by Gear [11] and considered to be the state-of-the-art in 1975, is available in the IMSL libraries of most main-frame computers. Using this algorithm, the simultaneous integration of each model's set of differential equations was able to proceed much more quickly, depending on the accuracy of the results desired. This technique was employed in all of the flexible-link simulations and some of the results were later compared with the solutions produced using a 5th - 6th order Runge-Kutta technique.

Chapter 5

Results and Discussion

For all models, the same basic system configuration was used. Both the first and second links were modelled as slender Euler-Bernoulli beams one meter in length and consisting of the aluminum alloy 2014-T6 (properties found in Mark's M.E. Handbook). The motors that delivered power to each revolute joint were modelled after the Kollmorgan model 2045 servo, which is rated at a continuous torque output of $2.18N - M$ and a peak torque output of $9.09N - M$. Furthermore, the derivation of the gear ratios, as shown earlier, yielded optimal overall values of 400/1 for the base revolute joint, and 175/1 for the second revolute joint. Also, the payloads used ranged from $1kg$ to $14kg$, compared to a system mass of roughly $26kg$ (including the mass of the motors).

The optimal control scheme for the flexible models proved to be the combination of the IJC strategy and a ramped motor acceleration/deceleration profile. A “bang-bang” motor acceleration profile worked well with the rigid-link Model RR, however it was avoided with the flexible-link models because it was found that a step acceleration input would induce very high frequency structural vibrations quite early in the motion. This result, coupled with the system’s nonlinear effects proved to make the numerical integration of the governing equations over the course of the manipulator’s full trajectory far too time consuming even when Gear’s method was used . Also, in order to exclude the effects of alternating positive and negative gravitational influences, and to avoid singularity positions, it was decided to restrict the manipulator to vertical motion with positive joint angle measures.

Generally speaking, the focus of these case studies has been to observe and compare the behavior of the two link manipulator as simulated by each flexible-link model to the behavior of an assumed rigid-link manipulator as simulated by Model RR, and to note any general trends or effects resulting from the torsional and/or lateral flexibility of each link. Moreover, it was expected that these studies would clearly illustrate the influences of eccentric load induced bending-torsion link vibrations, and thus permit a comparison between the effects of this phenomena and the effects of single-plane link bending.

Before beginning the case studies, the rigid-link model was validated since the equations governing this case formed the core of the gross robot arm motion simulated

in all of the subsequent models. The derived equations of motion for model RR were compared to the same equations as listed in Asada[1] and Fu[6]. Additionally, a "fall" test was conducted which consisted of letting the manipulator drop loose from an extended horizontal position with no applied motor torques, and then verifying that its ensuing motion due to the influence of gravity imitated the motion of a planar double pendulum. Each of the flexible-link models were also tested by ensuring that the rigid-link equations of motion would remain in their entirety after all of the flexibility variables were removed from each model's set of governing equations of motion. Finally, each flexible-link model was subject to the same "fall test" as previously described.

Once these tests were satisfactorily completed, model RR was tasked to move from an initial configuration of 15° at θ_1 and 15° at θ_2 , to a target configuration of 45° at θ_1 and 45° at θ_2 in a period of one second, while carrying a payload with its end-effector (see fig. 11). The resulting transient response of each joint angle trajectory was then saved for comparison to the same joint angle trajectories produced by the flexible link models.

Since all considered flexibility effects were included in model TTFEL, and the remaining flexible-link models may be derived from it, the case studies concentrated on the simulations produced by this model.

Perhaps the first observed consequence of the link flexibility while simulating the

described vertical motion, was the reactive upward-displacement of the end of link one due to the torque applied by the second joint motor, and the lack of motion of link two. Considering the system's configuration, this result can be explained since the inertial resistance to movement presented by the combination of the second link and payload was greater than the first link's resistance to elastic flexure. Reducing the length of the second link and lowering the mass of the payloads would certainly remedy this problem, but would also severely limit the case studies planned. Also, since most robot arm's in use today are configured with a longer second link, it was decided to shorten-up and strengthen link one instead.

With a non-eccentric payload gripped at the end of link two, the vertical motion of the manipulator towards the target configuration induced a normal downward planar flexure of link two, as expected, and a slight upward displacement of the end of link one (which was on the order of hundredths of a millimeter - see fig. 12). Moreover, once the target configuration was reached the end of the second link would begin to vibrate about its resting position, eventually damping out (see fig. 13). It is important to consider this behavior because the ensuing fine-motion control of an end-effector mounted at the tip of link two would be affected by this vibration. Overall, though, no particularly adverse influences upon the joint angle trajectories were noted in this case.

In contrast, the joint angle trajectories and the resulting gross motion control of the two-link manipulator was significantly affected by the bending-torsion vibrations

that developed in each link as a result of the robot arm's efforts to move an eccentrically gripped payload. (Note that these vibrations move the case at hand from a planar to a three dimensional problem). Generally, the resulting transient response of each joint angle trajectory exhibited increases in maximum peak overshoot, and increases in settling time. There was also a noticeable, increased lag in the response of the second joint angle θ_2 . These conclusions were drawn after examining the performance of the two link manipulator while moving from the described initial configuration to the final vertical configuration in a period of one second while carrying eccentrically positioned loads ($e = 8cm$) ranging in size from $1kg$ to $14kg$.

Referring to the case where the eccentric load is $1kg$ (figs. 14,14.1, 14.2), which is 3.8 percent of the system's total mass, note the increased lag and hesitation of each joint angle history. Furthermore, an increase in peak overshoot and a slight increase in settling time is evident. Referring to the joint angle histories for the case of an eccentric $3kg$ payload (figs. 15,15.1,15.2), the same behavior is noticed. In fact, all of the loads considered produced these effects on the joint angle trajectories, and the severity of these effects was generally noted to increase in proportion to the size of the eccentric load (see figs. 18-21).

It is suspected that a reason for these disturbances of the transient response of each joint angle trajectory is the somewhat higher amplitude and frequency of the structural bending-torsion vibrations compared to the amplitude and frequency of the planar flexural vibrations, both of which are observed to occur when the manipulator

is closing in on its target configuration. It is at this time, when the gross motion is virtually complete and the torques are small that these vibrations have a significant influence upon the joint angle time histories. Consider the plots of the end-effector lateral vibrations for each case compared to the lateral planar-vibrations that occur when the load is not held eccentrically. The increased amplitude and frequency of the vibrations that occur is depicted in many of the plots, indicating that the amount of time needed until they settled increased. Consider figs. 17.1,17.2, and 17.3, which pertain to the case when a 14kg payload - which is more than 50 percent of the system mass - is held eccentrically. Over ten seconds passes before the system settles and the end-effector vibrations cease. Even when the eccentric load is small many seconds pass before these vibrations settle down (see fig. 22). We must consider the average dynamic error of the end-effector due to these vibrations and note that this error is generally larger when produced by an eccentric payload (see fig. 23). Hence, the objective of high end-effector positional accuracy and its successful fine-motion control certainly appears to be difficult to attain in light of this phenomena. In fact, the objective of a reliable, and immediately stable response from the robot manipulator as a whole is not realistic in the presence of these high frequency structural vibrations. This difficulty is especially likely since most control schemes ignore the effects of link elasticity.

In order to reduce the detrimental effects of these vibrations and improve the accuracy of the manipulator, it was proposed to introduce additional structural damping into the system. In practise, this could be accomplished with passive damping tech-

niques such as coating the aluminum links with a polymer jacket, inserting in the hollow links removeable rubber baffles which would still permit conduits to pass, or utilizing layered composite materials to construct the links themselves. Note that attempting to diminish the high frequency vibrations through damping methods offers a far cheaper and easier first alternative to the use of sophisticated control techniques.

Thus, simulated positive damping was added to the differential equations governing the vibrations in both links one and two. Results from subsequent simulations indicated a definite improvement in the transient responses of each joint angle trajectory, and a reduction in the severity of the bending-torsion vibrations at the end-effector (see figs. 24 & 25). Just how much damping to introduce was also evaluated. Referring to fig. 26, it is evident that the damping ratio required increased as a function of the size of the payload.

Since they are a function of the joint angle velocities, Coriolis and centripetal effects are often justifiably ignored in the real-time control schemes of robot manipulators in order to speed-up the rate of the numerical solution to the system's equations of motion. However, the arm is then restricted to slow speeds of movement, which may not be desirable in many applications. An advantage provided in simulation studies is that prior knowledge of the complete closed form equations of motion enables one to readily identify these terms, and experiment with compensation methods. Thus, some brief attempts were also made to account for the system's Coriolis and centripetal effects with nonlinear feedback control methods. This is accomplished by

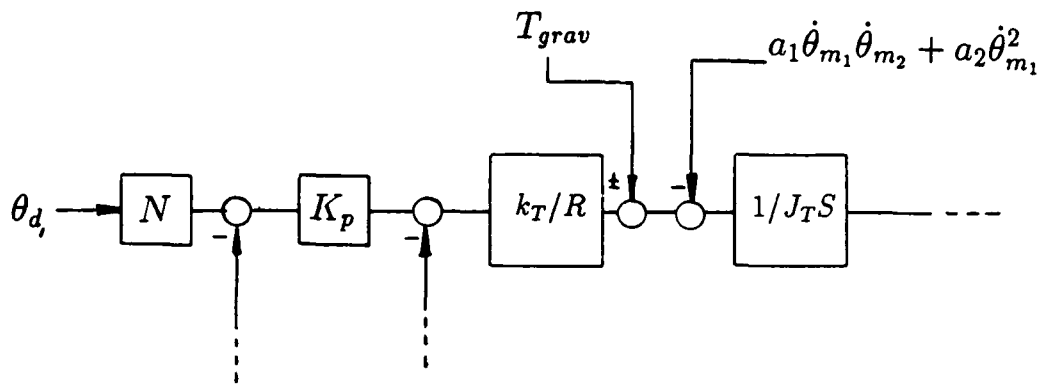


Fig. 27

coupling the separate joint servocontrollers with velocity feedback paths, and treating the Coriolis and centripetal effects as disturbance torques along with the gravity torques in each joint's control loop (see fig. 27). It was not necessary to account for all of the Coriolis and centripetal terms appearing in the system's equations of motion before slight improvements in performance were observed. Specifically, the transient responses of each joint angle trajectory indicated a drop in peak overshoot and settling time, and slightly quicker speeds of movement were permitted. It should also be mentioned that the material flexibility led to the presence of cross-product terms between joint velocities and material displacement velocities in the equations of motion; indeed, the system was fully coupled. These terms mathematically describe the form of some of the peculiarities and reverse-effects caused by the material elasticity. No attempts were made to compensate for these phenomena, however, this could be attempted after examining the equations of motion as listed in Appendix B. One suggestion, as a matter of fact, is to feed forward the flexibility terms (i.e. the

FFC method as suggested by Book [3]).

Chapter 6

Summary and Conclusions

Current trends and research efforts in the field of robotics indicate a definite desire to obtain a greater understanding of the consequences of material flexibility. An increased awareness of the effects of joint elasticity and link displacements permits the development of sophisticated manipulator control schemes and other techniques aimed at minimizing the dynamic and static errors inevitably seen in the manipulator's trajectory and end-effector positioning as a result of link flexure and vibration. In this light, much noteworthy work has been accomplished in the U.S. and abroad. Single-link robot models and two-link robot models with a variety of joints and degrees of material flexibility have been derived using many methods. Resulting suggestions for compensation are many, and more are being published yearly.

It has been the intention of this study to also focus on the example of a two-link revolute-joint robot manipulator and to develop models to simulate its motion when each link is permitted to elastically deform. Specifically, five system models are developed, the last of which allows each of the manipulator links to displace in torsion and in flexure - yielding a total of six degrees freedom. The crux of each of these models is a set of coupled governing differential equations of motion, which are second order and nonlinear and have been derived using the Lagrange-Euler technique and a proper kinematic description of each system. Material displacements have been represented through the method of assumed modes in a single-mode approximation. Moreover, proportional plus tachometric feedback positional control policies are used to operate the servos which provide power to each system at their revolute joints. Finally, the models are all run on a VAX 8650 digital computer wherein quick vertical motion is simulated while the manipulator holds a payload at its end-effector.

Unlike any of the aforementioned articles, the models developed in this study also consider the effects of carrying an inertially asymmetric payload. In fact, Model TFT-FEL simulates the elasto-dynamic behavior of the manipulator seen as a result of the coupled bending-torsion vibrations in each link that are driven by the manipulator's movement while carrying such a load. Case studies are conducted to determine the detrimental effects of this behavior on the joint angle trajectories of the manipulator. Specifically, it is seen that the transient response of each joint angle trajectory exhibits rises in maximum peak overshoot and settling time, and a hesitation in response - especially in the second joint angles. Moreover, lateral vibrations are observed at

the manipulator's end-effector, and it is readily apparent that the average amplitude and frequency of these displacements as caused by the coupled bending-torsion of the links were greater than the amplitude and frequency of the single plane displacements as driven by a properly positioned payload. Hence, more time would be necessary to settle this motion to allow for accurate end-effector fine motion control. It has been asserted that since most control algorithms ignore this phenomena completely, then the objective of a smooth, reliable and accurate manipulator reponse as a whole is indeed questionable. Artificial passive damping techniques used to eliminate or at least reduce the severity of these high-frequency vibrations were also attempted, and resulted in marked improvements in the two joint angle trajectories. It was found that by increasing the damping ratio in the equations governing torsional and lateral elastic link displacements, the detrimental effects of the bending- torsion vibrations could be almost completely subdued, and the end-effector displacements would follow as the planar vibrations had.

An additional aspect of this study is the inclusion of the complete closed-form governing equations of motion. Having the full listing of the differential equations for Model TTFEL enables one to pose studies of the effectiveness of various control policies such as FFC (the feed-forward of flexibility coefficients). Although time did not permit full studies of this kind to be carried out, some attempts were made with nonlinear feedback techniques with motor speed in order to compensate for the system's centripetal and Coriolis effects. Results indicated an improvement in the accuracy of the transient responses of each joint angle trajectory with reductions in

target position overshoot and settling times.

Overall, this study has been conducted for the purpose of deriving models which are intended to be used as tools to aid further investigation into the effects of elastic link displacements and how to compensate for this phenomena. Although the method chosen to derive the governing equations for each case did not lead to the most computationally efficient models, the resulting closed-form equations do have the advantage of being explicitly a function of the manipulator's physical characteristics, and therefore, much can be learned from them. Much time was also expended in an effort to make all of the steps in the derivation as clear as possible and it is hoped that this will also aid further studies of this kind. Finally, it should be mentioned that although the packaged numerical technique used for the simultaneous integration of the equations of motion in each model is highly advanced and fast compared to standard Runge-Kutta methods (which are not suited for the stiff systems of equations seen in these flexible-link models), it still has its limitations and tends to be very sensitive to its many inputs. As a result, the extent of the variations in manipulator speeds, trajectories, and payload sizes that could be tried was somewhat limited. Perhaps efforts in nondimensionalization with respect to material stiffness EI would increase the bandwidth of possibilities in the study of the manipulator's motion.

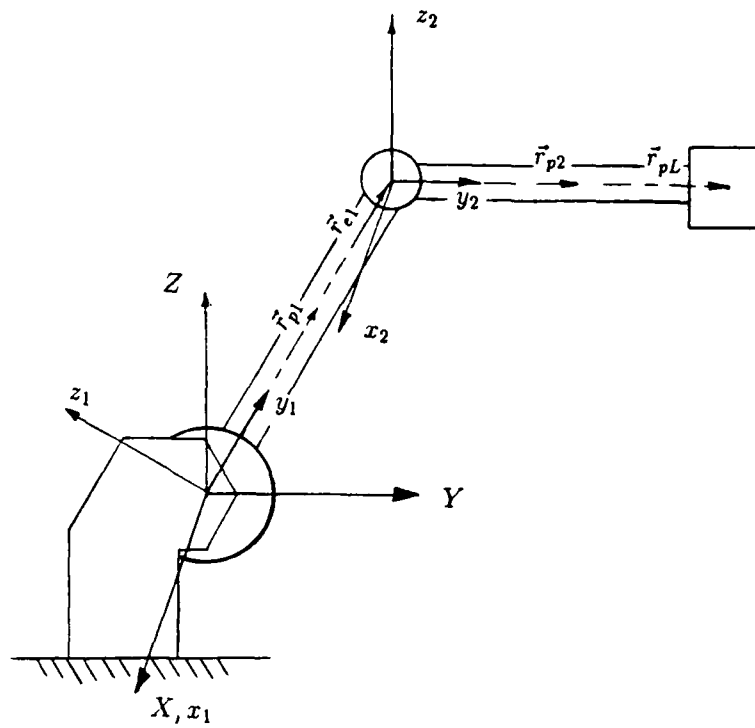


Fig. 2 Model RR

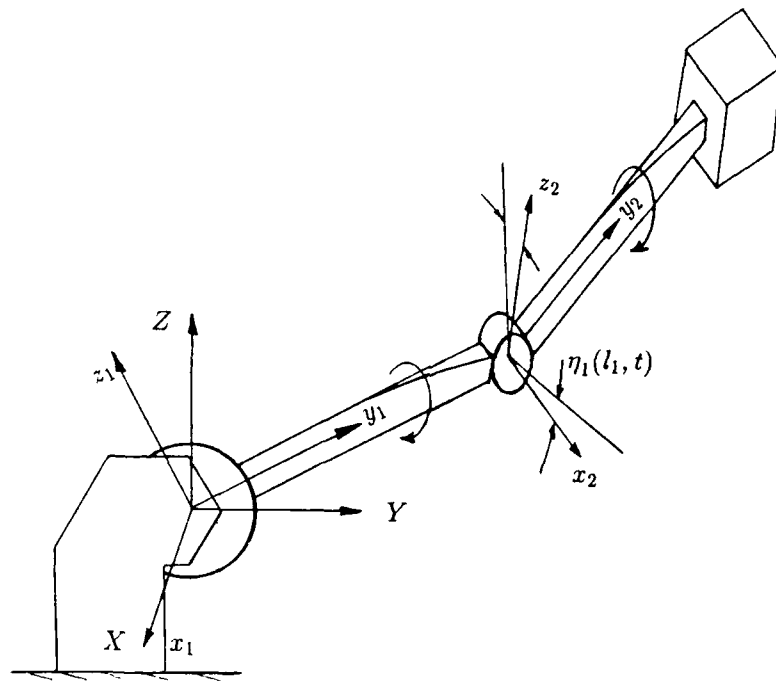


Fig. 3 Model TT

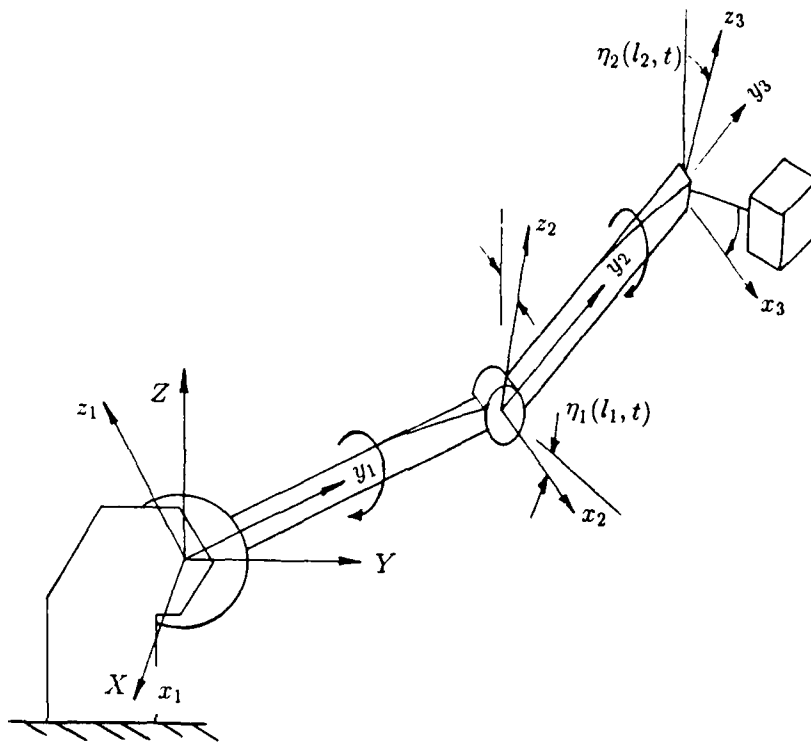


Fig. 4 Model TTEL

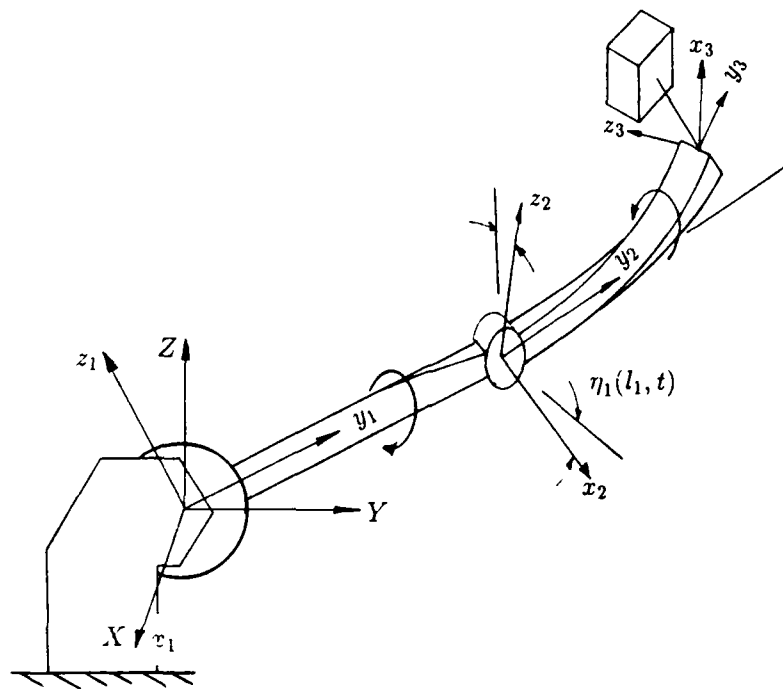


Fig. 5 Model TTFEL

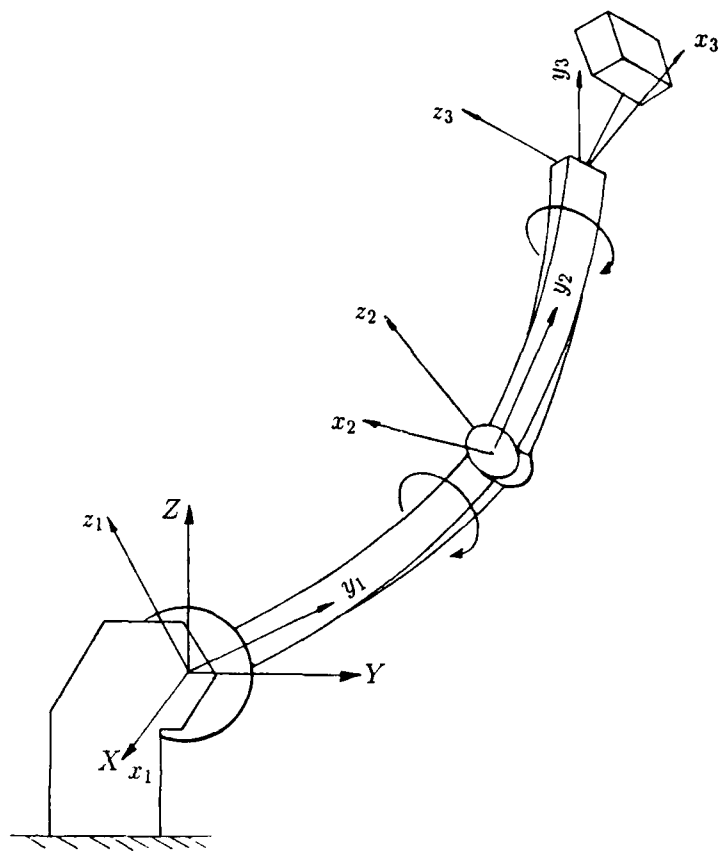


Fig. 6 Model TTFEL

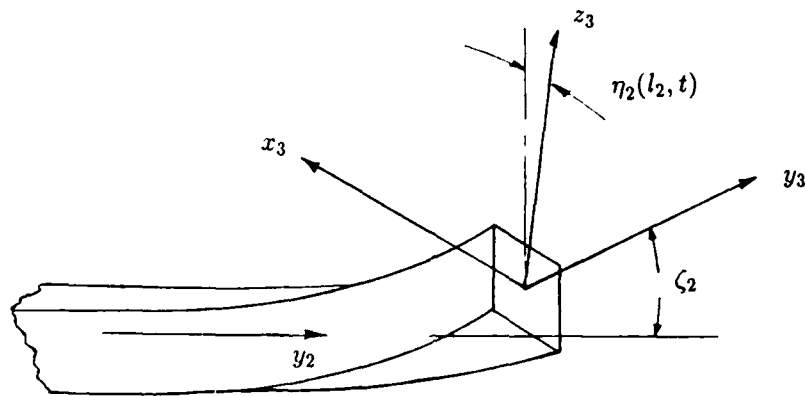


Fig. 7 Bending-Torsion of Link 2

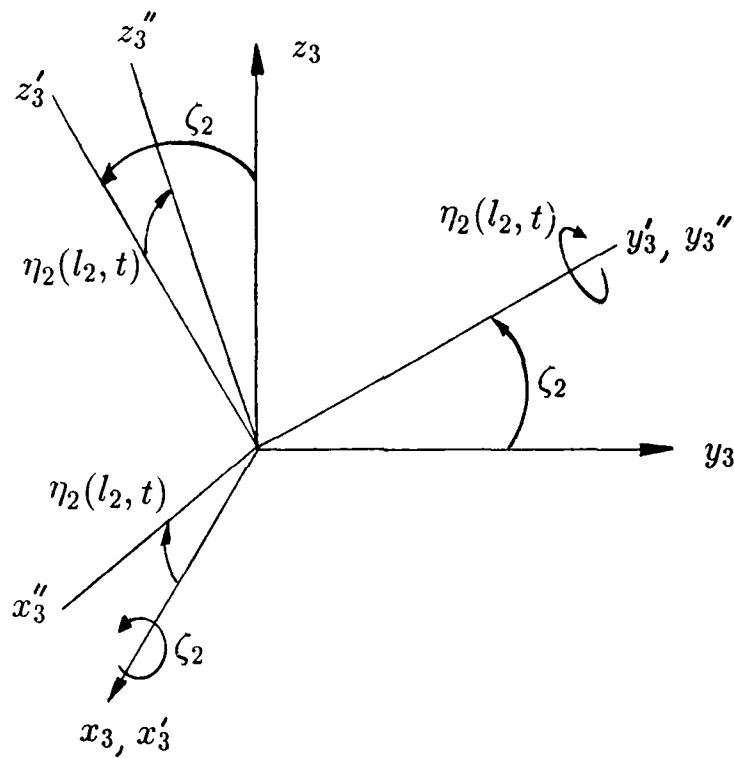


Fig. 7.1 Rotation of the $x_3y_3z_3$ Frame in Models TTFEL and TFTEL

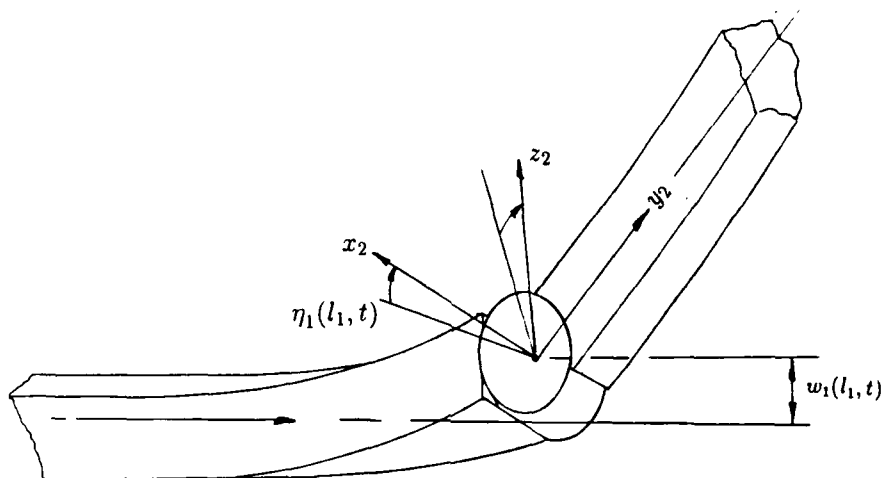


Fig. 8 Bending-Torsion of Link 1

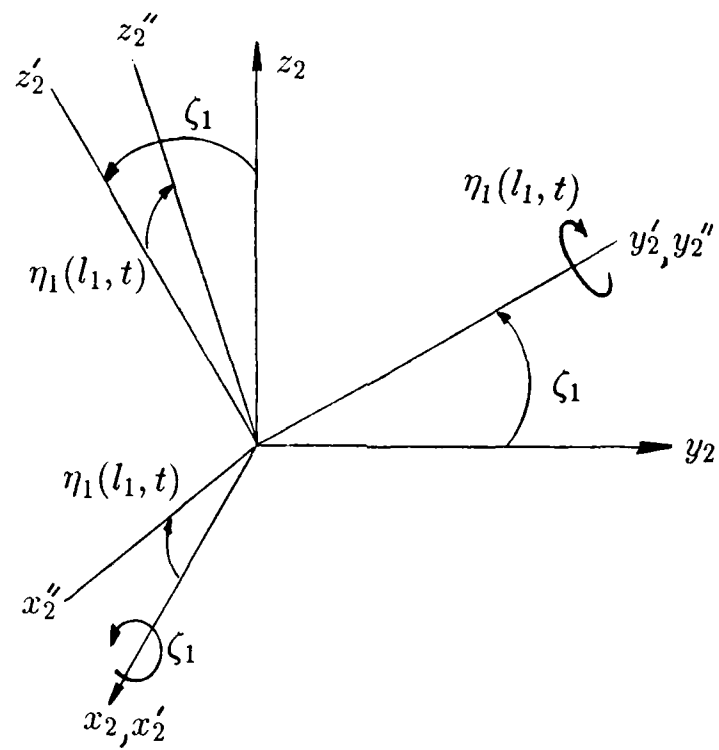


Fig. 8.1 Rotation of the $x_2y_2z_2$ Frame in Model TTFEL

Bang-Bang Acceleration Profile

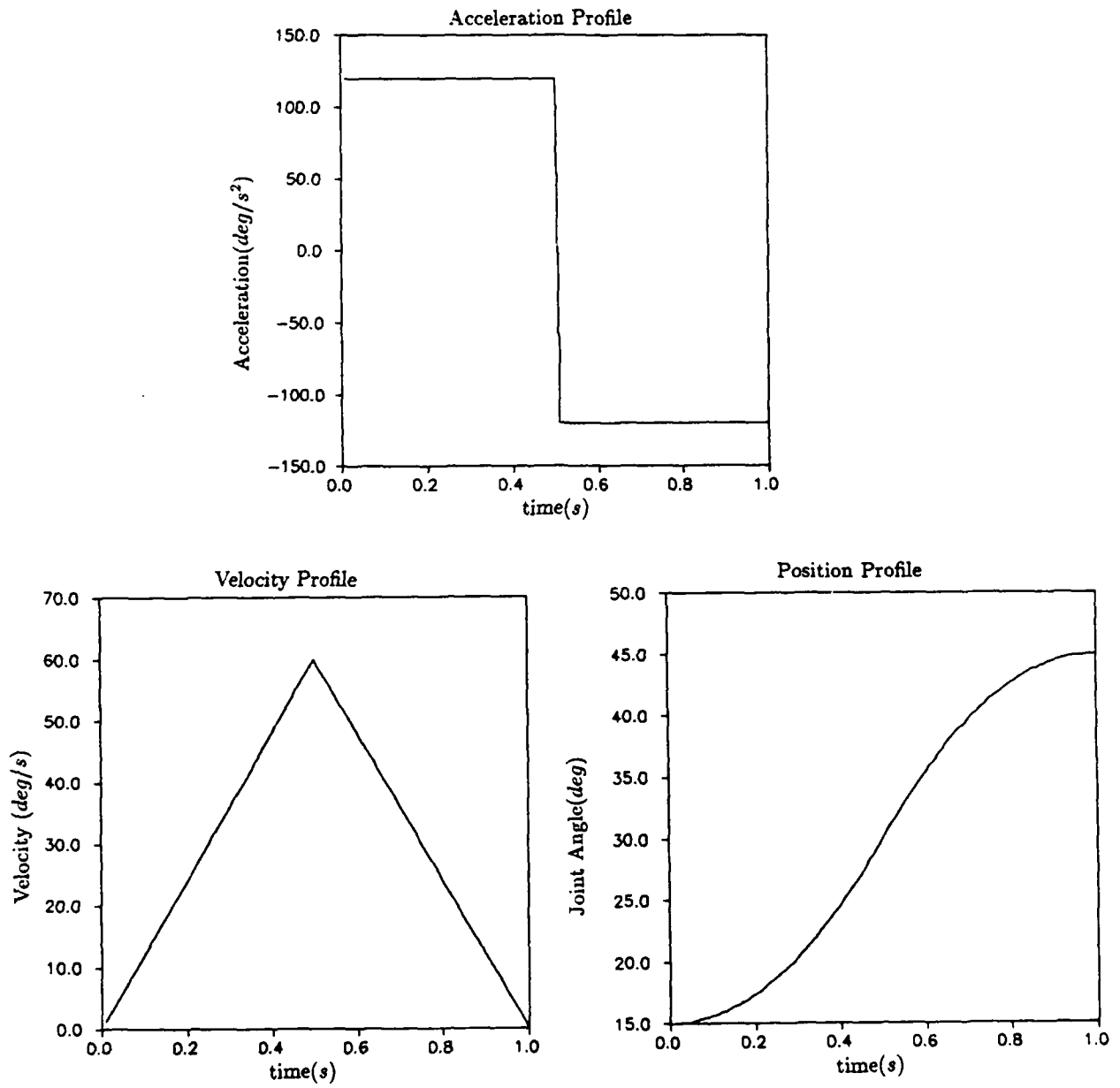


Fig. 10.1

Ramped Acceleration/Deceleration Profile

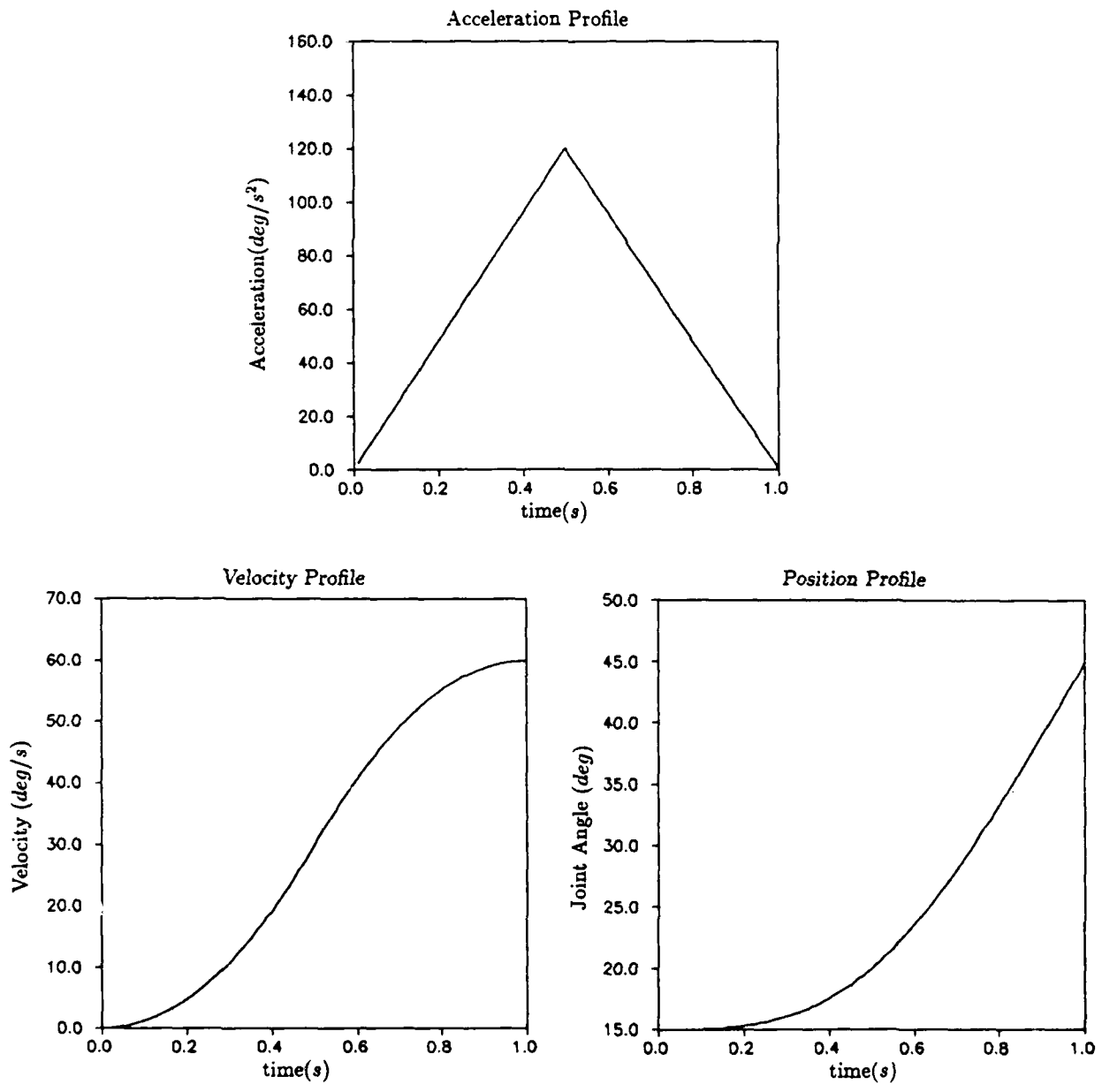


Fig. 10.2

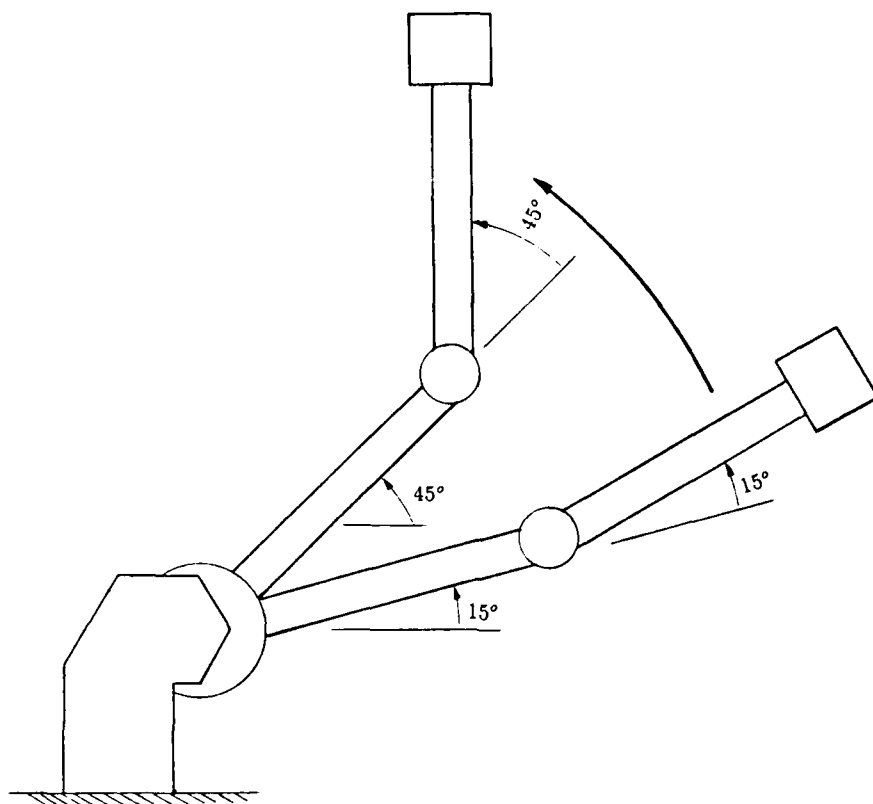


Fig. 11 Simulated Vertical
Arm Motion

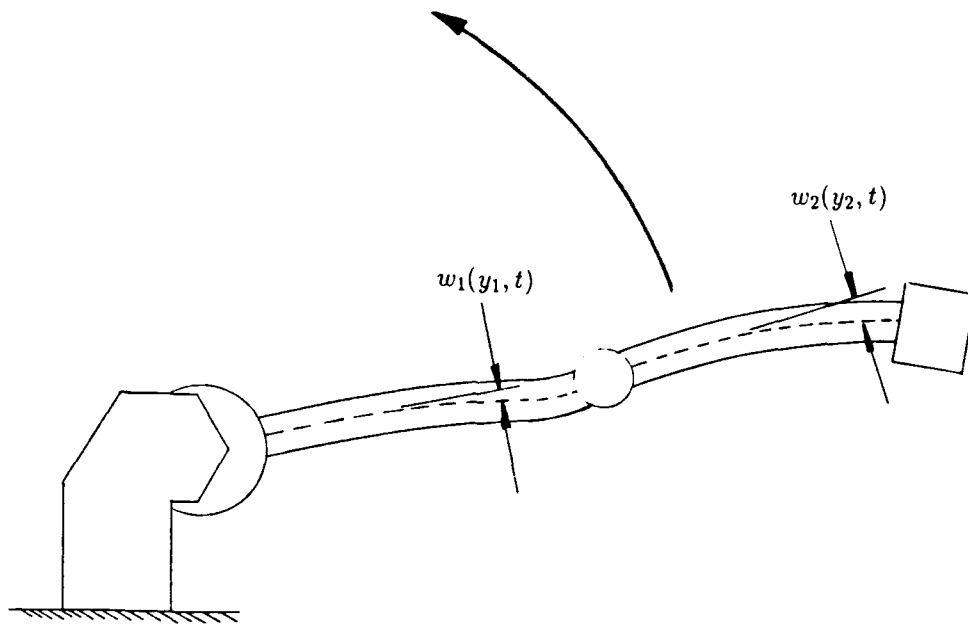


Fig. 12 Single-Plane Flexure
of Manipulator Links

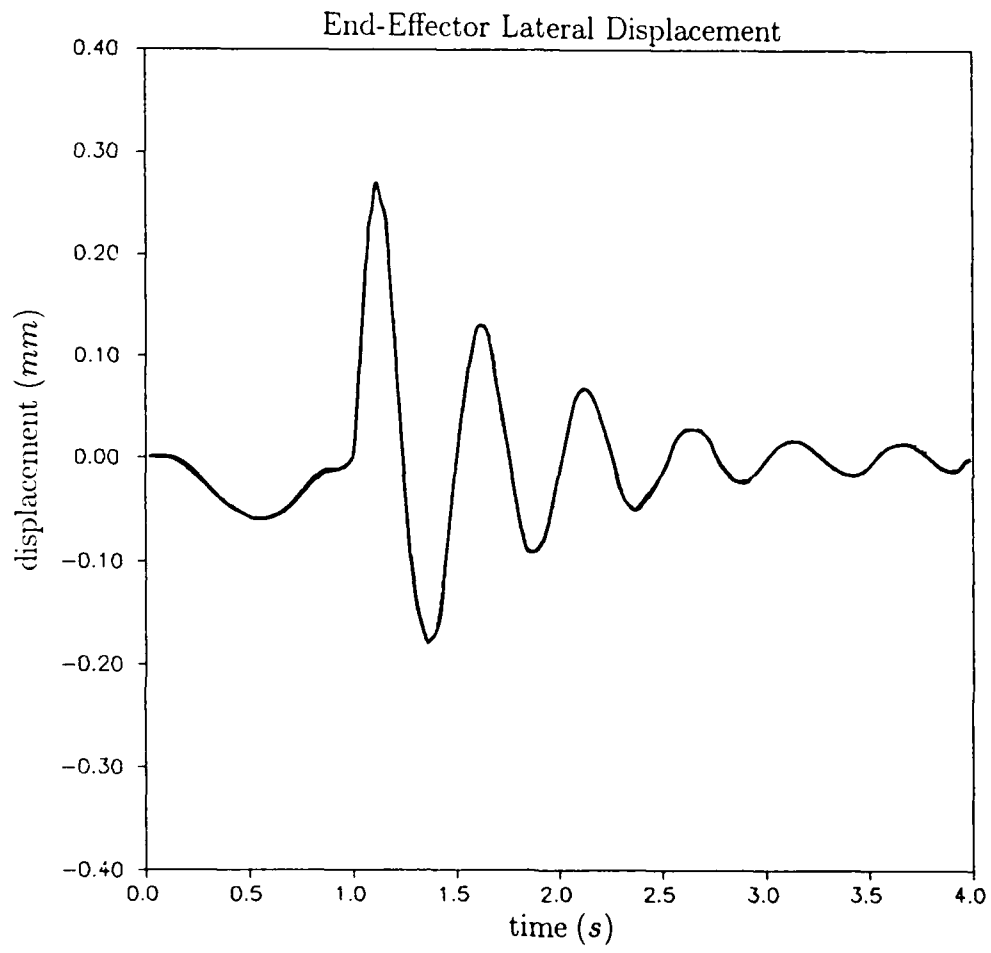


Fig. 13

First Joint Angle Transient Response
(eccentric load = 1kg)

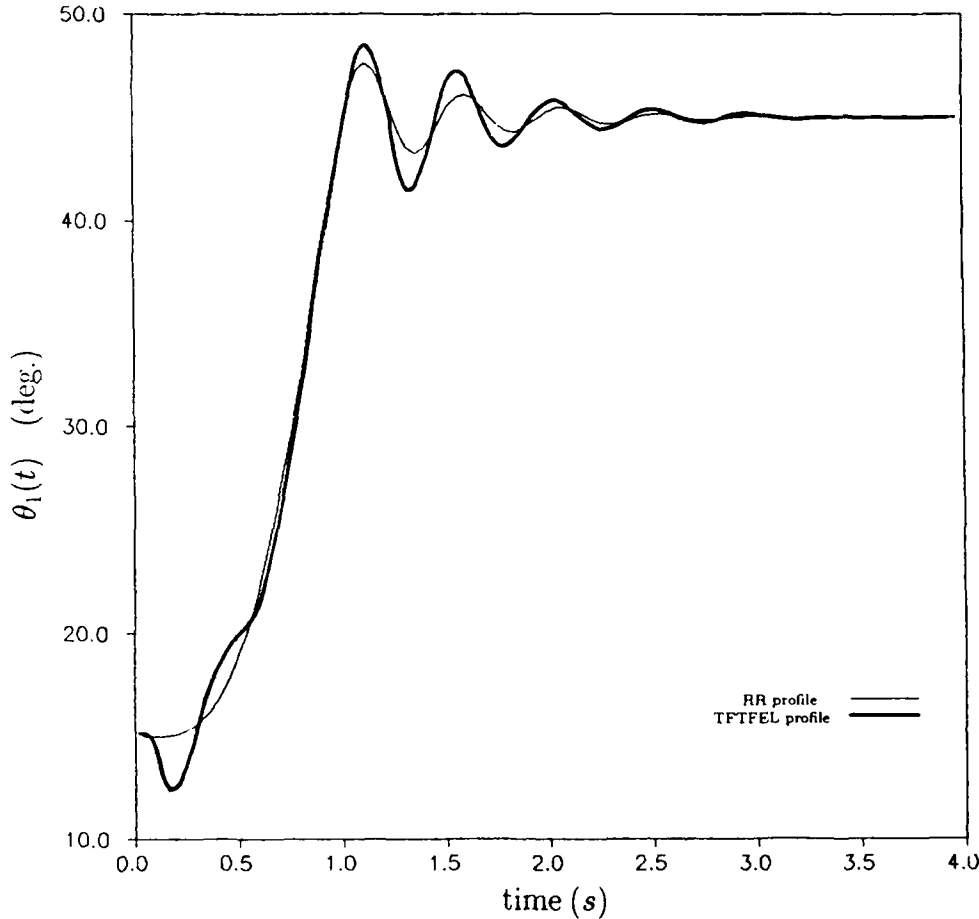


Fig. 14

Second Joint Angle Transient Response
(eccentric load = 1kg)

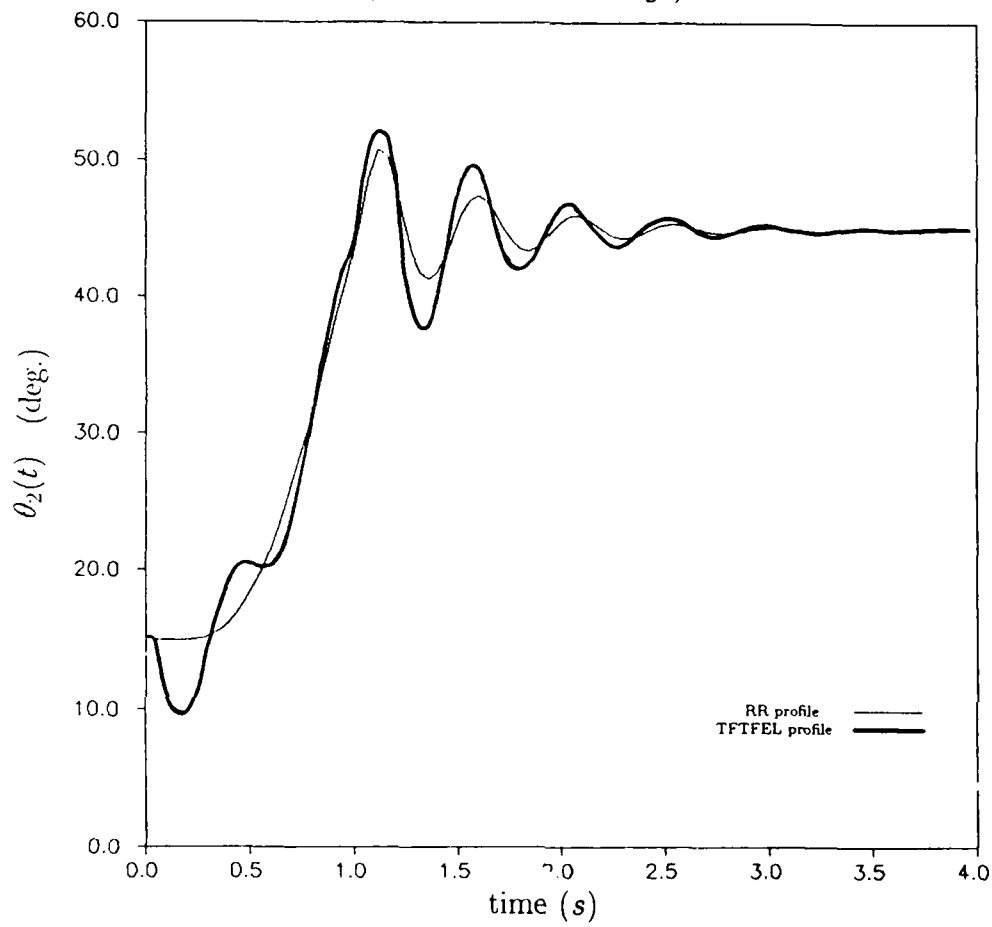


Fig. 14.1

End-Effector Lateral Displacement

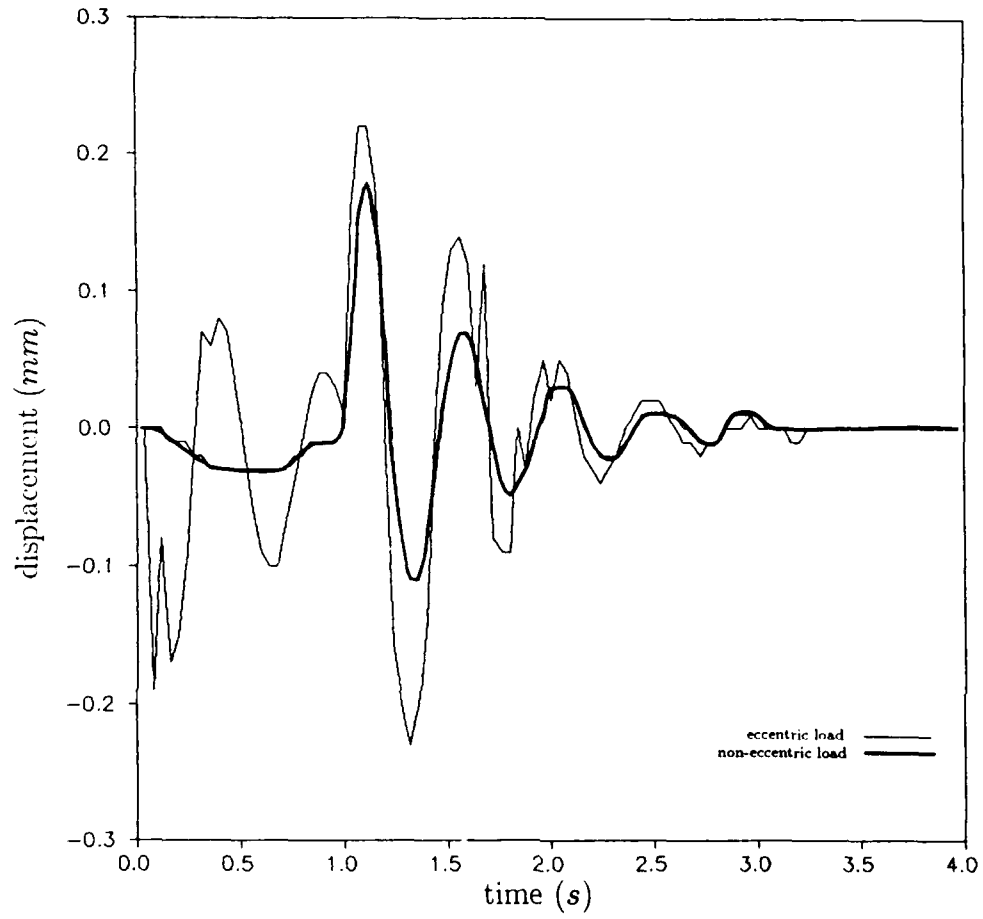


Fig. 14.2

First Joint Angle Transient Response
(eccentric load = 3kg)

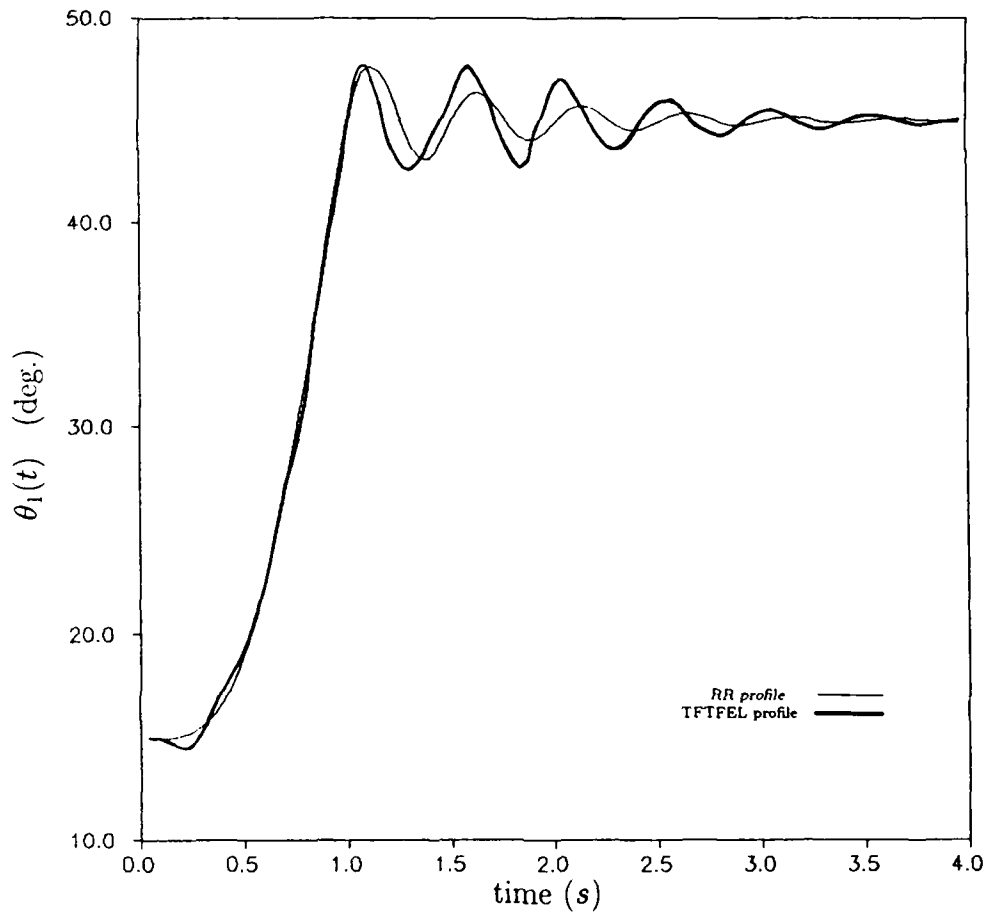


Fig. 15

Second Joint Angle Transient Response
(eccentric load = 3kg)

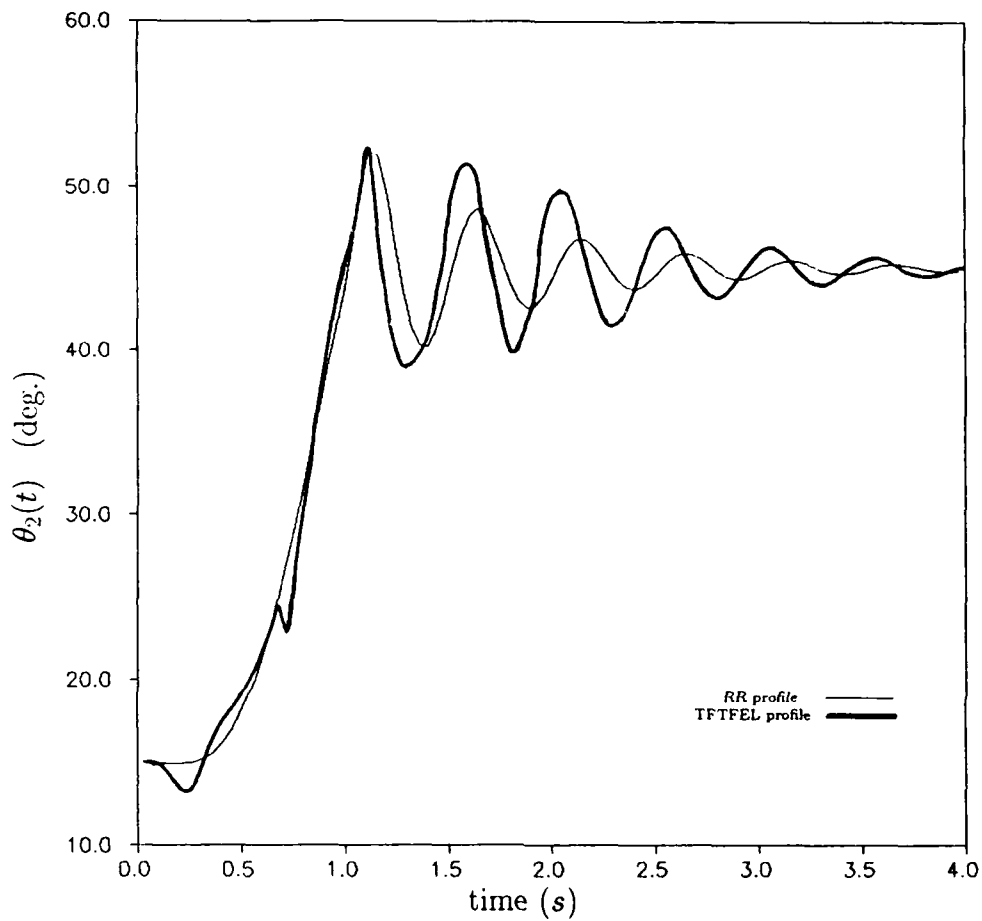


Fig. 15.1

End-Effector Lateral Displacement

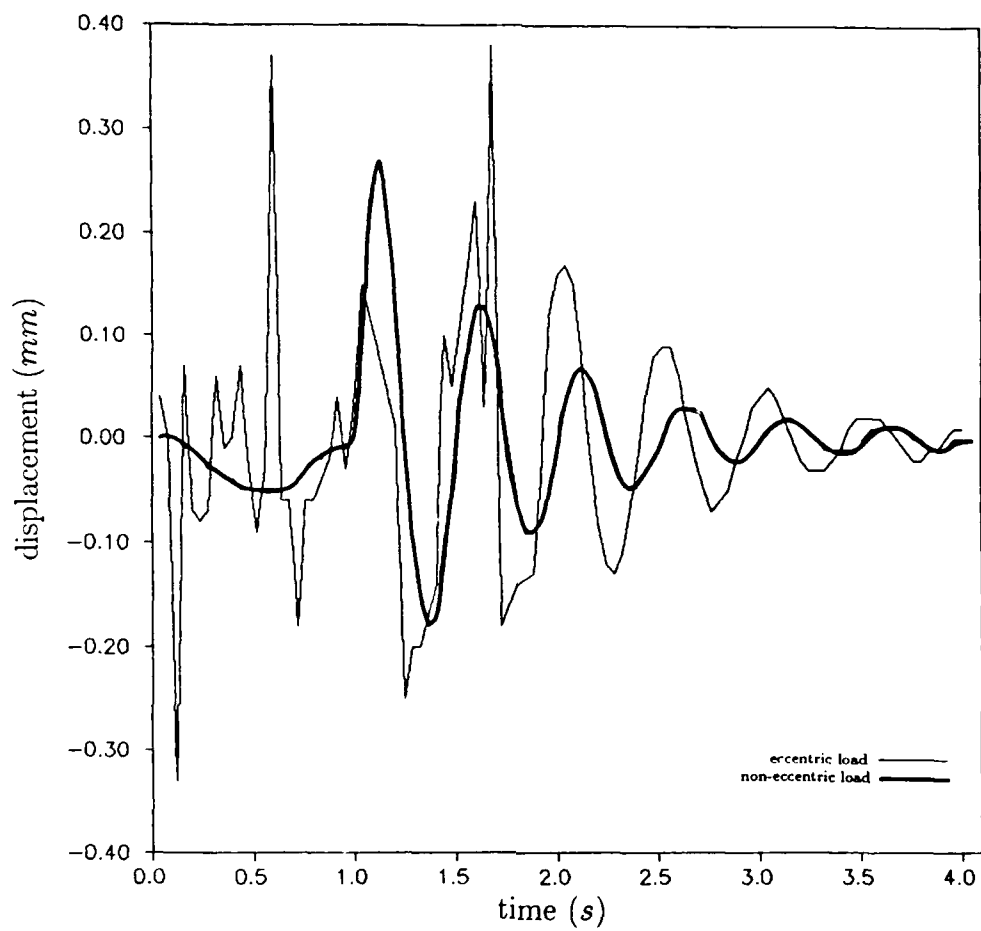


Fig. 15.2

First Joint Angle Transient Response
(eccentric load = 4.7kg)

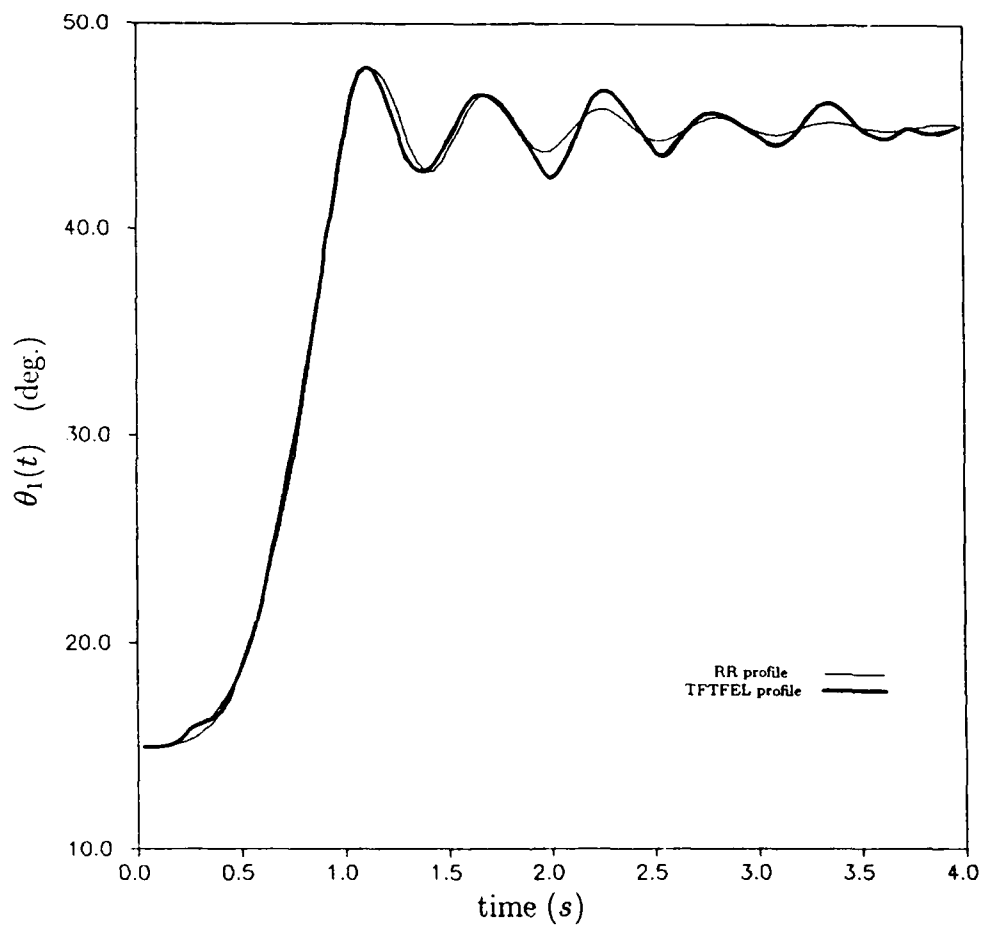


Fig. 16

Second Joint Angle Transient Response
(eccentric load = 4.7kg)

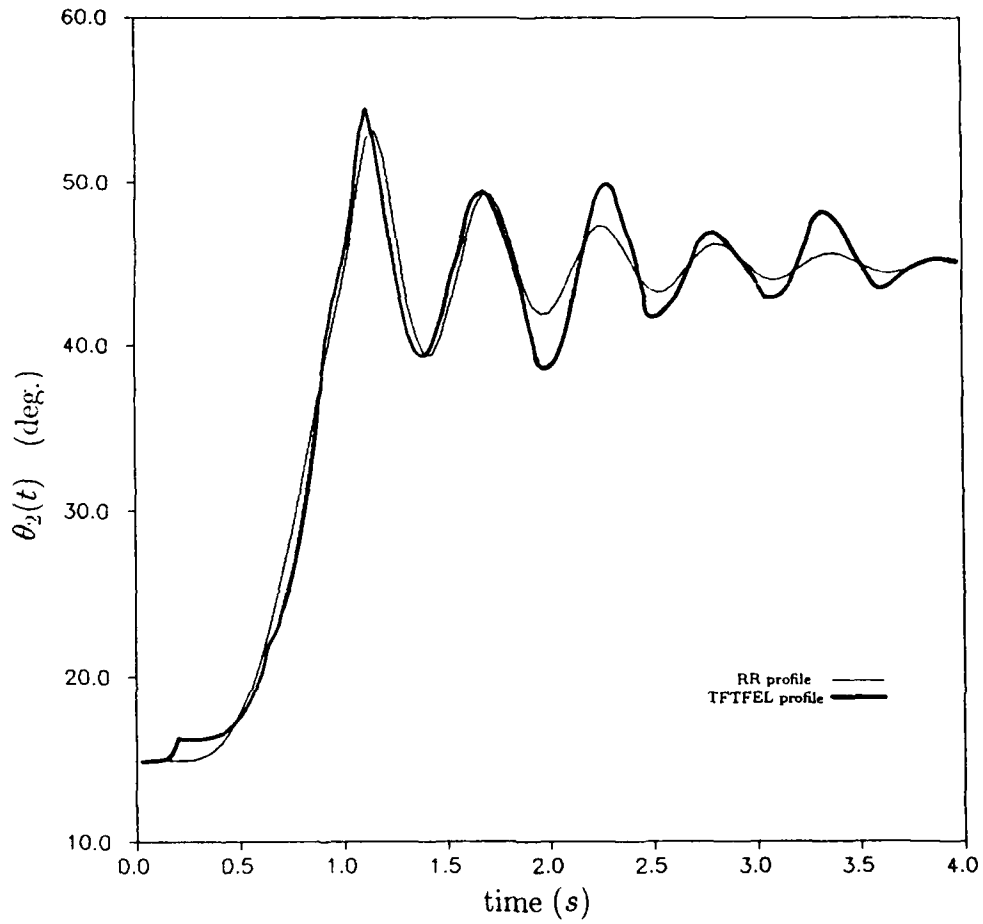


Fig. 16.1

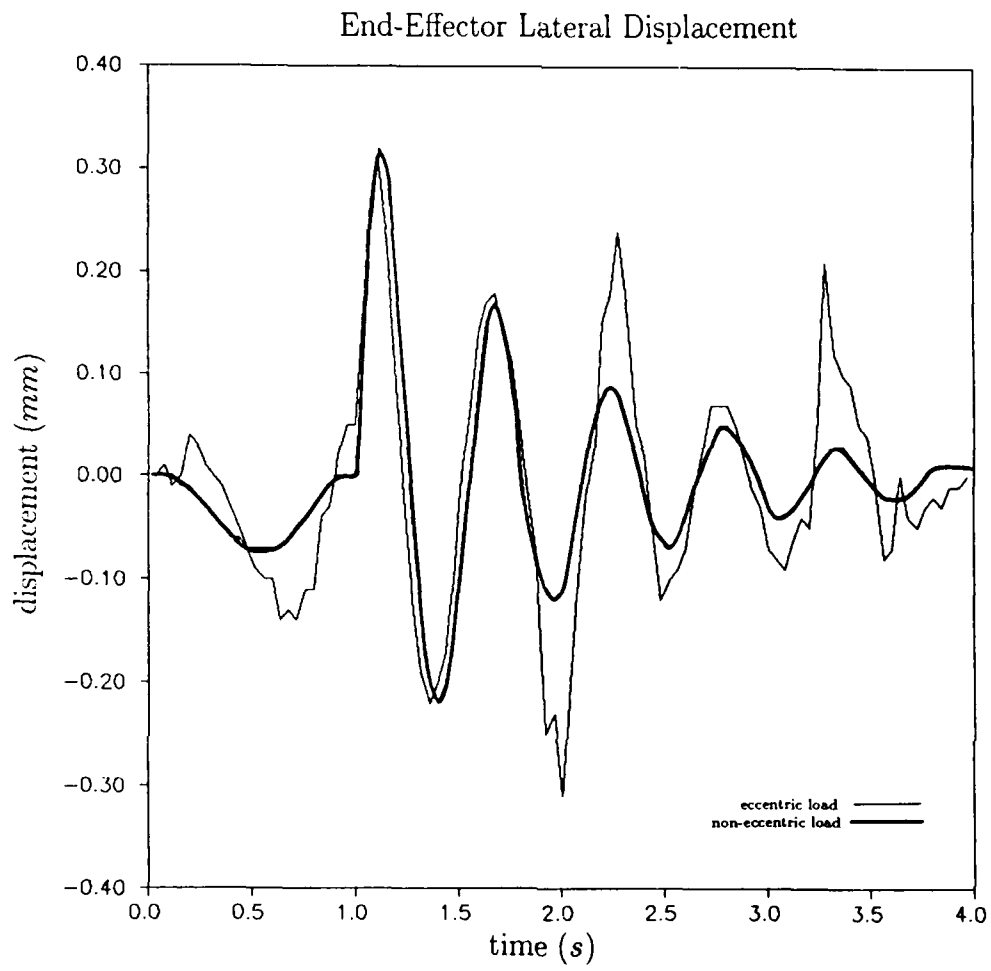


Fig. 16.2

First Joint Angle Transient Response
(eccentric load = 14kg)

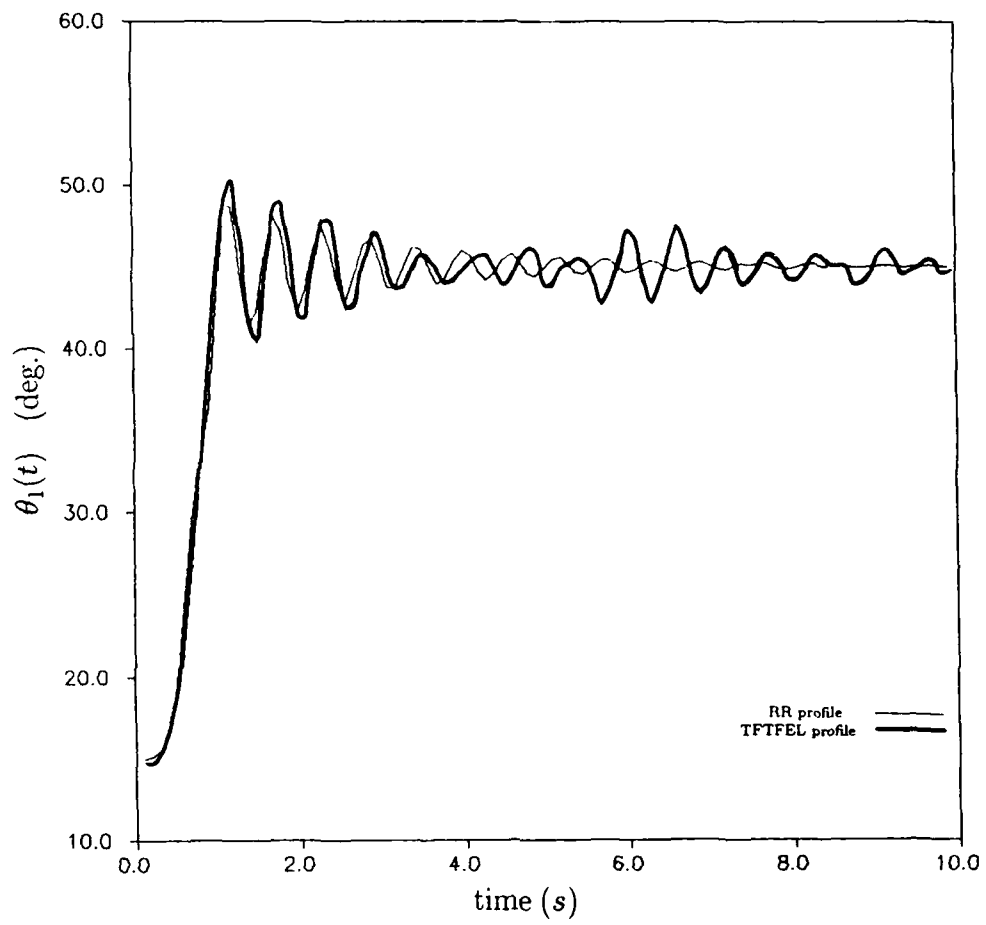


Fig. 17

Second Joint Angle Transient Response
(eccentric load = 14kg)

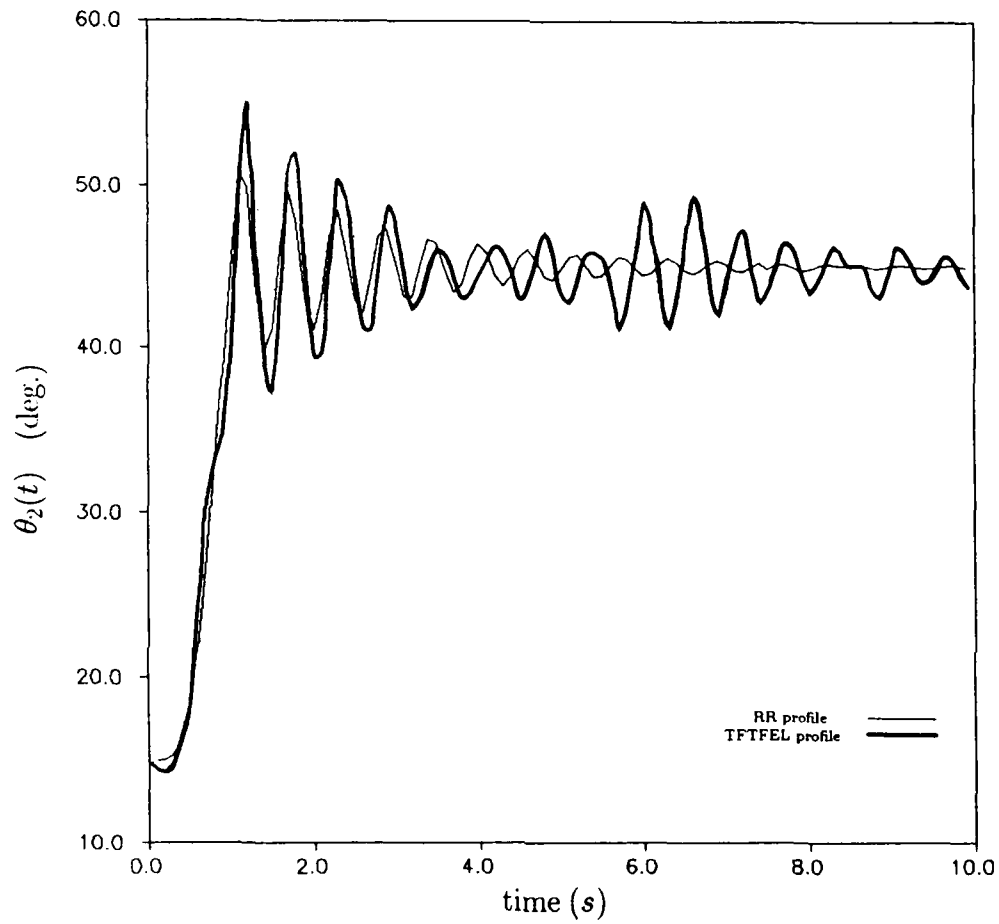


Fig. 17.1

End-Effector Lateral Displacement

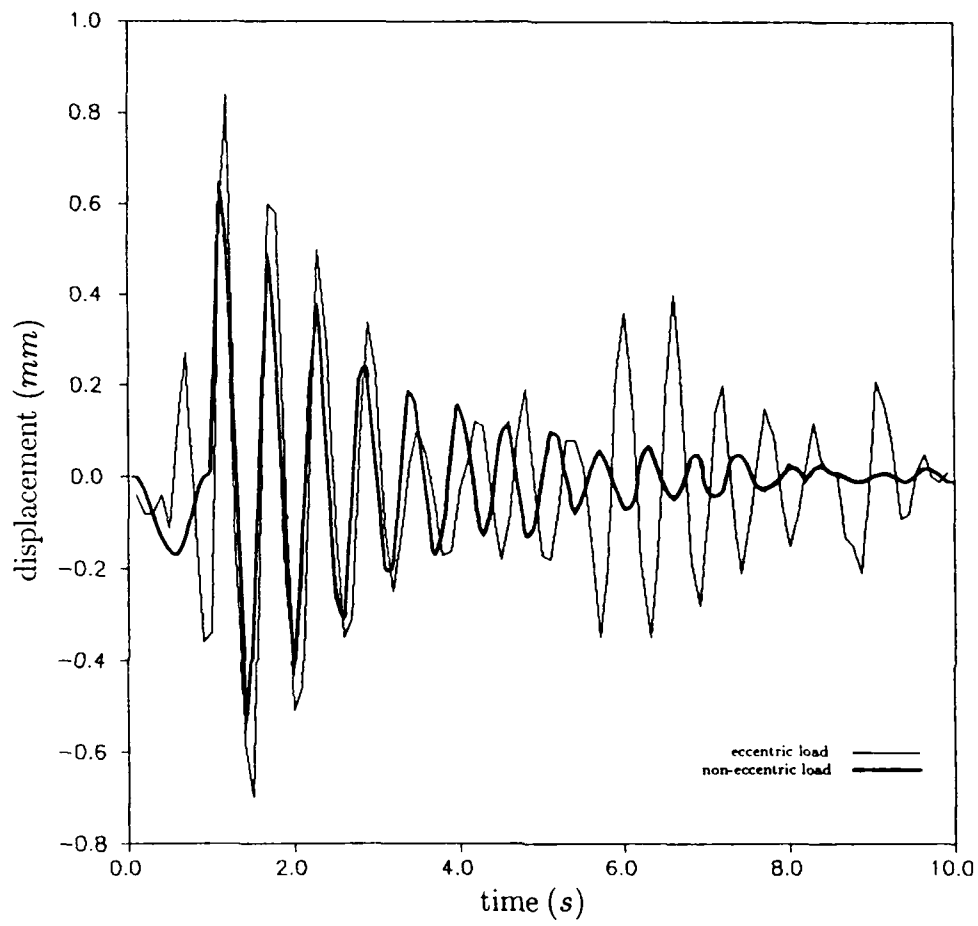


Fig. 17.2

Increase in Settling Time Vs. Mass of Eccentric Load
First Joint Angle

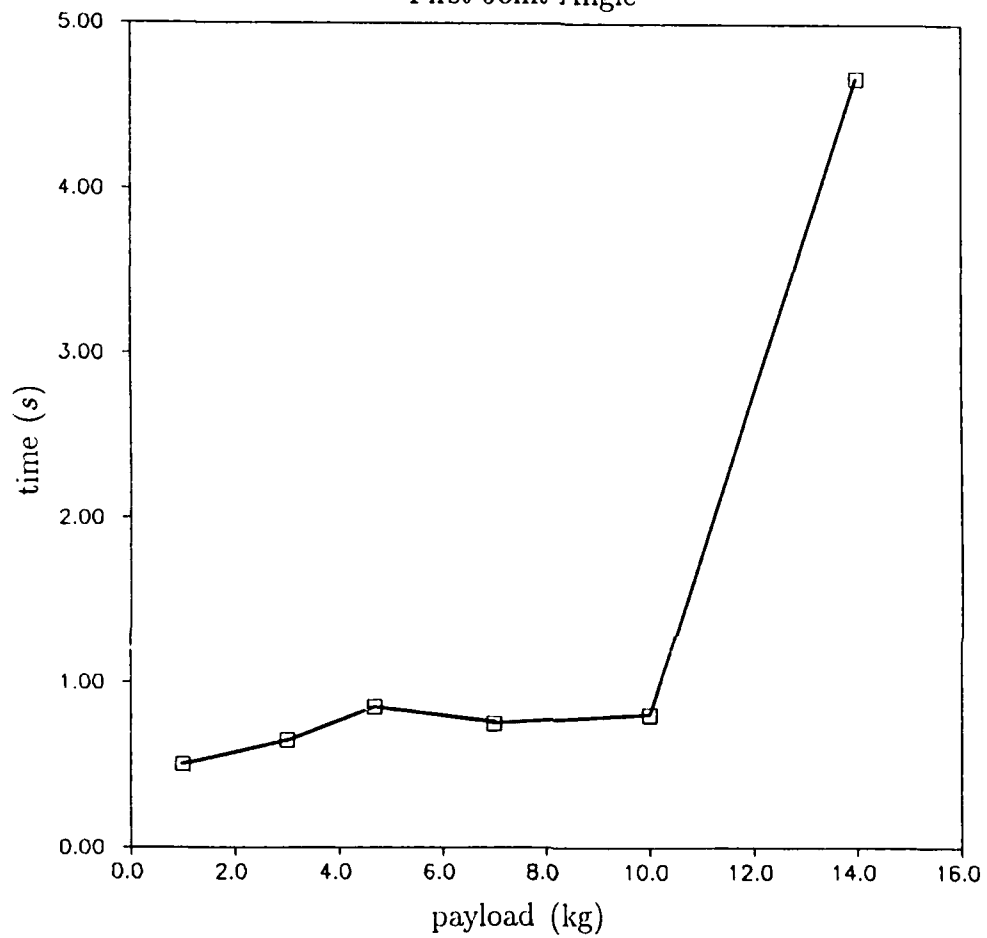


Fig. 18

Increase in Settling Time Vs. Mass of Eccentric Load
Second Joint Angle

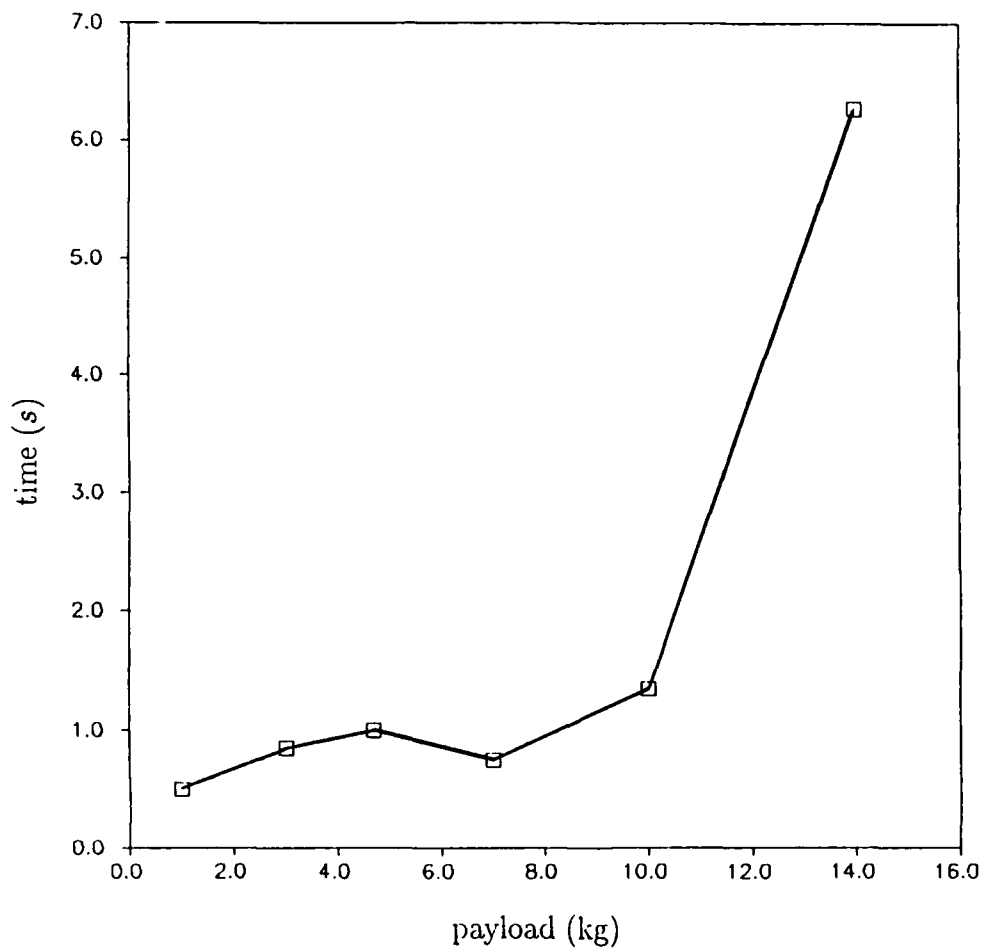


Fig. 19

Maximum Peak Overshoot Vs. Mass of Eccentric Load
First Joint Angle

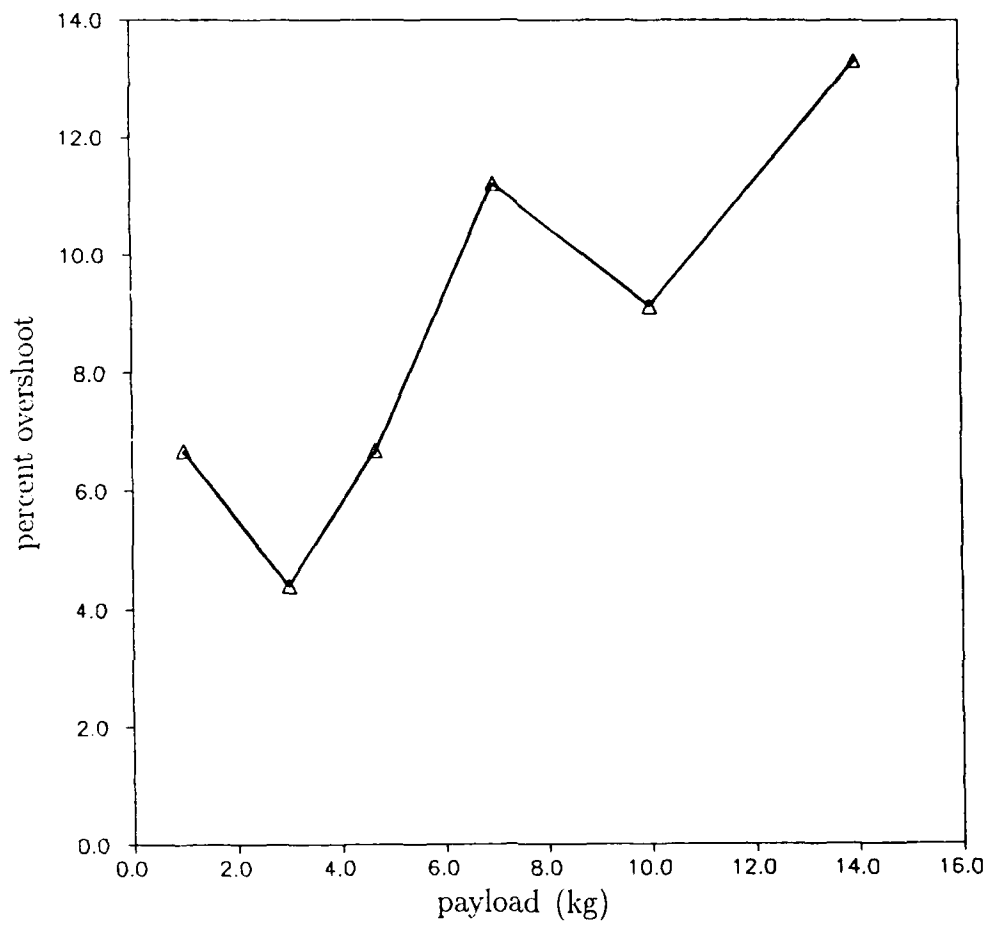


Fig. 20

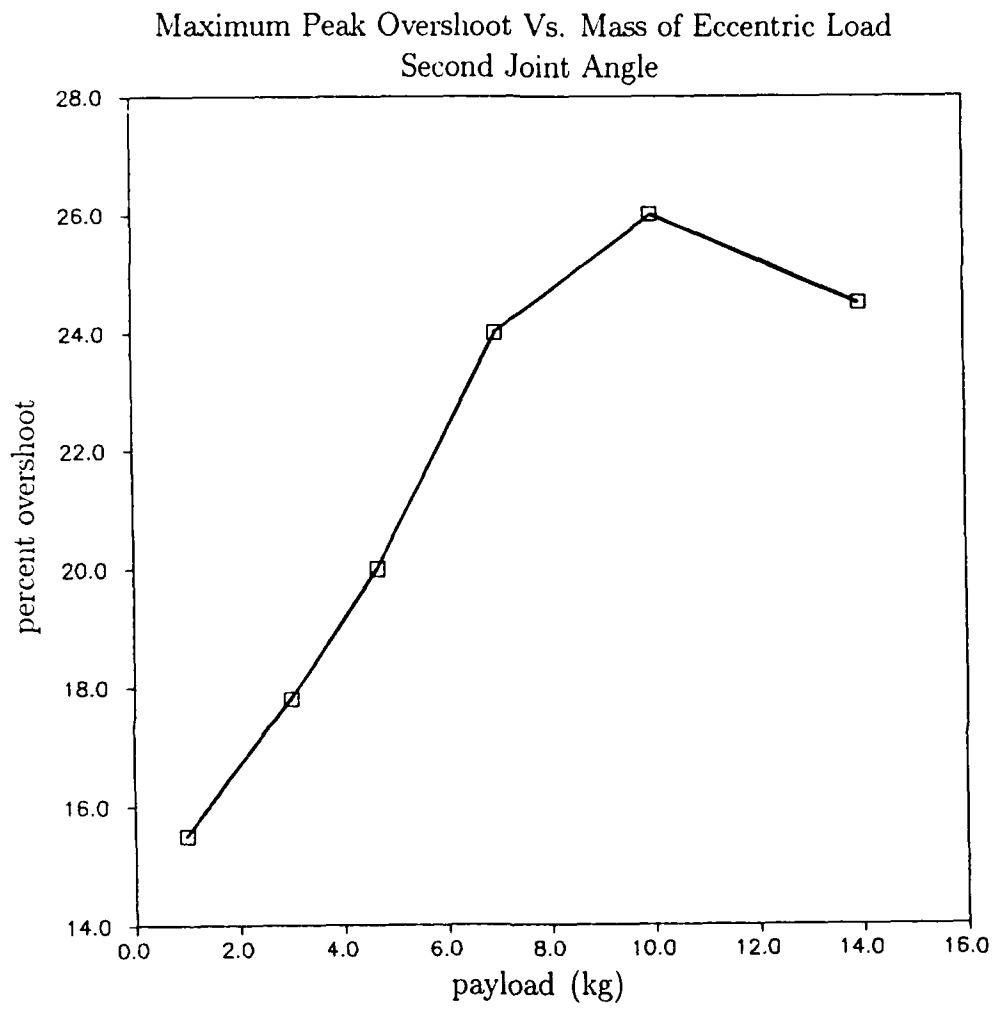


Fig. 21

Required Settling Time for End-Effector
Vibration

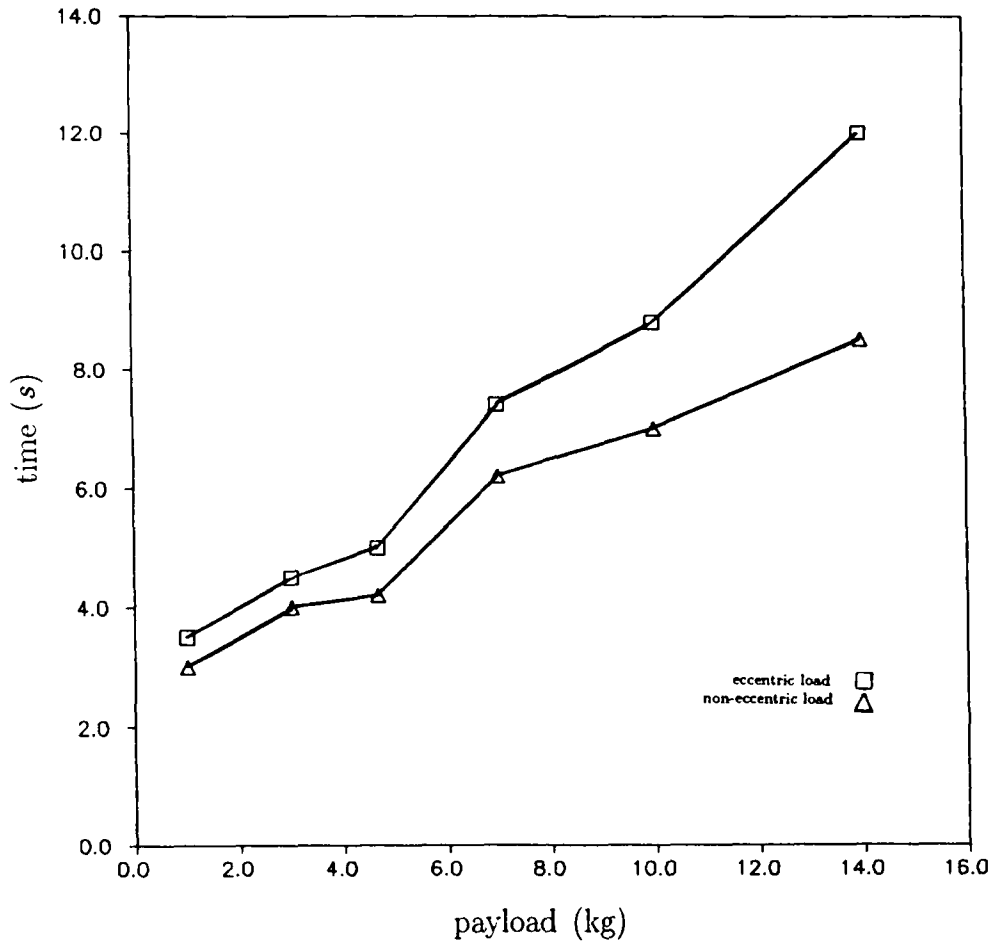


Fig. 22

Average Maximum End-Effector Lateral Displacement
at Target Time

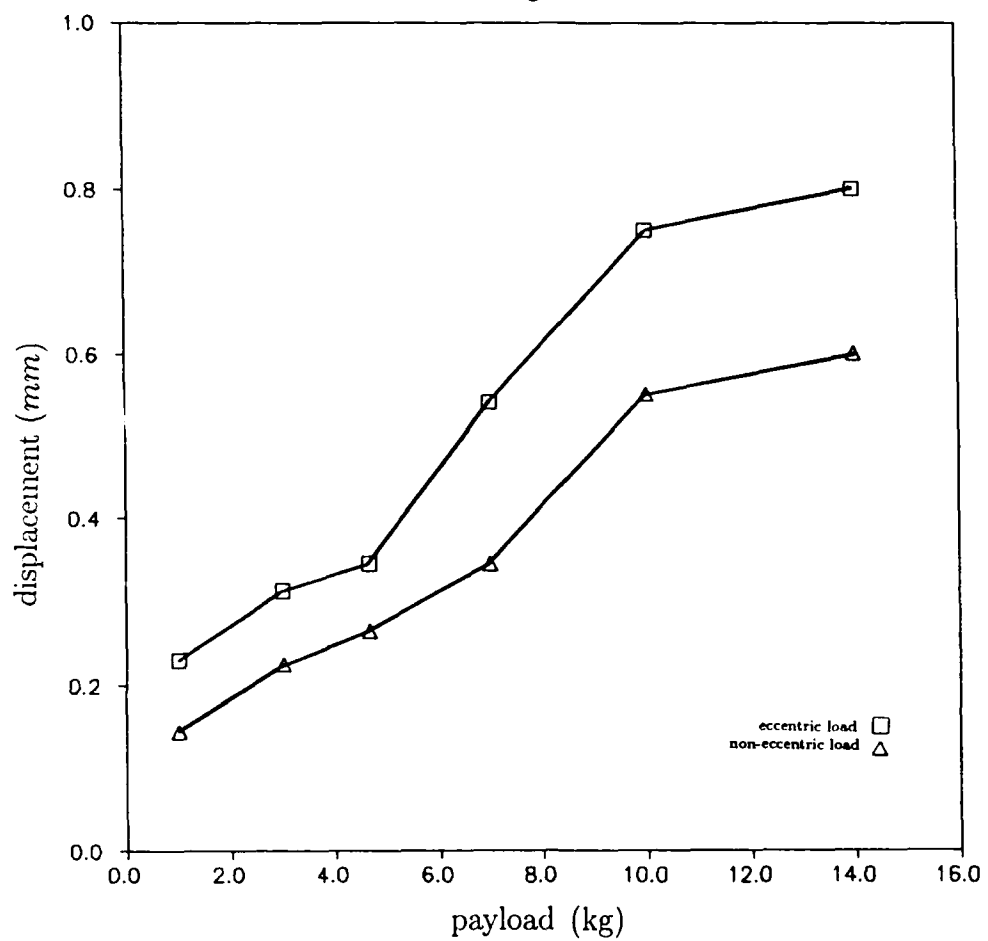


Fig. 23

Required Settling Time for End-Effector Vibration

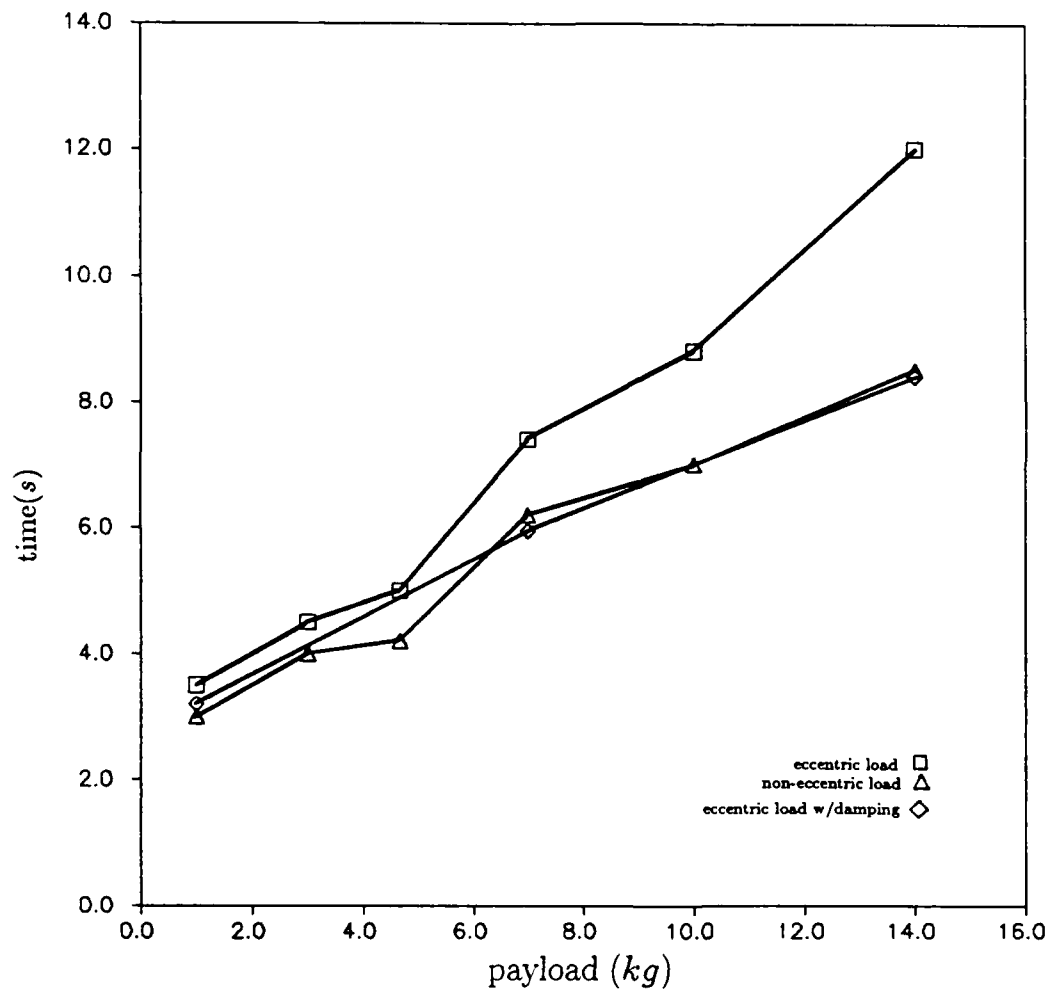


Fig. 24

Average Maximum End-Effector Lateral Displacement
at Target Time

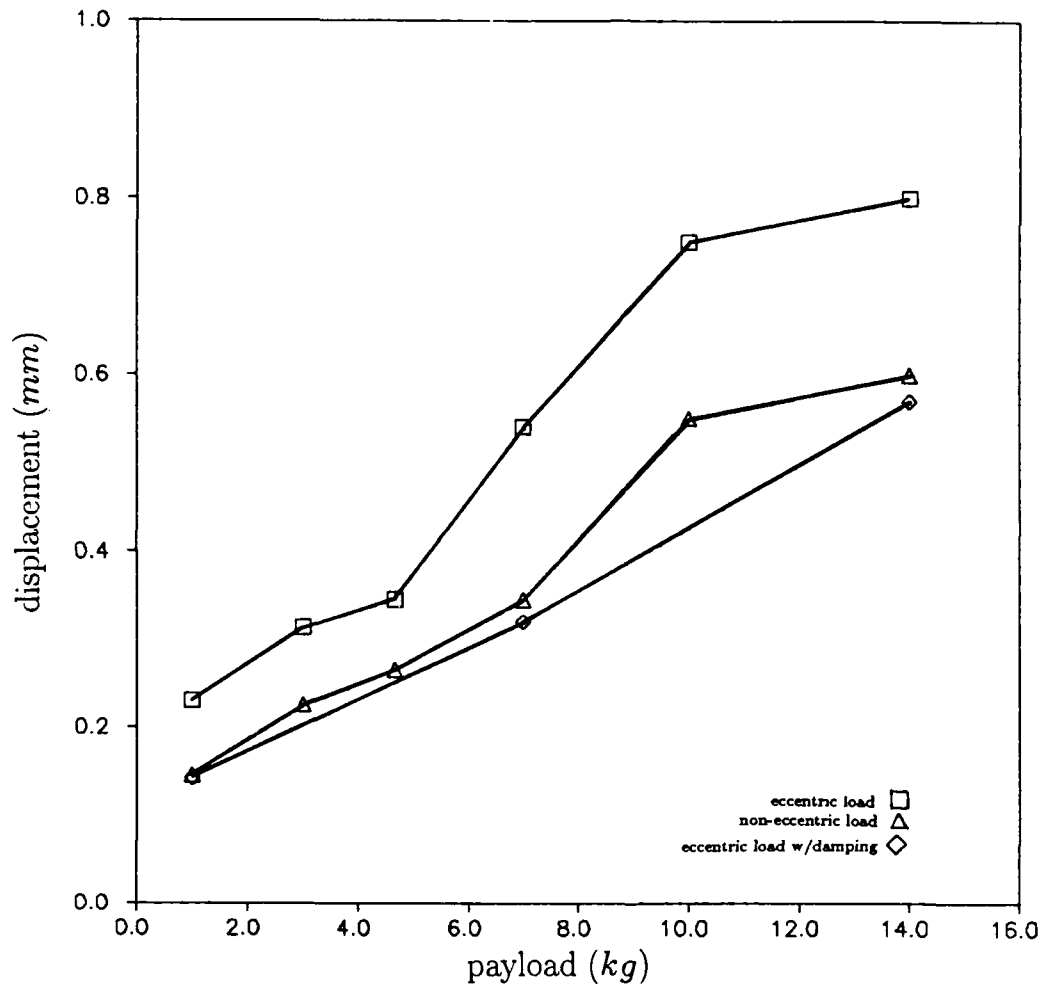


Fig. 25

Increase in Damping Ratio Required to Subdue Bending-Torsion Vibrations

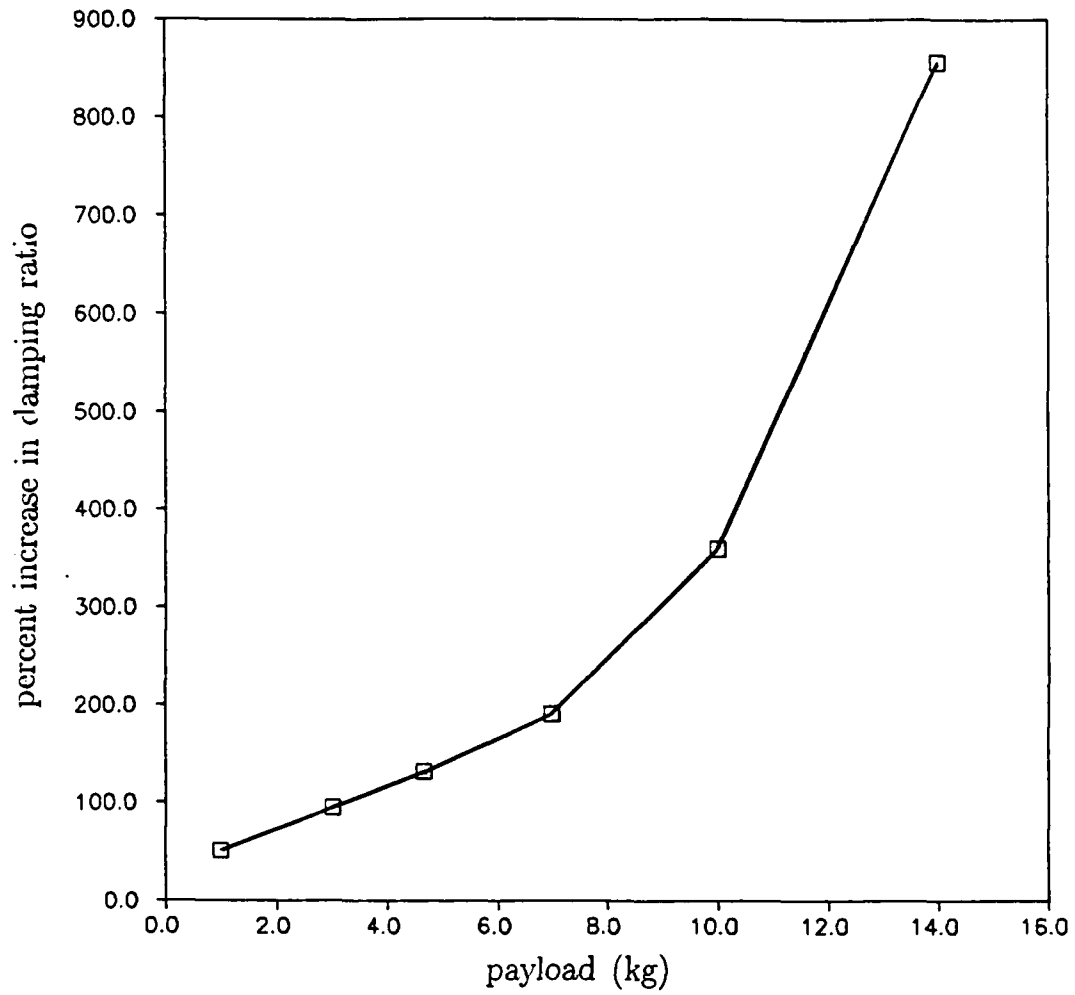


Fig. 26

Chapter 7

Appendix A

The boundary value problem for a cantilever bar in torsion is governed by the following equation for its free vibration

$$\frac{\partial}{\partial x} \left[GJ \frac{\partial \theta(x, t)}{\partial x} \right] = I \frac{\partial^2 \theta(x, t)}{\partial t^2}$$

(... assuming a uniform bar). If a payload is fixed to its end, we have the following boundary conditions:

$$\theta(0, t) = 0$$

$$GJ \frac{\partial \theta(l, t)}{\partial x} = -I_{pL} \frac{\partial^2 \theta(l, t)}{\partial t^2}$$

This problem is solved through separation of variables, and special attention is paid to the fact that the system eigenvalue also appears in the second boundary condition. The resulting transcendental frequency equation is

$$\tan \beta l = \frac{I l}{I_{pL}} \frac{1}{\beta l}$$

and the natural modes are given by:

$$\phi_r(x) = A_r \sin \beta_r x \quad r = 1, 2 \dots$$

In our particular case, the problem is somewhat extended since $I_{pL} = I_{pL}(\theta_2)$, where $\theta_2 = \theta_2(t)$ is the manipulator's second joint angle. Therefore, $I_{pL} = I_{pL}(t)$, and β , which is found iteratively using the transcendental frequency equation, is now

$$\beta = \beta(\theta_2) = \beta(t)$$

Therefore, the expression for the solution to the torsion problem using a single mode approximation

$$\theta(x, t) = q(t)\phi(x)$$

... becomes

$$\theta(x, t) = q(t)A \sin \beta(t)x$$

If this is the case, then the complete expression for the defined free vibration problem would become

$$\begin{aligned} -\beta^2 GJq \sin \beta x &= I\ddot{q} \sin \beta x + 2I\dot{q}\dot{\beta} \cos \beta x \\ &+ Iq\ddot{\beta} \cos \beta x - Iq\dot{\beta}^2 \sin \beta x \end{aligned}$$

Multiplying by $\sin \beta x$ and integrating both sides of the equation with respect to x yields

$$\begin{aligned} -\beta^2 GJq \int_0^l \sin^2 \beta x dx &= I\ddot{q} \int_0^l \sin^2 \beta x dx \\ &+ 2I\dot{q}\dot{\beta} \int_0^l \sin \beta x \cos \beta x dx \\ &+ Iq\ddot{\beta} \int_0^l \sin \beta x \cos \beta x dx - Iq\dot{\beta}^2 \int_0^l \sin^2 \beta x dx \end{aligned}$$

Since the $\int_0^l \sin^2 \beta x dx$ & $\int_0^l \sin \beta x \cos \beta x dx$ are of the order l at most (where l is the length of the bar), we can neglect the spatial dependence on x

$$-\beta^2 GJq = I\ddot{q} + 2I\dot{q}\dot{\beta} + Iq\ddot{\beta} - Iq\dot{\beta}^2$$

Instead of carrying the full extent of the details surrounding this time dependent boundary condition to the simulation, it was decided to make the simplifying assumption that $\dot{\beta}$ and $\ddot{\beta}$ and the three terms from the above equation involving these terms were small in comparison to \ddot{q} . Note that the algorithm used in the FORTRAN code *does* adjust β for each iteration, but the full consequences of its time dependence are neglected. This is based on the following reasoning:

$$\ddot{q} = \omega^2 q \gg \begin{cases} \dot{q}\dot{\beta} \\ q\ddot{\beta} \\ q\dot{\beta}^2 \end{cases}$$

or equivalently

$$\omega^2 \gg \begin{cases} \dot{q}\dot{\beta}/q \\ \ddot{\beta} \\ \dot{\beta}^2 \end{cases}$$

If this inequality is satisfied, then the following relationship stands as a close estimate to the free vibration equation:

$$-\beta^2 GJ q \sin \beta x = I \omega^2 q \sin \beta x$$

... and

$$\frac{-\beta^2 GJ}{I} = \omega^2$$

Hence, for this assumption to be valid, we require that the following must be true:

$$\omega = \sqrt{\frac{-\beta^2 GJ}{I}} \gg \dot{\beta}$$

A permitted assumption is that β is small. Therefore, from the frequency equation we can obtain an estimate for $\dot{\beta}$ in the following manner :

$$\tan \beta l = \frac{Il}{I_p L} \frac{1}{\beta l}$$

$$\text{let } \mu = \frac{H}{I_{pL}}$$

$$\tan \beta l = \frac{\mu}{\beta l}$$

... with β small we have

$$(\beta l)^2 = \mu$$

therefore

$$\dot{\beta} = \frac{\dot{\mu}}{2l\sqrt{\mu}}$$

If we consider as an example the case where the payload is $1kg$ and the bar is $1m$ in length and configured as the manipulator links were, calculations lead to the following values:

$$\omega^2 \approx 3700$$

$$\omega \approx 61$$

$$\dot{\beta} \approx 0.027$$

... and indeed $\omega \gg \dot{\beta}$. Thus, the previous approximation is justified. A similar argument can be used in the case of the lateral vibration of the links.

Chapter 8

Appendix B

The governing set of equations of motion for each separate model may be derived from the full expression of the equations of motion for the six -degree-of-freedom model TTFEL by removing non-applicable terms.

Specifically, for model TTFEL, all terms involving the variables representing first link lateral vibration, $q(t)$ and $\psi(y_1)$, should be removed and the resulting five equations of motion will result.

Furthermore, for model TTEL, all terms involving the variables that represent second link lateral vibration, $b(t)$ and $\epsilon(y_2)$, should be removed as well thus yielding the desired four coupled equations of motion.

Finally, for model TT, all terms involving an eccentrically positioned load are also removed, and for model RR, only the rigid-link terms should remain.

8.1 Equations for Model TTFEL

The full form of the equations of motion for the six degree of freedom model will be listed as compactly as possible by defining the terms that appear in the matrix form of the system as shown below.

$$\begin{bmatrix} I_{11} & I_{12} & I_{13} & I_{14} & I_{15} & I_{16} \\ I_{21} & I_{22} & I_{23} & I_{24} & I_{25} & I_{26} \\ I_{31} & I_{32} & I_{33} & I_{34} & I_{35} & I_{36} \\ I_{41} & I_{42} & I_{43} & I_{44} & I_{45} & I_{46} \\ I_{51} & I_{52} & I_{53} & I_{54} & I_{55} & I_{56} \\ I_{61} & I_{62} & I_{63} & I_{64} & I_{65} & I_{66} \end{bmatrix} \begin{bmatrix} \ddot{\theta}_1 \\ \ddot{\theta}_2 \\ \ddot{\Lambda}_1 \\ \ddot{\alpha}_1 \\ \ddot{q}_1 \\ \ddot{b}_1 \end{bmatrix} + \begin{bmatrix} \dot{\theta}_1 B_{11} \\ \dot{\theta}_2 B_{21} \\ \dot{\Lambda}_1 B_{31} \\ \dot{\alpha}_1 B_{41} \\ \dot{q} B_{51} \\ \dot{b} B_{61} \end{bmatrix} + \begin{bmatrix} C_{11} \\ C_{21} \\ C_{31} \\ C_{41} \\ C_{51} \\ C_{61} \end{bmatrix} = \begin{bmatrix} T_1 \\ T_2 \\ 0 \\ 0 \\ 0 \\ 0 \end{bmatrix}$$

$$\begin{aligned}
 I_{11} = & A_1(S_1 + q^2 V_5) + A_2 l_1^2 S_4 + A_2 S_2 \\
 & + 2A_2 S_3 [l_1 C(\theta_2 + \zeta_1) + q\psi S(\theta_2 + \zeta_1)] \\
 & + 2A_2 b V_3 [q\psi C(\theta_2 + \zeta_1) - l_1 S(\theta_2 + \zeta_1)] \\
 & + M_{pL} \{ l_1^2 + 2e\Lambda\Gamma l_1 S\zeta_1 + l_2^2 + 2e(\alpha\lambda - 1)l_2 S\zeta_2 \}
 \end{aligned}$$

$$\begin{aligned}
& + 2M_{pL}[l_1 l_2 C(\theta_2 + \zeta_1) + S(\theta_2 + \zeta_1)(l_2 q \psi - l_1 b \epsilon) + e \Lambda \Gamma l_2 S \theta_2 - e l_1 S(\theta_2 + \zeta_1 + \zeta_2)] \\
I_{12} = & A_2 S_2 + A_2 S_3 [l_1 C(\theta_2 + \zeta_1) + q \psi S(\theta_2 + \zeta_1)] \\
& + A_2 b V_3 [q \psi C(\theta_2 + \zeta_1) - l_1 S(\theta_2 + \zeta_1)] \\
& + M_{pL} \{ l_2^2 + 2e(\alpha \lambda - 1) l_2 S \zeta_2 + l_1 l_2 C(\theta_2 + \zeta_1) \} \\
& + M_{pL} \{ S(\theta_2 + \zeta_1)(l_2 q \psi - l_1 b \epsilon) + e \Lambda \Gamma l_2 S \theta_2 - e l_1 S(\theta_2 + \zeta_1 + \zeta_2) \} \\
I_{13} = & M_{pL} e \Gamma (\alpha \lambda + 1) l_1 \\
& - M_{pL} e \Gamma [l_2 C \theta_2 - \Lambda \Gamma l_2 S \theta_2 S(\theta_2 + \zeta_2)] \\
I_{14} = & M_{pL} e \lambda \Lambda \Gamma (\alpha \lambda - 1) l_2 C \theta_2 \\
& - M_{pL} e \lambda \{ (\alpha \lambda + 1) l_2 + (\alpha \lambda + 1) l_1 C(\theta_2 + \zeta_1 + \zeta_2) \} \\
I_{15} = & A_1 V_4 + A_2 l_1 \psi S_4 + A_2 S_2 \psi' \\
& + A_2 S_3 \psi' [l_1 C(\theta_2 + \zeta_1) + q \psi S(\theta_2 + \zeta_1)] \\
& - A_2 b \psi S(\theta_2 + \zeta_1) V_3 + A_2 \psi C(\theta_2 + \zeta_1) S_3 \\
& + A_2 b \psi' [q \psi C(\theta_2 + \zeta_1) - l_1 S(\theta_2 + \zeta_1)] V_3 \\
& + M_{pL} \{ \psi (l_1 + e \Lambda \Gamma S \zeta_1) + \psi' (l_2^2 + 2e(\alpha \lambda - 1) l_2 S \zeta_2) \} \\
& + M_{pL} \psi' \{ l_1 l_2 C(\theta_2 + \zeta_1) + S(\theta_2 + \zeta_1)(l_2 q \psi - l_1 b \epsilon) + e \Lambda \Gamma l_2 S \theta_2 - e l_1 S(\theta_2 + \zeta_1 + \zeta_2) \} \\
& + M_{pL} \psi [l_2 C(\theta_2 + \zeta_1) + e(\alpha \lambda - 1) S(\theta_2 + \zeta_1 + \zeta_2)] \\
& + M_{pL} \psi' l_1 S \zeta_1 e \Lambda (\alpha \lambda + 1) \\
I_{16} = & A_2 l_1 C(\theta_2 + \zeta_1) V_3 + A_2 V_2 \\
& + M_{pL} \{ \epsilon (l_1 C(\theta_2 + \zeta_1) - e \Lambda \Gamma S \theta_2) + \epsilon (l_2 + e(\alpha \lambda - 1) S \zeta_2) \} \\
& + M_{pL} \epsilon' e (\alpha \lambda - 1) l_2 S \zeta_2 - \epsilon' S \theta_2 e \Lambda \Gamma l_2 \\
& + M_{pL} \epsilon' e (\alpha \lambda - 1) l_1 S(\theta_2 + \zeta_1 + \zeta_2) \\
I_{22} = & A_2 S_2 + M_{pL} [C^2 \theta_2 l_2^2 (\Lambda \Gamma)^2 + l_2^2 \\
& + 2e(\alpha \lambda - 1) l_2 S \zeta_2] \\
I_{23} = & A_2 / 2 \Lambda \Gamma^2 S(2\theta_2) S_2 + A_2 b \Lambda \Gamma^2 C(2\theta_2) V_2
\end{aligned}$$

$$\begin{aligned}
& -M_{pL}\Gamma[e l_2 C\theta_2 - e\Lambda\Gamma l_2 S\theta_2 S(\theta_2 + \zeta_2)] \\
& + M_{pL}\Gamma\{1/2S(2\theta_2)l_2^2\Lambda\Gamma + e\Lambda\Gamma[S(\theta_2 + \zeta_2)(\alpha\lambda - 1)S\theta_2 l_2 - l_2 C\theta_2(\alpha\lambda + 1)C(\theta_2 + \zeta_2)]\} \\
I_{24} & = -\lambda l_2 e(\alpha\lambda + 1)M_{pL} \\
I_{25} & = A_2 S_2 \psi' - A_2 b \psi S(\theta_2 + \zeta_1) V_3 + A_2 \psi C(\theta_2 + \zeta_1) S_3 \\
& + M_{pL}\{l_2^2 + 2e(\alpha\lambda - 1)l_2 S\zeta_2 \psi\} \\
& + M_{pL}\psi\{l_2 C(\theta_2 + \zeta_1) + e(\alpha\lambda - 1)S(\theta_2 + \zeta_1 + \zeta_2)\} \\
I_{26} & = A_2 V_2 + M_{pL}\epsilon(l_2 + e(\alpha\lambda - 1)S\zeta_2) \\
& + M_{pL}\epsilon'e(\alpha\lambda - 1)l_2 S\zeta_2 - M_{pL}e\Lambda\Gamma l_2 S\theta_2 \epsilon' \\
I_{33} & = S_7 + A_2 \Gamma^2 S^2 \theta_2 S_2 + A_2 b \Gamma^2 S(2\theta_2) V_2 + S_8 \\
& + M_{pL}\Gamma^2\{S^2 \theta_2 l_2^2 + 2e^2 + S(2\theta_2)l_2 b \epsilon\} \\
& + 2M_{pL}\Gamma^2\{e l_2 S\theta_2 \Lambda\Gamma - e l_2 S\theta_2 \alpha \lambda C(\theta_2 + \zeta_2)\} \\
I_{34} & = C\theta_2 S_5 \\
I_{35} & = -M_{pL}\Gamma\psi[\Lambda\Gamma l_2 S\theta_2 + e(\alpha\lambda + 1)] \\
& - M_{pL}\Gamma\psi'l_2 e[C\theta_2 - \Lambda\Gamma S\theta_2 S(\theta_2 + \zeta_2)] \\
I_{36} & = A_2/2\Lambda\Gamma^2 S(2\theta_2) V_2 + A_2 \Lambda\Gamma^2 C^2 \theta_2 b V_1 \\
& + M_{pL}\Gamma\epsilon[S(2\theta_2)l_2 \Lambda\Gamma - e C\theta_2] \\
I_{44} & = S_9 \\
I_{45} & = eM_{pL}\lambda\psi'\{\Lambda\lambda(\alpha\lambda - 1)l_2 C\theta_2 - (\alpha\lambda + 1)l_2\} \\
& - eM_{pL}\lambda\psi[\Lambda\Gamma + (\alpha\lambda + 1)C(\theta_2 + \zeta_1 + \zeta_2)] \\
I_{46} & = -\epsilon\lambda e(\alpha\lambda + 1)M_{pL} \\
I_{55} & = A_1 V_5 + A_2 \psi^2 S_4 + A_2 \psi'\psi' \\
& + 2A_2 \psi\psi'[C(\theta_2 + \zeta_1)S_3 - bS(\theta_2 + \zeta_1)V_3] \\
& + M_{pL}\{\psi^2 + \psi'\psi'[l_2 + 2e(\alpha\lambda - 1)l_2 S\zeta_2]\} \\
& + 2M_{pL}\psi\psi'\{l_2 C(\theta_2 + \zeta_1) + e(\alpha\lambda - 1)S(\theta_2 + \zeta_1 + \zeta_2)\}
\end{aligned}$$

$$\begin{aligned}
& + 2M_{pL}\psi\psi'e\Lambda\Gamma S\zeta_1(\alpha\lambda + 1) \\
I_{56} = & A_2\psi C(\theta_2 + \zeta_1)V_3 + A_2\psi'V_2 + M_{pL}\psi\epsilon C(\theta_2 + \zeta_1) \\
& + M_{pL}\epsilon\psi' \{l_2 + e(\alpha\lambda - 1)S\zeta_2 + e(\alpha\lambda - 1)S(\theta_2 + \zeta_1 + \zeta_2)\} \\
& + M_{pL}\psi'\epsilon' \{e(\alpha\lambda - 1)l_2S\zeta_2 - e\Lambda\Gamma l_2S\theta_2\} \\
I_{66} = & A_2V_1 + M_{pL} \{\epsilon^2 + 2\epsilon'\epsilon eS\zeta_2\}
\end{aligned}$$

Note that the mass matrix is symmetric, therefore:

$$I_{21} = I_{12}$$

$$I_{31} = I_{13}$$

$$I_{41} = I_{14}$$

$$I_{51} = I_{15}$$

⋮

At this point, the other terms can be defined as well:

$$\dot{\theta}_1 B_{11} + C_{11} \equiv$$

$$\begin{aligned}
& 2A_1\dot{\theta}_1 q \dot{q} V_5 - A_2\dot{b}l_1 S(\theta_2 + \zeta_1)(\dot{\theta}_2 + \dot{q}\psi')V_3 \\
& + A_2S_3(2\dot{\theta}_1 + \dot{\theta}_2 + \dot{q}\psi') \left[-l_1(\dot{\theta}_2 + \dot{q}\psi')S(\theta_2 + \zeta_1) + \dot{q}\psi S(\theta_2 + \zeta_1) + q\psi C(\theta_2 + \zeta_1)(\dot{\theta}_2 + \dot{q}\psi') \right] \\
& - A_2\dot{b}q\psi S(\theta_2 + \zeta_1)V_3 \\
& - A_2\dot{b}q\psi C(\theta_2 + \zeta_1)(\dot{\theta}_2 + \dot{q}\psi')V_3 \\
& - A_2\dot{q}\psi S(\theta_2 + \zeta_1)(\dot{\theta}_2 + \dot{q}\psi')S_3 \\
& A_2\dot{b}(2\dot{\theta}_1 + \dot{\theta}_2 + \dot{q}\psi') [q\psi C(\theta_2 + \zeta_1) - l_1S(\theta_2 + \zeta_1)] V_3
\end{aligned}$$

$$\begin{aligned}
& +A_2b(2\dot{\theta}_1 + \dot{\theta}_2 + \dot{q}\psi') \left[\dot{q}\psi C(\theta_2 + \zeta_1) - q\psi S(\theta_2 + \zeta_1)(\dot{\theta}_2 + \dot{q}\psi') - l_1 C(\theta_2 + \zeta_1)(\dot{\theta}_2 + \dot{q}\psi') \right] V_3 \\
& \quad + 2M_{pL}e\dot{\theta}_1\Gamma l_1(\dot{\Lambda}S\zeta_1 + \Lambda\dot{q}\psi') \\
& \quad - M_{pL}\dot{b}\epsilon \left[l_1 S(\theta_2 + \zeta_1)(\dot{\theta}_2 + \dot{q}\psi') + e\dot{\Lambda}\lambda S\theta_2 + e\Lambda\Gamma C\theta_2\dot{\theta}_2 \right] + M_{pL}qe\Gamma(\dot{\Lambda}S\zeta_1 + \Lambda\dot{q}\psi') \\
& \quad + 2eM_{pL}(\dot{\theta}_1 + \dot{\theta}_2 + \dot{q}\psi') \left[\dot{\alpha}\lambda l_2 S\zeta_2 + (\alpha\lambda - 1)l_2\dot{b}\epsilon' \right] \\
& + e\dot{\Lambda}\Gamma M_{pL} \left[\dot{\Lambda}\Gamma l_2 S\theta_2 S(\theta_2 + \zeta_2) + \Lambda\Gamma C\theta_2\dot{\theta}_2 S(\theta_2 + \zeta_2) + \Lambda\Gamma l_2 S\theta_2 C(\theta_2 + \zeta_2)(\dot{\theta}_2 + \dot{b}\epsilon') + l_2 S\theta_2\dot{\theta}_2 \right] \\
& \quad + (2\dot{\theta}_1 + \dot{\theta}_2 + \dot{q}\psi')M_{pL} \left[-l_1 l_2 S(\theta_2 + \zeta_2)(\dot{\theta}_2 + \dot{q}\psi') + C(\theta_2 + \zeta_1)(\dot{\theta}_2 + \dot{q}\psi')(l_2 q\psi - l_1 b\epsilon) \right] \\
& \quad + (2\dot{\theta}_1 + \dot{\theta}_2 + \dot{q}\psi')M_{pL} \left[S(\theta_2 + \zeta_1)(l_2 \dot{q}\psi - l_1 \dot{b}\epsilon) \right] \\
& \quad + (2\dot{\theta}_1 + \dot{\theta}_2 + \dot{q}\psi')M_{pL} \left[e\dot{\Lambda}l_2 S\theta_2 + e\Lambda\Gamma l_2 C\theta_2\dot{\theta}_2 - e l_1 C(\theta_2 + \zeta_1 + \zeta_2)(\dot{\theta}_2 + \dot{q}\psi' + \dot{b}\epsilon') \right] \\
& \quad + \dot{q}\psi M_{pL} \left[-l_2 S(\theta_2 + \zeta_1)(\dot{\theta}_2 + \dot{q}\psi') + e\dot{\alpha}\lambda S(\theta_2 + \zeta_1 + \zeta_2) \right] \\
& \quad + \dot{q}\psi M_{pL} e(\alpha\lambda - 1)C(\theta_2 + \zeta_1 + \zeta_2)(\dot{\theta}_2 + \dot{q}\psi' + \dot{b}\epsilon') \\
& \quad + \dot{b}\epsilon e M_{pL} \left[\dot{\alpha}\lambda S\zeta_2 + (\alpha\lambda - 1)\dot{b}\epsilon' \right] + \dot{\Lambda}\Gamma e\dot{\alpha}\lambda l_1 \\
& \quad + \dot{\alpha}\lambda e M_{pL} \left[\dot{\Lambda}\lambda(\alpha\lambda - 1)l_2 C\theta_2 - \Lambda\lambda(\alpha\lambda - 1)l_2 S\theta_2\dot{\theta}_2 - \dot{\alpha}\lambda l_2 \right] \\
& \quad + \dot{b}\epsilon' e M_{pL} \dot{\alpha}\lambda l_2 S\zeta_2 + \dot{b}\epsilon' e(\alpha\lambda - 1)l_2 \dot{b}\epsilon' \\
& \quad - \dot{b}\epsilon' C\theta_2\dot{\theta}_2 e\Lambda\Gamma M_{pL} l_2 - \dot{b}\epsilon' S\theta_2 M_{pL} e\dot{\Lambda}\Gamma l_2 \\
& \quad + \dot{b}\epsilon' e\dot{\alpha}\lambda M_{pL} l_1 S(\theta_2 + \zeta_1 + \zeta_2) \\
& \quad + \dot{b}\epsilon' e(\alpha\lambda - 1)M_{pL} l_1 C(\theta_2 + \zeta_1 + \zeta_2)(\dot{\theta}_2 + \dot{q}\psi' + \dot{b}\epsilon') \\
& \quad - \dot{\alpha}\lambda e\dot{\alpha}\lambda M_{pL} l_1 C(\theta_2 + \zeta_1 + \zeta_2) \\
& \quad + \dot{\alpha}\lambda e M_{pL}(\alpha\lambda + 1)S(\theta_2 + \zeta_1 + \zeta_2)(\dot{\theta}_2 + \dot{q}\psi' + \dot{b}\epsilon') \\
& \quad + \dot{q}\psi' M_{pL} l_1 \dot{b}\epsilon' e\Lambda\Gamma(\alpha\lambda + 1) \\
& \quad + \dot{q}\psi' M_{pL} l_1 S\zeta_1 e\dot{\Lambda}\Gamma(\alpha\lambda + 1) \\
& \quad + \dot{q}\psi' M_{pL} l_1 S\zeta_1 e\Lambda\Gamma\dot{\alpha}\lambda
\end{aligned}$$

$$+M_{pL}g[l_1C\theta_1 + l_2C\beta - eS(\beta + \zeta_2)]$$

$$+m_1gC\theta_1l_1/2$$

$$+m_2g[l_1C\theta_1 + C\beta l_2/2]$$

... Also

$$\dot{\theta}_2 B_{21} + C_{21} \equiv$$

$$A_2\dot{\theta}_1 S_3 \left\{ \dot{q}\psi S(\theta_2 + \zeta_1) + [q\psi C(\theta_2 + \zeta_1) - l_1 S(\theta_2 + \zeta_1)](\dot{\theta}_2 + \dot{q}\psi') \right\}$$

$$+ A_2 b \dot{\theta}_1 [q\psi C(\theta_2 + \zeta_1) - l_1 S(\theta_2 + \zeta_1)] V_3$$

$$+ A_2 V_3 b \dot{\theta}_1 \left[\dot{q}\psi C(\theta_2 + \zeta_1) - (\dot{\theta}_2 + \dot{q}\psi') [q\psi S(\theta_2 + \zeta_1) + l_1 C(\theta_2 + \zeta_1)] \right]$$

$$- \dot{\theta}_2^2 C\theta_2 S\theta_2 l_2^2 \Lambda^2 \Gamma^2 M_{pL} + 2\dot{\theta}_2 C^2 \theta_2 l_2 \Lambda \dot{\Lambda} \Gamma^2 M_{pL}$$

$$+ 2e(\dot{\theta}_1 + \dot{\theta}_2 + \dot{q}\psi') l_2 \left[\dot{\alpha} \lambda S\zeta_2 + (\alpha\lambda - 1) \dot{b}e' \right] M_{pL}$$

$$+ \dot{\Lambda} \Gamma e l_2 \left[S\theta_2 \dot{\theta}_2 + \dot{\Lambda} \Gamma S\theta_2 S(\theta_2 + \zeta_2) + \Lambda \Gamma C\theta_2 \dot{\theta}_2 S(\theta_2 + \zeta_2) + \Lambda \Gamma S\theta_2 C(\theta_2 + \zeta_2) (\dot{\theta}_2 + \dot{b}e') M_{pL} \right]$$

$$+ \dot{\theta}_1 M_{pL} \left[-S(\theta_2 + \zeta_1) (\dot{\theta}_2 + \dot{q}\psi') l_1 l_2 + C(\theta_2 + \zeta_1) (\dot{\theta}_2 + \dot{q}\psi') (l_2 q\psi - l_1 b e) + S(\theta_2 + \zeta_1) (l_2 \dot{q}\psi - l_1 \dot{b}e) \right]$$

$$+ \dot{\theta}_1 M_{pL} e \left[\dot{\Lambda} \Gamma l_2 S\theta_2 + \Lambda \Gamma \dot{\theta}_2 C\theta_2 \right]$$

$$- \dot{\theta}_1 M_{pL} e l_1 C(\theta_2 + \zeta_1 + \zeta_2) (\dot{\theta}_2 + \dot{q}\psi' + \dot{b}e')$$

$$+ \dot{q}\psi M_{pL} \left[-l_2 S(\theta_2 + \zeta_1) (\dot{\theta}_2 + \dot{q}\psi') + e \dot{\alpha} \lambda S(\theta_2 + \zeta_1 + \zeta_2) \right]$$

$$+ \dot{q}\psi M_{pL} e (\alpha\lambda - 1) C(\theta_2 + \zeta_1 + \zeta_2) (\dot{\theta}_2 + \dot{q}\psi' + \dot{b}e')$$

$$+ \dot{b}e e M_{pL} \left[\dot{\alpha} \lambda S\zeta_2 + (\alpha\lambda - 1) \dot{b}e' \right]$$

$$\dot{\Lambda} \Gamma^2 l_2 M_{pL} \left[\dot{\theta}_2 C(2\theta_2) l_2 \Lambda + l_2 \dot{\Lambda} S(2\theta_2) / 2 + e \dot{\Lambda} \{ S(\theta_2 + \zeta_2) (\alpha\lambda - 1) S\theta_2 - C\theta_2 (\alpha\lambda + 1) C(\theta_2 + \zeta_2) \} \right]$$

$$+ \dot{\Lambda} \Gamma l_2 e \Lambda \Gamma M_{pL} \left[(\dot{\theta}_2 + \dot{b}e') C(\theta_2 + \zeta_2) (\alpha\lambda - 1) S\theta_2 + S(\theta_2 + \zeta_2) \dot{\alpha} \lambda S\theta_2 + S(\theta_2 + \zeta_2) (\alpha\lambda - 1) C\theta_2 \dot{\theta}_2 \right]$$

$$+ \dot{\Lambda} \Gamma l_2 e \Lambda \Gamma M_{pL} \left[-C\theta_2 \dot{\alpha} \lambda C(\theta_2 + \zeta_2) + C\theta_2 (\alpha\lambda + 1) S(\theta_2 + \zeta_2) (\dot{\theta}_2 + \dot{b}e') \right]$$

$$- \dot{\alpha} \lambda e \dot{\alpha} \lambda l_2 M_{pL} + \dot{b}e' e \dot{\alpha} \lambda l_2 M_{pL} S\zeta_2$$

$$+ \dot{b}e' e (\alpha\lambda - 1) l_2 \dot{b}e' M_{pL}$$

$$\begin{aligned}
& -e\dot{\Lambda}\Gamma l_2 S\theta_2 \dot{b}\epsilon' M_{pL} \\
& -e\dot{\Lambda}\Gamma l_2 C\theta_2 \dot{\theta}_2 \dot{b}\epsilon' M_{pL} \\
& +A_2 \dot{\theta}_1 \dot{b} l_1 S(\theta_2 + \zeta_1) V_3 \\
& -A_2 \dot{\theta}_1 (\dot{\theta}_1 + \dot{\theta}_2 + \dot{q}\psi') [-l_1 S(\theta_2 + \zeta_1) + q\psi C(\theta_2 + \zeta_1)] S_3 \\
& +A_2 b \dot{\theta}_1 V_3 \dot{q}\psi C(\theta_2 + \zeta_1) + A_2 \dot{q}\psi \dot{\theta}_1 S_3 S(\theta_2 + \zeta_1) \\
& +A_2 b \dot{\theta}_1 (\dot{\theta}_1 + \dot{\theta}_2 + \dot{q}\psi') [q\psi S(\theta_2 + \zeta_1) + l_1 C(\theta_2 + \zeta_1)] V_3 \\
& +A_2 \dot{\Lambda}\Gamma^2 S(2\theta_2) \dot{b} b \dot{\Lambda} V_1 \\
& +\dot{\theta}_1 \dot{b} \epsilon [l_1 S(\theta_2 + \zeta_1) + e\dot{\Lambda}\Gamma C\theta_2] M_{pL} + \dot{q} \dot{b} \psi \epsilon S(\theta_2 + \zeta_1) M_{pL} \\
& -(\dot{\Lambda}\Gamma)^2 M_{pL} l_2 [S\theta_2 C\theta_2 l_2 + C(2\theta_2) b \epsilon + eC\theta_2 \dot{\Lambda}\Gamma - e\alpha \lambda C(2\theta_2 + \zeta_2)] \\
& -\dot{\Lambda} \dot{b} \Gamma \epsilon M_{pL} [C(2\theta_2) l_2 \dot{\Lambda}\Gamma + eS\theta_2 + l_2 \dot{\Lambda}\Gamma C(2\theta_2)] \\
& -(\dot{\theta}_1 + \dot{\theta}_2 + \dot{q}\psi') \dot{\Lambda} \Gamma \epsilon l_2 M_{pL} [\dot{\Lambda}\Gamma S(2\theta_2 + \zeta_2) + S\theta_2] \\
& -\dot{\theta}_1 (\dot{\theta}_1 + \dot{\theta}_2 + \dot{q}\psi') M_{pL} [-S(\theta_2 + \zeta_1) l_1 l_2 + C(\theta_2 + \zeta_1) (l_2 q\psi - l_1 b \epsilon) + e\dot{\Lambda}\Gamma l_2 C\theta_2 - e l_1 C(\theta_2 + \zeta_1 + \zeta_2)] \\
& -\dot{q}\psi (\dot{\theta}_1 + \dot{\theta}_2 + \dot{q}\psi') [-l_2 S(\theta_2 + \zeta_1) + e(\alpha \lambda - 1) C(\theta_2 + \zeta_1 + \zeta_2)] M_{pL} \\
& +\dot{\Lambda} \dot{q} \Gamma \psi C\theta_2 \dot{\Lambda}\Gamma l_2 M_{pL} \\
& -\dot{\theta}_2 \dot{\Lambda}\Gamma^2 \Lambda [C(2\theta_2) l_2^2 + e l_2 \{S(2\theta_2 + \zeta_2)(\alpha \lambda - 1) + (\alpha \lambda + 1) S(2\theta_2 + \zeta_2)\}] M_{pL} \\
& -\dot{\alpha} \lambda \dot{\theta}_2 e(\alpha \lambda - 1) \dot{\Lambda}\Gamma S\theta_2 l_2 M_{pL} + \dot{\alpha} \lambda (\dot{\theta}_1 + \dot{\theta}_2 + \dot{q}\psi') e \dot{\Lambda}\Gamma (\alpha \lambda - 1) l_2 S\theta_2 M_{pL} \\
& +M_{pL} (\dot{\theta}_1 + \dot{\theta}_2 + \dot{q}\psi') \dot{b} \epsilon' e \dot{\Lambda}\Gamma l_2 C\theta_2 - M_{pL} \dot{b} \epsilon' \dot{\theta}_1 e(\alpha \lambda - 1) l_1 C(\theta_2 + \zeta_1 + \zeta_2) \\
& -\dot{\theta}_1 \dot{\alpha} \lambda e(\alpha \lambda + 1) l_1 S(\theta_2 + \zeta_1 + \zeta_2) M_{pL} \\
& +M_{pL} g [l_2 C\beta - eS(\beta + \zeta_2)] + m_2 g C\beta l_2 / 2
\end{aligned}$$

... Also

$$\begin{aligned}
& \dot{\Lambda} B_{31} + C_{31} \equiv \\
& A_2 \dot{b} \dot{\Lambda}\Gamma^2 \dot{\theta}_2 C(2\theta_2) V_2
\end{aligned}$$

$$\begin{aligned}
& -a_2 \Lambda \Gamma^2 S(2\theta_2) \dot{\theta}_2 \dot{b} \dot{b} V_1 \\
& + A_2 \Lambda \Gamma^2 C^2 \theta_2 \dot{b} \dot{b} V_1 \\
& + A_2 \Gamma^2 \dot{\theta}_2 \left[\dot{\Lambda} S(2\theta_2) + \dot{\theta}_2 \Lambda C(2\theta_2) \right] S_2 \\
& + A_2 \dot{b} \left[\Lambda \dot{\theta}_2 C(2\theta_2) + \dot{\Lambda} S(2\theta_2) \right] V_2 \Gamma^2 \\
& + 2A_2 b \Gamma^2 \left[\dot{\Lambda} C(2\theta_2) - \Lambda \dot{\theta}_2 S(2\theta_2) \right] \dot{\theta}_2 V_2 \\
& + \dot{\Lambda} \Gamma^2 l_2 S(2\theta_2) \left[\dot{\theta}_2 l_2 + \dot{b} \epsilon \right] M_{pL} \\
& + 2\dot{\Lambda} \Gamma^2 l_2 M_{pL} \left[C(2\theta_2) \dot{\theta}_2 b \epsilon + e C \theta_2 \dot{\theta}_2 \Lambda \Gamma + e S \theta_2 \dot{\Lambda} \Gamma \right] \\
& + 2\dot{\Lambda} \Gamma^2 l_2 M_{pL} \left[-e \dot{\theta}_2 C \theta_2 \alpha \lambda C(\theta_2 + \zeta_2) - e S \theta_2 \dot{\alpha} \lambda C(\theta_2 + \zeta_2) + e S \theta_2 \alpha \lambda S(\theta_2 + \zeta_2) (\dot{\theta}_2 + \dot{b} \epsilon') \right] \\
& + \dot{b} \Gamma \epsilon M_{pL} \left[2\dot{\theta}_2 C(2\theta_2) l_2 \Lambda \Gamma + S(2\theta_2) l_2 \dot{\Lambda} \Gamma + e \dot{\theta}_2 S \theta_2 \right] \\
& + (\dot{\theta}_1 + \dot{\theta}_2 + \dot{q} \psi') \Gamma \epsilon l_2 M_{pL} \left[S \theta_2 \dot{\theta}_2 + \dot{\Lambda} S \theta_2 S(\theta_2 + \zeta_2) \right] \\
& + (\dot{\theta}_1 + \dot{\theta}_2 + \dot{q} \psi') \Gamma \epsilon l_2 M_{pL} \left[\Lambda \Gamma C \theta_2 \dot{\theta}_2 S(\theta_2 + \zeta_2) + \Lambda \Gamma S \theta_2 C(\theta_2 + \zeta_2) (\dot{\theta}_2 + \dot{b} \epsilon') \right] \\
& + \dot{\theta}_1 \Gamma l_1 e \dot{\alpha} \lambda M_{pL} \\
& - \dot{q} \Gamma \psi M_{pL} \left[\dot{\Lambda} \Gamma l_2 S \theta_2 + \Lambda \Gamma l_2 C \theta_2 \dot{\theta}_2 + e \dot{\alpha} \lambda \right] \\
& + \dot{\theta}_2 \Gamma^2 \dot{\theta}_2 C(2\theta_2) l_2^2 \Lambda \Gamma M_{pL} \\
& + \dot{\theta}_2 \Gamma e \Lambda \Gamma l_2 M_{pL} \left[C(\theta_2 + \zeta_2) (\dot{\theta}_2 + \dot{b} \epsilon') (\alpha \lambda - 1) S \theta_2 + S(\theta_2 + \zeta_2) \dot{\alpha} \lambda S \theta_2 + S(\theta_2 + \zeta_2) (\alpha \lambda - 1) C \theta_2 \dot{\theta}_2 \right] \\
& + \dot{\theta}_2 \Gamma e \Lambda \Gamma l_2 M_{pL} \left[S \theta_2 \dot{\theta}_2 (\alpha \lambda + 1) C(\theta_2 + \zeta_2) - C \theta_2 \dot{\alpha} \lambda C(\theta_2 + \zeta_2) + C \theta_2 (\alpha \lambda + 1) S(\theta_2 + \zeta_2) (\dot{\theta}_2 + \dot{b} \epsilon') \right] \\
& - \dot{\alpha} S \theta_2 \dot{\theta}_2 S_5 \\
& - \dot{\theta}_1^2 S \zeta_1 e \Gamma l_1 M_{pL} - \dot{\theta}_2^2 C^2 \theta_2 l_2^2 \Lambda \Gamma^2 M_{pL} \\
& + \dot{\theta}_1 \dot{b} \epsilon S \theta_2 e \Gamma M_{pL} - \dot{\theta}_1 \dot{q} \psi e \Gamma S \zeta_1 M_{pL} \\
& - (\dot{\Lambda} \Gamma)^2 \Gamma \epsilon l_2 S \theta_2 M_{pL} - \dot{\Lambda} \dot{b} M_{pL} \Gamma \epsilon l_2 \Gamma S(2\theta_2) / 2 \\
& - (\dot{\theta}_1 + \dot{\theta}_2 + \dot{q} \psi') M_{pL} \dot{\Lambda} \Gamma e \Gamma l_2 S \theta_2 S(\theta_2 + \zeta_2) \\
& - \dot{\theta}_1 M_{pL} (\dot{\theta}_1 + \dot{\theta}_2 + \dot{q} \psi') e \Gamma l_2 S \theta_2
\end{aligned}$$

$$\begin{aligned}
& +\dot{\Lambda}\dot{q}\Gamma\psi S\theta_2\Gamma l_2 M_{pL} + \dot{\alpha}\lambda\dot{\theta}_2 e(\alpha\lambda - 1)\Gamma C\theta_2 l_2 M_{pL} \\
& -\dot{\alpha}\lambda M_{pL}(\dot{\theta}_1 + \dot{\theta}_2 + \dot{q}\psi')e\Gamma(\alpha\lambda - 1)l_2 C\theta_2 \\
& +(\dot{\theta}_1 + \dot{\theta}_2 + \dot{q}\psi')\dot{b}\epsilon' S\theta_2 e\Gamma l_2 M_{pL} \\
& +\dot{\alpha}\dot{q}\lambda\psi e\Gamma M_{pL} - \dot{q}^2\psi'\psi e\Gamma S\zeta_1(\alpha\lambda + 1)M_{pL} \\
& -\dot{\theta}_1\dot{q}\psi' l_1 S\zeta_1 e\Gamma M_{pL}(\alpha\lambda + 1) \\
& +\Lambda S_6
\end{aligned}$$

... Also

$$\begin{aligned}
& \dot{\alpha}B_{41} + C_{41} \equiv \\
& -\dot{\Lambda}S\theta_2\dot{\theta}_2 S_5 \\
& -\lambda\dot{\theta}_2 e(\alpha\lambda - 1)\dot{\Lambda}\Gamma C\theta_2 l_2 M_{pL} + \lambda\dot{\theta}_2 e(\alpha\lambda - 1)\Lambda\Gamma S\theta_2\dot{\theta}_2 l_2 M_{pL} \\
& +\lambda(\dot{\theta}_1 + \dot{\theta}_2 + \dot{q}\psi')eM_{pL}l_2 \left[\dot{\Lambda}\Gamma(\alpha\lambda - 1)C\theta_2 + \Lambda\Gamma\dot{\alpha}\lambda C\theta_2 \right] \\
& -\lambda(\dot{\theta}_1 + \dot{\theta}_2 + \dot{q}\psi')eM_{pL}l_2 \left[\Lambda\Gamma(\alpha\lambda - 1)S\theta_2\dot{\theta}_2 - \dot{\alpha}\lambda \right] \\
& +\dot{\theta}_1\lambda e(\alpha\lambda + 1)M_{pL}l_1 S(\theta_2 + \zeta_1 + \zeta_2)(\dot{\theta}_2 + \dot{q}\psi' + \dot{b}\epsilon') \\
& -\dot{q}\lambda\psi eM_{pL} \left[\dot{\Lambda}\Gamma + \dot{\alpha}\lambda C(\theta_2 + \zeta_1 + \zeta_2) \right] \\
& +\dot{q}\lambda\psi eM_{pL}(\alpha\lambda + 1)S(\theta_2 + \zeta_1 + \zeta_2) \left(\dot{\theta}_2 + \dot{q}\psi' + \dot{b}\epsilon' \right) \\
& +\alpha S_{10} + eM_{pL}l_2 S\theta_2\lambda C(\theta_2 + \zeta_2)\dot{\Lambda}^2\Gamma^2 \\
& -(\dot{\theta}_1 + \dot{\theta}_2 + \dot{q}\psi')^2 M_{pL}e\lambda l_2 S\zeta_2 \\
& -\dot{q}\psi(\dot{\theta}_1 + \dot{\theta}_2 + \dot{q}\psi')M_{pL}e\lambda S(\theta_2 + \zeta_1 + \zeta_2) \\
& -\dot{b}\epsilon(\dot{\theta}_1 + \dot{\theta}_2 + \dot{q}\psi')M_{pL}e\lambda S\zeta_2 \\
& -\dot{\theta}_1\dot{\Lambda}\Gamma e\lambda l_1 M_{pL} + \dot{\Lambda}\dot{q}\Gamma\psi e\lambda M_{pL} \\
& -\dot{\theta}_2\dot{\Lambda}\Gamma^2 l_2 e\Lambda\lambda M_{pL} [S(\theta_2 + \zeta_2)S\theta_2 - C\theta_2 C(\theta_2 + \zeta_2)] \\
& -\dot{\alpha}\lambda(\dot{\theta}_1 + \dot{\theta}_2 + \dot{q}\psi')M_{pL}e\lambda l_2 [\Lambda\Gamma C\theta_2 - 1]
\end{aligned}$$

$$\begin{aligned}
& -(\dot{\theta}_1 + \dot{\theta}_2 + \dot{q}\psi')\dot{b}\epsilon' M_{pL}e\lambda l_2 S\zeta_2 \\
& -\dot{b}e\lambda\epsilon' M_{pL}S(\theta_2 + \zeta_1 + \zeta_2) [\dot{\theta}_1 l_1 + \dot{q}\psi] \\
& +\dot{\alpha}\dot{q}\lambda^2\psi eC(\theta_2 + \zeta_1 + \zeta_2)M_{pL} \\
& -\dot{q}^2\psi'\psi e\Lambda\Gamma S\zeta_1\lambda M_{pL} \\
& -\dot{\theta}_1\dot{q}\psi' M_{pL}l_1 S\zeta_1 e\Lambda\Gamma\lambda
\end{aligned}$$

... Also

$$\begin{aligned}
& \dot{q}B_{51} + C_{51} \equiv \\
& -A_2\psi\dot{b}S(\theta_2 + \zeta_1)\dot{\theta}_2 V_3 \\
& -A_2\psi(\dot{\theta}_1 + \dot{\theta}_2 + 2\dot{q}\psi')S(\theta_2 + \zeta_1) [(\dot{\theta}_2 + \dot{q}\psi')S_3 + \dot{b}V_3] \\
& +A_2S_3\dot{\theta}_1\psi'\dot{q}\psi S(\theta_2 + \zeta_1) \\
& +A_2S_3\dot{\theta}_1\psi' [(\dot{\theta}_2 + \dot{q}\psi') [C(\theta_2 + \zeta_1)q\psi - l_1S(\theta_2 + \zeta_1)]] \\
& -A_2\psi(\dot{\theta}_1 + \dot{\theta}_2 + 2\dot{q}\psi')\dot{b}C(\theta_2 + \zeta_1)(\dot{\theta}_2 + \dot{q}\psi')V_3 \\
& +A_2V_3\dot{b}\dot{\theta}_1\psi' [q\psi C(\theta_2 + \zeta_1) - l_1S(\theta_2 + \zeta_1)] \\
& +A_2V_3\dot{b}\dot{\theta}_1\psi\dot{q}\psi C(\theta_2 + \zeta_1) \\
& -A_2V_3\dot{b}\dot{\theta}_1\psi(\dot{\theta}_2 + \dot{q}\psi') [q\psi S(\theta_2 + \zeta_1) + l_1C(\theta_2 + \zeta_1)] \\
& +\dot{\theta}_1\psi M_{pL}\Gamma e [\dot{\Lambda}S\zeta_1 + 2\Lambda\dot{q}\psi'] \\
& -\dot{b}\psi eM_{pL}S(\theta_2 + \zeta_1)(\dot{\theta}_2 + \dot{q}\psi') \\
& +2(\dot{q}\psi'^2 + \dot{\theta}_1\psi' + \dot{\theta}_2\psi')e l_2 [\dot{\alpha}\lambda S\zeta_2 + (\alpha\lambda - 1)\dot{b}\epsilon'] M_{pL} \\
& +\psi'\dot{\Lambda}\Gamma e l_2 M_{pL} [S\theta_2\dot{\theta}_2 + \dot{\Lambda}\Gamma S\theta_2 S(\theta_2 + \zeta_2)] \\
& +\psi'\dot{\Lambda}\Gamma e l_2 M_{pL}\Lambda\Gamma [C\theta_2\dot{\theta}_2 S(\theta_2 + \zeta_2) + S\theta_2 C(\theta_2 + \zeta_1)(\dot{\theta}_2 + \dot{b}\epsilon')] \\
& -\dot{\theta}_1\psi' M_{pL}S(\theta_2 + \zeta_1)(\dot{\theta}_2 + \dot{q}\psi')l_1 l_2 \\
& +\dot{\theta}_1\psi' M_{pL}C(\theta_2 + \zeta_1)(\dot{\theta}_2 + \dot{q}\psi')(l_2 q\psi - bl_1\epsilon)
\end{aligned}$$

$$\begin{aligned}
& +\dot{\theta}_1 \psi' M_{pL} S(\theta_2 + \zeta_1) (l_2 \dot{q} \psi - \dot{b} l_1 \epsilon) \\
& +\dot{\theta}_1 \psi' M_{pL} e \Gamma l_2 \left[\dot{\Lambda} S \theta_2 + \Lambda C \theta_2 \dot{\theta}_2 \right] \\
& -\dot{\theta}_1 \psi' M_{pL} e l_1 \left[S(\theta_2 + \zeta_1 + \zeta_2) + C(\theta_2 + \zeta_1 + \zeta_2)(\dot{\theta}_2 + \dot{q} \psi' + \dot{b} \epsilon') \right] \\
& +\psi M_{pL} (\dot{\theta}_1 + \dot{\theta}_2 + 2\dot{q} \psi') e \dot{\alpha} \lambda S(\theta_1 + \zeta_1 + \zeta_2) \\
& -\psi M_{pL} (\dot{\theta}_1 + \dot{\theta}_2 + 2\dot{q} \psi') l_2 S(\theta_2 + \zeta_1) (\dot{\theta}_2 + \dot{q} \psi') \\
& +\psi M_{pL} (\dot{\theta}_1 + \dot{\theta}_2 + 2\dot{q} \psi') e M_{pL} (\alpha \lambda - 1) C(\theta_2 + \zeta_1 + \zeta_2) (\dot{\theta}_2 + \dot{q} \psi' + \dot{b} \epsilon') \\
& +\dot{b} \epsilon \psi' e M_{pL} \left[\dot{\alpha} \lambda S \zeta_2 + (\alpha \lambda - 1) \dot{b} \epsilon' \right] \\
& +\dot{b} \epsilon \psi' e M_{pL} \left[\dot{\alpha} \lambda S(\theta_2 + \zeta_1 + \zeta_2) + (\alpha \lambda - 1) C(\theta_2 + \zeta_1 + \zeta_2) (\dot{\theta}_2 + \dot{q} \psi' + \dot{b} \epsilon') \right] \\
& -\dot{\Lambda} \Gamma \psi M_{pL} \left[\dot{\Lambda} \Gamma l_2 S \theta_2 + \Lambda \Gamma l_2 C \theta_2 \dot{\theta}_2 + e \dot{\alpha} \lambda \right] \\
& +\dot{\alpha} \lambda \psi' e l_2 M_{pL} \left[\dot{\Lambda} \Gamma (\alpha \lambda - 1) C \theta_2 - \Lambda \Gamma (\alpha \lambda - 1) S \theta_2 \dot{\theta}_2 - \dot{\alpha} \lambda \right] \\
& +\psi' \dot{b} \epsilon' e l_2 \left[\dot{\alpha} \lambda S \zeta_2 + (\alpha \lambda - 1) \dot{b} \epsilon' \right] \\
& +\psi' \dot{b} \epsilon' e l_2 M_{pL} \left[\dot{\alpha} \lambda S \zeta_2 + (\alpha \lambda - 1) \dot{b} \epsilon' \right] \\
& -\psi' \dot{b} \epsilon' e l_2 \Gamma M_{pL} \left[\dot{\Lambda} S \theta_2 + \Lambda C \theta_2 \dot{\theta}_2 \right] \\
& -\dot{\alpha} \lambda \psi e M_{pL} \left[\dot{\alpha} \lambda C(\theta_2 + \zeta_1 + \zeta_2) - (\alpha \lambda + 1) S(\theta_2 + \zeta_1 + \zeta_2) (\dot{\theta}_2 + \dot{\zeta}_1 + \dot{\zeta}_2) \right] \\
& +2\dot{q} \psi' \psi e \Gamma M_{pL} \left[\dot{\Lambda} S \zeta_1 (\alpha \lambda + 1) + \Lambda \dot{q} \psi' (\alpha \lambda + 1) / 2 + \Lambda S \zeta_1 \dot{\alpha} \lambda \right] \\
& +\dot{\theta}_1 \psi' e \Gamma l_1 M_{pL} \left[\dot{\Lambda} S \zeta_1 (\alpha \lambda + 1) + \Lambda \dot{q} \psi' (\alpha \lambda + 1) + \Lambda S \zeta_1 \dot{\alpha} \lambda \right] \\
& -A_1 \dot{\theta}_1^2 q V_5 + A_2 \dot{\theta}_1 \dot{b} l_1 S(\theta_2 + \zeta_1) \psi' V_3 \\
& -S_3 A_2 \dot{\theta}_1 (\dot{\theta}_1 + \dot{\theta}_2 + \dot{q} \psi') S(\theta_2 + \zeta_1) [\psi - l_1 \psi'] \\
& -S_3 A_2 \dot{\theta}_1 (\dot{\theta}_1 + \dot{\theta}_2 + \dot{q} \psi') q \psi C(\theta_2 + \zeta_1) \psi' \\
& +A_2 b (\dot{\theta}_1 + \dot{\theta}_2 + \dot{q} \psi') \dot{q} \psi C(\theta_2 + \zeta_1) \psi' V_3 \\
& +A_2 \dot{q} \psi (\dot{\theta}_1 + \dot{\theta}_2 + \dot{q} \psi') S(\theta_2 + \zeta_1) \psi' S_3 \\
& -A_2 b \dot{\theta}_1 (\dot{\theta}_1 + \dot{\theta}_2 + \dot{q} \psi') C(\theta_2 + \zeta_1) V_3 [\psi - l_1 \psi']
\end{aligned}$$

$$\begin{aligned}
& +A_2 b \dot{\theta}_1 (\dot{\theta}_1 + \dot{\theta}_2 + \dot{q} \psi') V_3 q \psi S(\theta_2 + \zeta_1) \psi' \\
& \quad - \dot{\theta}_1^2 \psi' e \Lambda \Gamma l_1 M_{pL} \\
& \quad + \dot{\theta}_1 b \epsilon \psi' l_1 S(\theta_2 + \zeta_1) M_{pL} \\
& \quad + \dot{q} b \psi \epsilon S(\theta_2 + \zeta_1) \psi' M_{pL} \\
& - (\dot{\theta}_1 + \dot{\theta}_2 + \dot{q} \psi') \dot{\theta}_1 M_{pL} [C(\theta_2 + \zeta_1) \psi' (l_2 q \psi - l_1 b \epsilon) - S(\theta_2 + \zeta_1) \psi' l_1 l_2] \\
& \quad - (\dot{\theta}_1 + \dot{\theta}_2 + \dot{q} \psi') \dot{\theta}_1 M_{pL} [S(\theta_2 + \zeta_1) l_2 \psi - e l_1 C(\theta_2 + \zeta_1 + \zeta_2) \psi'] \\
& \quad + \psi' \dot{q} \psi (\dot{\theta}_1 + \dot{\theta}_2 + \dot{q} \psi') l_2 M_{pL} S(\theta_2 + \zeta_1) \\
& - \psi' \dot{q} \psi (\dot{\theta}_1 + \dot{\theta}_2 + \dot{q} \psi') M_{pL} e (\alpha \lambda - 1) C(\theta_2 + \zeta_1 + \zeta_2) \\
& \quad - b \epsilon' \dot{\theta}_1 e (\alpha \lambda - 1) M_{pL} l_1 C(\theta_2 + \zeta_1 + \zeta_2) \psi' \\
& \quad - \dot{\theta}_1 \dot{\alpha} \lambda e (\alpha \lambda + 1) M_{pL} l_1 S(\theta_2 + \zeta_1 + \zeta_2) \psi' \\
& \quad - b \dot{q} \epsilon' \psi e (\alpha \lambda - 1) C(\theta_2 + \zeta_1 + \zeta_2) \psi' M_{pL} \\
& \quad - \dot{\alpha} \dot{q} \lambda \psi e (\alpha \lambda + 1) S(\theta_2 + \zeta_1 + \zeta_2) \psi' M_{pL} \\
& \quad - \dot{\theta}_1 \dot{q} \psi' l_1 \psi' e \Lambda \Gamma (\alpha \lambda + 1) M_{pL} \\
& \quad + q V_6 \\
& + g M_{pL} [l_2 C \beta \psi' - e S(\beta + \zeta_2) \psi'] \\
& \quad + g m_2 l_2 C \beta \psi' / 2
\end{aligned}$$

... And finally

$$\begin{aligned}
& \dot{b} B_{61} C_{61} \equiv \\
& -A_2 \dot{\theta}_1 l_1 (\dot{\theta}_2 + \dot{q} \psi') S(\theta_2 + \zeta_1) V_3 \\
& \quad + A_2 \dot{\Lambda} \Gamma^2 C^2 \theta_2 b \dot{\Lambda} V_1 \\
& \quad - 2A_2 \dot{\Lambda} \Gamma^2 C \theta_2 S \theta_2 \dot{\theta}_2 b \dot{\Lambda} V_1 \\
& \quad - \dot{\theta}_1 \epsilon M_{pL} l_1 S(\theta_2 + \zeta_1) (\dot{\theta}_2 + \dot{q} \psi')
\end{aligned}$$

$$\begin{aligned}
& -\dot{\theta}_1 \epsilon e \Gamma M_{pL} \left[\dot{\Lambda} S \theta_2 + \Lambda C \theta_2 \dot{\theta}_2 \right] \\
& -\dot{q} \psi \epsilon S (\theta_2 + \zeta_1) (\dot{\theta}_2 + \dot{q} \psi') M_{pL} \\
& + \dot{\Lambda} \Gamma \epsilon M_{pL} \left[2\dot{\theta}_2 C (2\theta_2) l_2 \Lambda \Gamma + S (2\theta_2) l_2 \dot{\Lambda} \Gamma + S \theta_2 \dot{\theta}_2 e \right] \\
& + \epsilon M_{pL} (\dot{\theta}_1 + \dot{\theta}_2 + \dot{q} \psi') e \left[\dot{\alpha} \lambda S \zeta_2 + (\alpha \lambda - 1) \dot{b} \epsilon' \right] \\
& + (\dot{\theta}_1 + \dot{\theta}_2 + \dot{q} \psi') M_{pL} \epsilon' e l_2 \left[\dot{\alpha} \lambda S \zeta_2 - \dot{b} \epsilon' \right] \\
& - (\dot{\theta}_1 + \dot{\theta}_2 + \dot{q} \psi') M_{pL} \epsilon' e l_2 \left[\dot{\Lambda} \Gamma S \theta_2 + \Lambda \Gamma C \theta_2 \dot{\theta}_2 \right] \\
& + \epsilon' \dot{\theta}_1 e l_1 M_{pL} \left[\dot{\alpha} \lambda S (\theta_2 + \zeta_1 + \zeta_2) - C (\theta_2 + \zeta_1 + \zeta_2) (\dot{\theta}_2 + \dot{b} \epsilon' + \dot{q} \psi') \right] \\
& - \dot{b}^2 \epsilon' \epsilon e \epsilon' M_{pL} \\
& + \dot{q} \epsilon' \psi e M_{pL} \left[\dot{\alpha} \lambda S (\theta_2 + \zeta_1 + \zeta_2) + C (\theta_2 + \zeta_1 + \zeta_2) (\dot{\theta}_2 + \dot{b} \epsilon' + \dot{q} \psi') \right] \\
& - \dot{\alpha}^2 \epsilon \lambda^2 e M_{pL} \\
& + A_2 \dot{\theta}_1 \dot{q} \psi S (\theta_2 + \zeta_1) V_3 \\
& - A_2 \dot{\theta}_1 (\dot{\theta}_1 + \dot{\theta}_2 + \dot{q} \psi') [q \psi C (\theta_2 + \zeta_1) - l_1 S (\theta_2 + \zeta_1)] V_3 \\
& - \dot{\Lambda}^2 \Gamma^2 l_2 [S \theta_2 C \theta_2 \epsilon + e S \theta_2 \alpha \lambda S (\theta_2 + \zeta_2) \epsilon'] M_{pL} \\
& - (\dot{\theta}_1 + \dot{\theta}_2 + \dot{q} \psi')^2 l_2 \epsilon' e (\alpha \lambda - 1) M_{pL} \\
& - (\dot{\theta}_1 + \dot{\theta}_2 + \dot{q} \psi') \dot{\Lambda} \Gamma^2 e \Lambda l_2 S \theta_2 C (\theta_2 + \zeta_2) \epsilon' M_{pL} \\
& + \dot{\theta}_1 (\dot{\theta}_1 + \dot{\theta}_2 + \dot{q} \psi') l_1 [S (\theta_2 + \zeta_1) \epsilon + e C (\theta_2 + \zeta_1 + \zeta_2) \epsilon'] M_{pL} \\
& - \dot{q} \psi (\dot{\theta}_1 + \dot{\theta}_2 + \dot{q} \psi') e (\alpha \lambda - 1) C (\theta_2 + \zeta_1 + \zeta_2) \epsilon' M_{pL} \\
& - \dot{b} \epsilon (\dot{\theta}_1 + \dot{\theta}_2 + \dot{q} \psi') e (\alpha \lambda - 1) \epsilon' M_{pL} \\
& - \dot{\theta}_2 \dot{\Lambda} \Gamma \epsilon' [e \Lambda \Gamma C (\theta_2 + \zeta_1) (\alpha \lambda - 1) S \theta_2 + C \theta_2 (\alpha \lambda + 1) S (\theta_2 + \zeta_2)] l_2 M_{pL} \\
& - (\dot{\theta}_1 + \dot{\theta}_2 + \dot{q} \psi') \dot{b} \epsilon' \epsilon' e (\alpha \lambda - 1) l_2 M_{pL} \\
& - \dot{b} \epsilon' \dot{\theta}_1 \epsilon' e (\alpha \lambda - 1) l_1 C (\theta_2 + \zeta_1 + \zeta_2) M_{pL} \\
& - \dot{\theta}_1 \dot{\alpha} \lambda e (\alpha \lambda + 1) l_1 S (\theta_2 + \zeta_1 + \zeta_2) \epsilon' M_{pL}
\end{aligned}$$

$$\begin{aligned}
& -b\dot{q}\epsilon'\psi\epsilon'e(\alpha\lambda - 1)C(\theta_2 + \zeta_1 + \zeta_2)M_{pL} \\
& -\dot{\alpha}\dot{q}\lambda\psi\epsilon'e'(\alpha\lambda + 1)S(\theta_2 + \zeta_1 + \zeta_2)M_{pL} \\
& +bV_7 - gM_{pL}eS(\beta + \zeta_2)\epsilon'
\end{aligned}$$

Some of the variables appearing in these equations ,such as $S_1, S_2 \dots$ and $V_1, V_2 ,$ have not been previously defined, and therefore will be listed below :

$$S_1 = \int_0^{l_1} \rho y_1^2 dy_1$$

$$S_2 = \int_0^{l_2} \rho y_2^2 dy_2$$

$$S_3 = \int_0^{l_2} \rho y_2 dy_2$$

$$S_4 = \int_0^{l_2} \rho dy_2$$

$$S_5 = I\Gamma_1(l_1) \int_0^{l_2} \lambda_1(y_2) dy_2$$

$$S_6 = \int_0^{l_1} GJ(y_1)\Gamma_1'(y_1)\Gamma_1'(y_1) dy_1$$

$$S_7 = \int_0^{l_1} I(y_1)\Gamma_1(y_1)\Gamma_1(y_1) dy_1$$

$$S_8 = \Gamma_1^2(l_1)Il_2$$

$$S_9 = \int_0^{l_2} I(y_2)\lambda_1(y_2)\lambda_1(y_2) dy_2$$

$$S_{10} = \int_0^{l_2} GJ(y_2)\lambda_1'(y_2)\lambda_1'(y_2) dy_2$$

$$V_1 = \int_0^{l_2} \rho \epsilon_1^2(y_2) dy_2$$

$$V_2 = \int_0^{l_2} \rho y \epsilon_1(y_2) dy_2$$

$$V_3 = \int_0^{l_2} \rho \epsilon_1(y_2) dy_2$$

$$V_4 = \int_0^{l_1} \rho y_1 \psi_1(y_1) dy_1$$

$$V_5 = \int_0^{l_1} \rho \psi_1^2(y_1) dy_1$$

$$V_6 = \int_0^{l_1} EI(y_1) (\psi'')^2 dy_1$$

$$V_7 = \int_0^{l_2} EI(y_2) (\epsilon'')^2 dy_2$$

Bibliography

- [1] Asada, H. and J. Slotine ; *Robot Analysis and Control*, John Wiley and Sons, N.Y., 1986.
- [2] Book, W.J. and G. Hastings, "Verification of a Linear Dynamic Model For Flexible Robot Manipulators," *IEEE International Conference on Robotics and Automation*, 1986, pp. 1024-1029.
- [3] Book, W.J., O. Maizza-Neto and D. Whitney, "Feedback Control of Two Beam, Two Joint Systems with Distributed Flexibility," *Transactions of the ASME; Journal of Dynamic Systems, Measurement, and Control*, Dec. 1975, pp. 424-431.
- [4] Clark, S.; *Dynamics of Continuous Systems*, Prentice Hall, Inc., Englewood Cliffs, N.J., 1972.
- [5] Dubowsky, S. and W.H. Sunada, "On the Dynamic Analysis and Behavior of Industrial Robotic Manipulators with Elastic Members," *Transactions of the ASME - Journal of Mechanical Design*, March 1982, paper 82-det-45.
- [6] Fu, K.S., Gonzales, and Lee ; *Robotics - Control, Sensing, Vision, and Intelligence*, McGraw-Hill, N.Y., 1987.
- [7] Gebler, B., "Feed Forward Control Strategy for an Industrial Robot with Elastic Links and Joints," *IEEE International Conference on Robotics and Automation*, 1987, pp. 923-928.
- [8] Gorman, Daniel J.; *Free Vibration Analysis of Beams and Shafts*, John Wiley and Sons, N.Y., 1975.

- [9] Hennessey, M.P., Priebe, Huang, and Gross, "Design of a Lightweight Robotic Arm and Controller," *IEEE International Conference on Robotics and Automation*, 1987, pp.779-785.
- [10] Hollerbach, J., "A Recursive Lagrangian Formulation of Manipulator Dynamics and a Comparative Study of Dynamics Formulation Complexity," *IEEE Transactions on Systems, Man, and Cybernetics*, Vol. sm-10, No. 11, Nov. 1980, pp. 730-736.
- [11] Hornbeck, Robert W.; *Numerical Methods*, Prentice Hall, Inc., Englewood Cliffs, N.J., 1975, pp. 185-208.
- [12] Marino, R. and M.W. Spong, "Nonlinear Control Techniques for Flexible Joint Manipulators: A Single Link Case Study," *IEEE International Conference on Robotics and Automation*, 1986, pp. 1030-1036.
- [13] Meirovitch, L.; *Analytic Methods in Vibrations*, Macmillan Co., N.Y., 1967.
- [14] Naganathan, G. and A.H. Soni, "Nonlinear Flexibility Studies for Spatial Manipulators," *IEEE International Conference on Robotics and Automation*, 1987, pp. 373-378.
- [15] Nicosia, S., Tomei and Tornambe, "Dynamic Modelling of Flexible Robot Manipulators," *IEEE International Conference on Robotics and Automation*, 1986, pp. 365-372.
- [16] Rakhsha, F. and A. Goldenberg, "Dynamic Modelling of a Single Link Flexible Robot," *IEEE International Conference on Robotics and Automation*, 1985, pp.984-989.
- [17] Tang, S. and C. Wang, "Computation of the Effects of Link Deflections and Joint Compliance on Robot Positioning," *IEEE International Conference on Robotics and Automation*, 1987, pp. 910-915.
- [18] Thomson, W.T.; *Theory of Vibrations with Applications*, Prentice Hall, Inc., Englewood Cliffs, N.J., 1981.
- [19] Timoshenko, S.; *Vibration Problems in Engineering*, D.Van Nostrand Comp., Inc. N.Y., 1955.
- [20] Tse, Morse and Hinkle; *Mechanical Vibrations - Theory and Applications*, Allyn and Bacon, Inc., Boston 1978

[21] Walshaw, A.C.; *Mechanical Vibrations with Applications*, Ellis Horwood Lmtd, West Sussex, Eng., 1984.